The E48 antigen as target for radioimmunotherapy of head and neck cancer

Martijn Gerretsen

The E48 antigen as target for radioimmunotherapy of head and neck cancer

Martijn Gerretsen

Drukkerij Tessel Offset bv, De Meern

Cover: Litho dating from 1975, Huub (Goofy) Gerretsen (1897-1978)

VRIJE UNIVERSITEIT

The E48 antigen as target for radioimmunotherapy of head and neck cancer

ACADEMISCH PROEFSCHRIFT

ter verkrijging van de graad van doctor aan
de Vrije Universiteit te Amsterdam,
op gezag van de rector magnificus
dr. C. Datema,
hoogleraar aan de faculteit der letteren,
in het openbaar te verdedigen
ten overstaan van de promotiecommissie
van de faculteit der geneeskunde
op vrijdag 11 juni 1993 te 10.30 uur
in het hoofdgebouw van de universiteit,
De Boelelaan 1105
door

Martijn Gerretsen

geboren te Haarlem

*Ter nagedachtenis aan Goofy, mijn grootvader, die voor mij altijd
een bron van inspiratie is gebleven*

Aan Dominique

Contents

 Parts of this and following chapters will be published in the
 European Journal of Cancer Part B: Oral Oncology, as an invited
 review, entitled "The feasibility of radioimmunotherapy in head
 and neck cancer".

Chapter 1

Introduction

Department of Otolaryngology / Head and Neck Surgery,
Free University Hospital, Amsterdam, The Netherlands

Introduction

Squamous cell carcinoma (SCC) represents the predominant histological type among tumors of the head and neck. They account for approximately 5% of all malignant neoplasms in Europe and the United States. The early stages are treated with single modality surgery or radiotherapy, advanced stages with combined surgery and radiation therapy. Failure to achieve tumor control above the clavicles has traditionally been regarded as the major cause of death in patients with advanced head and neck squamous cell carcinoma (HNSCC). The advent of modern reconstruction techniques has made wider excisions possible, and especially when combined with contemporary radiotherapy, locoregional control has been increased. However, the pattern of failure is changing due to the fact that more patients are exposed to the risk of developing distant metastases and "second primary" neoplasms. Consequently, the overall cure rate for patients with head and neck cancer has remained stationary. Disseminated disease has thus become an increasingly important cause of failure in patients with HNSCC. In order to identify risk factors predicting the development of distant metastases, Leemans *et al.* analyzed a group of 281 patients with SCC of the head and neck who did not develop recurrent disease above the clavicles [1]. All patients were primarily operated and received postoperative radiotherapy when three or more tumor infiltrated neck lymph nodes were found upon pathological examination. The 5-years overall incidence of distant metastases in this group was 10.7%. The number of involved nodes appeared to be an important prognostic factor: when 3 or more nodes contained tumor, the chance of developing distant metastases was found to be almost 50%. Even more unfavorable percentages are seen when patients are included who develop recurrent disease at the locoregional site: at least a doubling of the incidence of metastases is seen [2,3].

These data show that identification of patients with a high risk of developing distant metastases is possible. Development of an effective adjuvant systemic therapy is a major challenge. With respect to the application of (neo)adjuvant chemotherapy, unfortunately almost all studies have failed to show any improvement in survival [4-7]. Stell and Rawson evaluated the efficacy of neoadjuvant chemotherapy in 23 trials. No significant overall improvement in head and neck cancer mortality was found [8].

Among possible approaches for improved and more specific adjuvant therapy for this group of head and neck cancer patients at high risk of developing distant metastases is the use of monoclonal antibodies (MAbs).

MAbs in cancer immunotherapy

Since the introduction of the hybridoma technology by Köhler and Milstein [9], tremendous effort has been put in the realization of Ehrlich's concept of the magic bullet, which was proposed as early as the beginning of the century [10]. Based on the assumption that tumors possess specific antigens, he foresaw antibodies targeting toxic agents to tumor cells for the specific kill of these cells. Although there are for the majority of malignancies as yet no real tumor specific antigens (TSA), a considerable amount of evidence has accumulated during the last 15 years indicating that preferentially expressed tumor

antigens or tumor associated antigens (TAA) are excellent targets for cancer therapy.

With the increasing conceptual and technical knowledge in the fields of immunology, biochemistry, radiochemistry and molecular biology, various approaches to the use of MAbs in cancer therapy have evolved. In general, these strategies, all involving different mechanisms of action, can be classified in the following categories:

1. Delivery of toxic agents to tumor cells, e.g. radionuclides, toxins, or drugs.
2. Tumor site-specific targeting of cytokines, growth factors and enzymes with genetically engineered fusion proteins containing characteristics of both MAb and active agent.
3. Interference with tumor cell growth or differentiation by using MAbs directed to growth factor receptors.
4. Activation of components or effector cells of the immune system, resulting in complement- or antibody-dependent cellular cytotoxicity.
5. Redirection of effector cells to tumor sites by bispecific MAbs, e.g. MAbs directed to both tumor cell and T cell or monocyte surface antigens.

Of these strategies, the use of radiolabeled monoclonal antibodies may be particularly suitable for treatment of metastases of HNSCC due to the intrinsic radiosensitivity of this tumor type [11]. An other argument to use radiolabeled MAbs is the heterogeneity in antigen expression and/or the heterogenous penetration of the antibody into solid tumors. It is unnecessary for radiolabeled MAbs to bind to each single tumor cell to achieve maximal therapeutic effects, because most radionuclides in use are cytotoxic at a distance of several cell diameters. Antigen negative cells can thus be eliminated by "cross-fire" from a radioimmunoconjugate molecule bound to an adjacent antigen positive cell.

Monoclonal antibodies for targeting HNSCC.

Selection of appropriate antibodies is the first important step to successful radioimmunotherapy (RIT). Sofar, only a limited number of MAbs have been produced after immunization with head and neck cancer material. The most important characteristics of the majority of these MAbs and their suitability for HNSCC targeting wil be summarized. Zenner and Hermann were the first who described a MAb to a SCC cell surface antigen [12]. However, their reports are limited to the documentation of selective killing of laryngeal carcinoma cells with this antibody in an in vitro assay without further identification of the antigen [13]. In 1983 Carey et al. described the A9 and G10 antibodies directed against surface molecules of SCC [14]. Later studies revealed that MAb G10 reacts with a precursor blood group antigen [15] and that MAb A9 recognizes a basement membrane component [16,17]. Detailed studies on the reactivity of MAb A9 in normal human tissues were not presented, although they noted reactivity with normal blood vessels and epithelial basement membranes [16]. Recently, the antigen recognized by MAb A9 was identified as the $\alpha_6\beta_4$ integrin [18]. Boeheim et al. produced the SQM-1 antibody, a murine IgM antibody preferentially reactive with a SCC surface antigen of 48 kDa [19]. In general, the size and low affinity constants of IgM molecules render these immunoglobulins not very well suited for localization in tumors. A cytoplasmic antigen, recognized by MAb 17.13.C1.10

was found to be selectively expressed in squamous epithelia and myoepithelial cells [20,21]. An identical tissue distribution was found for MAb 174H64 [22]. Biochemical characterization made clear that this antigen has a relative molecular weight of 57 kDa and is probably a cytokeratin protein. Myoken *et al.* described two MAbs to oral SCC which were also found to be reactive with keratin proteins. These antibodies lack specificity for SCC [23].

Concerning the antibodies mentioned above we may conclude that these MAbs possess characteristics likely to hamper successful use for tumor-targeting. MAb A9 has been shown to react with normal blood vessels. This reactivity was also observed for the SQM-1 antibody. 17.1-3.C1.10 and 174H64 are highly selective reagents for SCC, but the location of the antigen is predominantly intracellular, and thus these Ag's are thought to be less accessible for an antibody than cell surface antigens.

At our department other MAbs, originally developed to non-SCC tumors but known to be reactive with SCC of the head and neck, were considered as potential tools for detection and therapy of SCC [25]. Among these antibodies, anti-CEA, anti-MAM-6 (episialine) and anti-epidermal growth factor receptor (EGFR) antibodies were evaluated on frozen sections in an indirect immunoperoxidase assay. Anti-CEA antibodies were reactive in a minority of SCC as has been documented [25]. MAbs to the MAM-6 antigen have been used to identify the epithelial nature of head and neck tumors [26]. A decrease in the percentage of reactive cells was seen from well differentiated SCC to the poorly differentiated types. In addition, the MAM-6 antigen was shown to be predominantly expressed in the more differentiated

cells in the central layers of tumors. Anti-EGF receptor antibodies could be useful to fulfil our study purposes, since in a considerable number of investigations it has been reported that overexpression of the EGF receptor occurs frequently in SCC [27,28].

A few years ago the use of MAbs directed against the epidermal growth factor receptor (EGFR) and the carcinoembryonic antigen (CEA) in radioimmunoscintigraphy of patients with head and neck cancer has been reported [29,30]. The value of these antibodies in targeting HNSCC is not clear. In these studies, only a few patients showed tumors smaller than 2 cm in diameter. A limitation of these antibodies may be that they are not specifically directed against HNSCC as has been described for anti-CEA which provided false-positive scintigrams [31].

Based on these data, the development of new antibodies directed to HNSCC was pursued [32,33]. As a result, a panel of 5 high affinity MAbs of the IgG subclass directed to antigens located at the outer cell surface of HNSCC was generated. MAbs E48 and MAb U36, the latter being developed only recently, are selectively reactive with squamous and transitional epithelia and their neoplastic counterparts [34,35]. MAb K928 is reactive with HNSCC and with suprabasal keratinocytes in normal stratified squamous epithelia [36]. This antibody recognizes a so called pan-carcinoma marker expressed by SCC, small cell lung carcinoma, and adenocarcinomas of lung, breast and ovary. Antibodies with similar features to MAb K928 have not been described before. K984 is reactive with HNSCC and basal keratinocytes in normal stratified squamous epithelia. This antibody recognizes a pan-carcinoma marker expressed by SCC, small cell lung carcinoma, and

Table 1. Characteristics of monoclonal antibodies for targeting HNSCC

	E48	U36	K928	K984	K931
reactivity with normal squamous tissue	basal and suprabasal	basal and suprabasal	suprabasal	basal	none
HNSCC (0% pos.)	3/58 (5%)	0/60 (0%)	1/60 (2%)	2/59 (3%)	7/55 (13%)
HNSCC (<10% pos.)	5/58 (9%)	1/60 (2%)	3/60 (5%)	3/59 (5%)	12/55 (22%)
HNSCC (10-50% pos.)	12/58 (21%)	4/60 (6%)	8/60 (13%)	10/59 (17%)	15/55 (27%)
HNSCC (51-95% pos.)	25/58 (43%)	43/60 (72%)	42/60 (70%)	41/59 (70%)	19/55 (34%)
HNSCC (>95% pos.)	13/58 (22%)	12/60 (20%)	6/60 (10%)	3/59 (5%)	2/55 (4%)
Mol. weight antigen	22 kD	200 kD	50kD	90 kD	37 kD
Affinity constant (M^{-1})	3×10^{10}	3.5×10^{10}	7×10^{9}	1×10^{10}	3×10^{10}

adenocarcinomas of lung, breast, colon, and ovary. Biochemical characterization indicates that the antigen recognized by MAb K984 is similar to the antigen recognized by MAb SF-25, an antibody produced by the group of Wands[37]. K931 is reactive with HNSCC but not with normal stratified squamous epithelia [38]. This antibody recognizes a pan-carcinoma marker expressed by SCC, small cell lung cancer, and adenocarcinomas of lung, breast colon, and ovary. Biochemical characterization indicated that the antigen recognized by MAb K931 is similar to the one recognized by MAb 17-1A, an antibody produced by the group of Koprowski [39]. The reactivity of MAbs E48, U36, K928, K984 and K931 on lymph node metastases from neck dissection specimen showed a similar pattern as on primary tumors.

Clinical RIT trials: an overview

Since the early 1980s, a substantial number of radioimmunotherapy trials have been performed.

Without presuming to be complete, an overview of a substantial number of the clinical trials performed between 1982 and 1993 is given in Table 2. The types of tumor which have been the subject of these studies include ovarian carcinoma; haematologic malignancies like Hodgkin's disease, B-cell lymphoma and cutaneous T cell lymphoma; gastrointestinal cancers like hepatocellular carcinoma, colorectal carcinoma, gastric cancer, pancreatic carcinoma and intrahepatic cholangiocarcinoma (biliary cancer); malignancies of the central nervous system, like neuroblastoma and glioma; breast cancer; melanoma; germ testicular carcinoma; and non-small cell lung cancer. In addition, a number of studies in patients with a very heterogeneous group of neoplastic meningitis have been reported. Neoplastic meningitis is a collective denominator for tumor deposits on the leptomeninges or cerebral membranes. These deposits are derived from tumors that originate elsewhere in the body and have the propensity to metastasize to the brain. The primary tumors from which these neoplastic

meningitis arise include tumors like pineoblasto-ma, B-cell lymphoma, teratoma, medulloblas-toma, melanoma, ovarian carcinoma, bladder carcinoma, gliomatosis, leukemia, breast cancer and lung cancer.

An important point with respect to reviewing the literature on clinical RIT studies is the observa-tion that a substantial number of reports show considerable overlap in patient groups being discussed. This seriously hampers attempts to gain insight in the absolute numbers of responses in patients with a given neoplastic disease. How-ever, a number of important generalizations can be made, based on the experiences obtained with these studies. First of all, most success has been obtained in patients with haematologic neoplasia. These tumor types have a high intrinsic sensitivity for radiation. In addition, the extensive characte-rization of T- and B-cell antigens allows for well considered and well founded choices of targets for RIT of malignancies arising from these cells. Especially when combined with bone marrow preservation, high doses of upto 600 mCi have been shown to result in a very high percentage of complete remissions [40]. For solid tumors how-ever, it has become clear that despite the fact that partial and complete responses have been obtained in a number of cases, the percentage of injected dose (%ID) taken up in large solid tumors is still an order of magnitude too low, and therapeutic ratios are still very low [41]. This is especially true for radioimmunoconjugates administered intra-venously, in which case the $\%ID.g^{-1}$ in tumor is reported to range from 0.001-0.01. However, since several tumor types are confined to only one compartment, like the peritoneal cavity or the thecal cavity, locoregional administration of the radioimmunoconjugate might improve the %ID

and tumor-nontumor ratios. When RIT is per-formed locoregional, e.g. by intraperitoneal, intraarterial, intraventricular or intralesional administration, indeed higher $\%ID.g^{-1}$ have been observed. However, the advantage of for instance intraperitoneal administration over intravenous administration in the case of ovarian carcinoma is still a matter of debate [42].

An important parameter of influence on the accumulation in tumor is the size of the tumor as has been shown in a number of cases. In a study on intraperitoneal RIT for ovarian cancer, Stewart *et al.* showed that whereas in 10 patients with gross disease (nodules > 2 cm) no responses were observed, partial responses in 2 out of 15 patients with nodules < 2 cm and complete responses in 3 out of 6 patients with microscopic disease were observed [42]. In studies evaluating a multimodality treatment protocol, including external beam irradiation, chemotherapy and treatment with ^{131}I-labeled antiferritin, for the conversion of nonresactable hepatocellular carcinoma to resectable disease, a relation between tumor size and respons was also observed [43]. In patients with tumors < 2290 g, a higher percentage complete remissions and partial responses was observed. A clear correlation between tumor size and $\%ID.g^{-1}$ was shown in a biodistribution study by Chatal *et al.*. In this study with [111]I-labeled MAb OC125, low accumu-lation in large tumors was observed (0.0014-0.0032 $\%ID.g^{-1}$), whereas in small tumor nodules (0.13 $\pm$ 0.08 $\%ID.g^{-1}$) and malignant cell clusters (median 0.33 with a maximum of 4.16 $\%ID.g^{-1}$) a significantly higher accumulation was observed [44]. It can thus be assumed that the efficacy of RIT is inversely correlated with tumor size.

Dose-response relations in clinical trials

For most tumors, a radiation dose of 2,000-6,000 rads must be delivered over a one-week period to achieve sterilization [45]. With the %ID.g^{-1} currently observed in tumors (0.01% on average), such a dose would require the i.v. administration of 2670 mCi ^{131}I- or 670 mCi ^{90}Y-labeled antibodies. This would however result in whole body doses of respectively 1700 and 1480 rads, causing unacceptable bone marrow toxicity. Thus, effective therapy with acceptable toxicity would require at least 0.05 %ID.g^{-1} to accumulate in the tumor. Based on concentrations of ^{131}I-labeled H317 antibodies measured in human tumors *in vivo*, Epenetos *et al.* calculated that 200 mCi administered i.v. to treat ovarian carcinoma would deliver only 500 rads to a 1 gram tumor, and a whole-body dose of 200 rads [46]. Based on pharmacokinetic data taken from the literature, mathematical modeling estimating tumor and whole-body doses during RIT showed that in a hypothetical patient of 70 kg with a 500 gram solid tumor in the liver, i.v. administration of 100 mCi ^{90}Y or ^{131}I would deliver 1700 and 750 rads to the tumor, respectively, and would result in wholebody doses of 200 and 120 rads, respectively [47].

Thus it would seem that, theoretically, therapeutic doses are not obtainable with RIT. In the clinical RIT studies summarized in Table 2, only a small number provide dosimetric estimates, and only part of these can be considered therapeutic. Nevertheless, partial responses and complete remissions were obtained in several of these studies. In part, this discrepancy may be explained by inadequate methods of calculating radiation doses. For instance, the conventional medical internal radiation dose (MIRD) method assumes uniform distribution of radioactivity in the tumor, despite experimental evidence that this is not the case [48]. The heterogeneity of antigen expression and the nonuniform distribution of theconjugate in the tumor will result in areas with much higher and much lower radiation doses than predicted by the MIRD method. Another factor not taken into account by the MIRD method is the range of ß-radiation in comparison with the diameter of the tumor, a parameter especially of importance when calculating radiation doses to small tumors [49]. Thus, the MIRD method can result in large errors [50]. In addition, immunological effects can contribute to the number of responses observed.

It can be anticipated that dose fractionation will increase the therapeutic index by relatively decreasing toxic effects in normal tissues [51]. As a consequence, a larger dose may be administered in total. Results from early clinical and animal studies of fractionated delivery of RIT suggest that larger doses of radiation are able to be administered with less bone marrow supression than with single large doses [52-55]. The enhanced anti-tumor effects with fractionated schedules observed in these animal studies may be in part the result of a larger dose. Another possible contributing factor is that a prior exposure to radiolabeled MAb could increase the sensitivity of tumor cells to a second exposure to radiolabeled MAb [56]. Most MAbs used in clinical trials are murine MAbs. These murine MAbs can be recognized by the body as foreign, and can give rise to the generation of human anti mouse antibodies (HAMA's). Formation of such HAMA's no doubt will interfere with the biodistribution and pharmacokinetics of the immunoconjugate

and furthermore can give rise to severe complications for patients especially upon repeated administration of the immunoconjugate. To prevent HAMA responses, reshaping the MAb molecule by recombinant DNA techniques will be a prerequisite.

Normally, estimation of radioactivity localized in the tumor is carried out by quantitative external planar imaging with a γ-camera. Dosimetry estimates for tumors that lie deep in the body and that have organs containing significant amounts of activity overlying them are not accurate when performed by this method. Single photon emission computed tomography (SPECT) [57,58] or positron emission tomography (PET) [59,60,61] may provide more accurate and reliable dosimetry estimates of radioactivity accumulated in tumors.

In conclusion, when the %ID in large solid tumors can not be elevated above values currently obtained, the therapeutic area where RIT has the potential to be most usefull is in adjuvant therapy when minimal residual disease is present [41].

Table 2. Summary of clinical RIT studies (1982-1993)

Tumor type (Patients)	Antibody	Antigen (Ag)	Radionuclide, Dose, Route	Response (n)	Tumor dose (Rads)	Reference
Malignancies of the female and male genital tract						
Ovarian (1)	HMFG2	Human milk fat globule (HMFG)	[131]I 20 mCi i.p.	CR	5,000-7,000	62
Ovarian (1)	AUA1 HMFG2	40 kD GP HMFG	[131]I 39-49 mCi i.p.	CR	8,533-10,667	63
Ovarian (9)	HMFG2	HMFG	[131]I 100-150 mCi i.p.	NE 2, NR 6, PR 1	ND	64
Ovarian (24)	HMFG1 HMFG2 H17E2	HMFG HMFG placental alkaline phosphatase (PAP)	[131]I 20-205 mCi i.p.	NR 15, PR 5, CR 4[a]	8,000	65
Ovarian (31)	HMFG1 HMFG2 AUA1 H17E2	HMFG HMFG 40 kD GP PAP	[131]I 20-158 mCi i.p.	NR 26, PR 2, CR 3[a]	39-455	42
Ovarian (11)	HMFG2	HMFG	[131]I 30-150 mCi i.p.	NE 1, NR 10	ND	66
Ovarian (10)	HMFG1 HMFG2 H17E2 B72.3	HMFG HMFG PAP tumor associated GP 72	[131]I 92 mCi i.p.	NR 3, MR 4, PR 3[a]	ND	67
Ovarian (5)	2G3	330 kD GP	[131]I 1-50 mCi i.p.	NR 4, PR 1	ND	68
Ovarian (8)	MOv18	Folate receptor	[131]I 100 mCi i.p.	NR 3, SD 2, CR 3	ND	69

Table 2. (continued)

Tumor type (Patients)	Antibody	Antigen (Ag)	Radionuclide, Dose, Route	Response (n)	Tumor dose (Rads)	Reference
Ovarian (6)	HMFG1 HMFG2 AUA1 H17E2	HMFG 40 kD GP PAP	^{90}Y 6-17.6 mCi i.p.	NR 5, PR 1[a]	ND	70
Germ testicular carcinoma (2)	H17E2	PAP	^{131}I 108-121 mCi i.v.	NR 2	ND	71

Haematologic malignancies

Tumor type (Patients)	Antibody	Antigen (Ag)	Radionuclide, Dose, Route	Response (n)	Tumor dose (Rads)	Reference
Hodgkin's (38)	α-ferritin	ferritin	^{131}I 50-100 mCi i.v.	NR 23, PR 14, CR 1	ND	72
Hodgkin's (6)	α-ferritin	ferritin	^{90}Y 10-30 mCi i.v.	NR 2, PR 1, CR 3	ND	73
B-cell lymphoma (1)	LYM-1	protein on B-cells	^{131}I 225 mCi i.v.	PR	ND	74
B-cell lymphoma (18)	LYM-1	protein on B-cells	^{131}I 300 mCi i.v.	NR 5, SD 3, PR 8, CR 2	ND	75
B-cell lymphoma (1)	α-idiotype	B-cell Ig	^{90}Y 10 mCi i.v.	PR	ND	76
B-cell lymphoma (10)	MB-1	CD37	^{131}I 25-161 mCi i.v.	NE 1,NR 2, SD 1, MR 2, MXR 1, PR 2, CR 1	34-341	77
B-cell lymphoma/ leukemia (10)	LYM-1	protein on B-cells	^{131}I 37-384 mCi i.v.	NR 3, SD 3, PR 3, CR 1	ND	78
B-cell lymphoma (5)	MB-1 IF5	CD37 CD20	^{131}I 232-608 mCi i.v.	PR 1, CR 4	850-4,260	40
B-cell lymphoma (5)	LL2 (EPB-2)	protein on B-cells	^{131}I 19-94 mCi i.v.	NR 1, MXR/MR 2, PR 2, CR 1[*A]	60-356	79,80
B-cell lymphoma/ Acute Myelo- genous Leukemia (AML) (12)	OKB7	CR2 (Epstein-Barr virus receptor)	^{131}I 90-200 mCi i.v.	NR 5, MXR 8, PR 1	ND	81
Cutaneous T-cell lymphoma (CTL) (7)	T101	T65 Ag	^{131}I 101-150 mCi i.v.	NR 1, MR 4, PR 2	40-150	82,83
CTL (3)	T101	T65 Ag	^{131}I 100 mCi i.v.	NR 1, PR 2	ND	84
AML (8)	M195	CD33	^{131}I 88-158 mCi i.v.	MR 7, PR 1	ND	85

Gastro-intestinal malignancies

Tumor type (Patients)	Antibody	Antigen (Ag)	Radionuclide, Dose, Route	Response (n)	Tumor dose (Rads)	Reference
Intrahepatic cholangiocarcinoma (34)	α-CEA	carcinoembryonic antigen (CEA)	^{131}I 30 mCi i.v.[b]	NE 4, NR 18, SD 4, PR 8	6,200	86
Hepato cellular carcinoma (HCC) (66)	α-ferritin	ferritin	^{131}I 50 mCi i.v.[b]	NR 15, SD 21, PR 26, CR 4	1,000-1,200	43
HCC (41)	α-ferritin	ferritin	^{131}I (37), ^{125}I (4) 10-141 mCi i.a.[b]	NR 5, SD 8, PR 28	ND	87-89
HCC (11)	α-ferritin	ferritin	^{131}I 30-50 mCi i.v.[b]	NR 4, PR 7	ND	90
HCC (13)	α-ferritin	ferritin	^{90}Y 20-62 mCi i.v.[b]	NE 4, NR 6, PR 3	512-2153	91

Table 2. (continued)

Tumor type (Patients)	Antibody	Antigen (Ag)	Radionuclide, Dose, Route	Response (n)	Tumor dose (Rads)	Reference
Colon (16)	PK4S	CEA	^{131}I 38-152 mCi	NR 15, PR 1	30-304	57
Colon (1)	35	CEA	^{131}I 200 mCi i.a.	PR 1	1,000	92
	431	CEA				
Colon (18)	FO23C5	CEA	^{131}I 21-150 mCi	NE 3, NR 8, SD 3,	768-4,628	93
	BW494/32	CEA	i.p., i.v., i.p.+i.v.	PR 2, CR 2[a]		
	B72.3	TAG 72				
Colon (12)	chimeric B72.3	TAG 72	^{131}I 49-63 mCi i.v.	NR 8, SD 3, MR 1	ND	94
Colorectal, lung, gastric, ovarian, renal (46)	NR-LU-10 NR-CO-O2	40 kD GP CEA subspecies	^{186}Re 25-336 mCi i.v. or i.a.	NE 5, NR 40, PR 1[a]	284-1,638 100-1,344	95
Pancreatic (1)	α-CA 19-9 BW-494/32	CA 19-9 CA 19-9	^{131}I 200 mCi i.a.	NR	ND	96

Malignancies of the central nervous system

Tumor type (Patients)	Antibody	Antigen (Ag)	Radionuclide, Dose, Route	Response (n)	Tumor dose (Rads)	Reference
Neuroblastoma (5)	UJ13A	Ag on neuroectodermal cells	^{131}I 35-50 mCi i.v.	NR 3, MXR 1, PR 1	1,313-2,893	97
Neuroblastoma (3)	3F8	ganglioside G_{D2}	^{131}I 100 mCi i.v.	MR 3	ND	98
Glioma (1)	9A	epidermal growth factor receptor (EGFR)	^{131}I 45 mCi i.a.	PR 1	ND	99
Glioma (10)	EGFR1	EGFR	^{131}I 40-200 mCi i.v., i.a.	NR 3, PR 6, CR 1	1,250	100
Glioma (14)	425	EGFR	^{125}I 26-130 mCi i.a.	NR 14	ND	101
Glioma (10)	BC2	tenascin	^{131}I 15 mCi i.tu.	NR 4, SD 3, PR 2, CR 1	7,000-41,000	102
Glioma (6)	ERIC-1	neural cell adhesion molecule	^{131}I 30-60 mCi i.ca.	NR 4, SD 1, MR 1	ND	103

Miscellaneous

Tumor type (Patients)	Antibody	Antigen (Ag)	Radionuclide, Dose, Route	Response (n)	Tumor dose (Rads)	Reference
Melanoma (21)	8.2 Fab 96.5 Fab 48.7	p97 p97 HMWMAA	^{131}I 137-870 mCi i.v.	NE 10, NR 8, MR 1, PR 2	3,800-8,500	104,105
Neoplastic meningitis (3)	SB10	Human chorio-gonadotropine (HCG)	^{131}I 20-50 mCi i.ventr.	NR 3[a]	ND	106
	W14	HCG				
	UJ13A	Ag on primitive neuroectodermal cells (PNEC)				
	MEL-14	high molecular weight melanoma associated antigen (HMWMAA)				

Table 2. (continued)

Tumor type (Patients)	Antibody	Antigen (Ag)	Radionuclide, Dose, Route	Response (n)	Tumor dose (Rads)	Reference
Neoplastic meningitis (15)	UJ181.4	Ag on PNEC	^{131}I 17-62 mCi l.p., i.ventr.	NE 6, NR 3, PR 6[a]	ND	107,108
	F8.11.3	leukocyt common Ag				
	MEL-14	HMWMAA				
	81C6	tenascin				
	HMFG1	HMFG				
Neoplastic meningitis (20)	UJ181.4	Ag on PNEC	^{131}I 35-62 mCi l.p., i.ventr.	NE 3, NR 7, SD 1, PR 3, CR 6[a]	ND	109,110
	M340	ND				
	UJ13A	Ag on PNEC				
	MEL-14	HMWAA				
	WCMH15.14	CD10				
	HD37	CD19				
Breast (11)	chimeric L6	ND	^{131}I 35-123 mCi i.v.	NR 5, MR 2, PR 4	ND	111
Breast (1)	2G3	330 kD GP	^{131}I 25 mCi i.p.	NR 1	ND	69

NE = not evaluable, NR = no response, MXR = mixed response, SD = stable disease, MR = minor response, PR = partial response, CR = complete response, ND = no data provided, i.v. = intravenous, i.a. = intraarterial, i.tu. = intratumoral, i.ventr. = intraventricular, i.c. = intracavitary, l.p. = lumbar puncture, [a] response rates were not specified per antibody, [b] RIT incorporated in multimodality treatment protocols including external beam irradiation and chemotherapy.

Radioisotopes for RIT

The selection of a radionuclide for RIT is based on properties like emitted radiation, e.g. the percentage of ß- and γ-emission, the energies and path lengths of these forms of emission and its physical half-life. When used for therapeutic purposes, radiation should be preferably limited to tumor tissue in order to spare normal tissue. Due to the path length of γ-emission, this type of emission is not suitable. However, a limited percentage of γ-emission does allow imaging and can thus provide information on tissue distribution, of importance for dosimetry estimations. MAbs labeled with radionuclides with α- or ß-emission can cause cell death without having to enter the cell. Especially ß-emission can kill several cells in the vicinity of the cell to which the radioimmunoconjugate has attached. This "cross-fire" effect may in part overcome the disadvantages of heterogeneous expression of the antigen to which the MAb has to bind, and of heterogenous distribution of the MAb, phenomena often observed in tumors. As has become clear from the previous paragraph, the efficacy of RIT appears to be dependent on the size of the tumor. When aiming at clinical RIT studies, the penetrating ability of ß-particles of the radionuclide to be used should be considered. It has been demonstrated that high-energy ß-emitters, such as ^{90}Y and ^{188}Re, are more effective when treating large tumors (> 1 cm in diameter), whereas radionuclides with intermediate-energy ß-emission, like ^{67}Cu, ^{131}I and ^{186}Re, would yield

higher effects when treating smaller tumors (< 1 cm in diameter) [112]. The advantage of α-emitters like [211]As and [212]Bi, is the high linear energy transfer within a short range with concomittant high toxicity. However, the short range limits the "cross-fire" effect, thus making the need for homogenous distribution for α-particles more pronounced then for β-particles. Moreover, the lack of imageable γ-emission prevents dosimetric estimations with α-emitters. [125]I is a radionuclide with potential for therapy due to the emission of highly damaging Auger-electrons. However, to exert its toxic effect, the radionuclide has to be in the direct proximity of the nucleus, which implies that the radioimmunoconjugate has to be internalized. In addition, the very long half-life of this radionuclide is a important disadvantage. In Table 3, radionuclides presently under investigation for (pre)clinical application in RIT are listed. As has become clear from the previous paragraph, up to this moment the β-emitters ^{131}I and ^{90}Y are the most widely used isotopes in clinical RIT studies (see Table 2). Advantages and disadvantages of these isotopes have been clearly documented. [131]I is easy to label and has a appropriate physical half-life (8 days), particle energy (β; E = 0.6 MeV) and path length (r_{90} = 0.83 mm, r_{90} being the range in which 90% of the energy is released) [113]. A problem with ^{131}I is the instability of the radioimmunoconjugate, both in serum and at the tumor site [114]. This problem may be solved in the near future by introduction of new labeling techniques [115,116]. Another problem is the γ-emission which represents 65% of the released energy and poses hazard to the patient and to medical personnel. [90]Y has the advantages of high particle energy (β; E_{max}, 2.2 MeV), comparatively long path length (r_{90} = 5.34 mm), and an appropriate

physical half-life (2.7 days). For binding ^{90}Y to an antibody, the chelate DTPA has been used most frequently. This antibody-chelate conjugate appeared instable, resulting in sequestering of ^{90}Y in non-target organs like spleen, liver and especially bone marrow [117]. This latter resulted in dose-limiting myelotoxicity [118]. Strategies to overcome this problem include the use of better chelators [119], EDTA to chelate free ^{90}Y in the circulation, and hematopoietic growth factors to counteract myelosuppression. Introduction of the new macrocyclic chelating agent DOTA for the generation of ^{90}Y conjugates however has come upon new difficulties. The use of this chelating agent has been reported to lead to the development of immune responses in patients [120]. In addition, imageable γ-emission, which is helpful for monitoring tumor targeting and for dosimetry estimates, is absent and thus another disadvantage of [90]Y [118]. Most recently, the conjugation of β-emitters such as [67]Cu [121], [153]Sm [122], [177]Lu [55], [186]Re [123], and [188]Re [124] has become possible, opening new avenues for effective RIT.

Wessels and Rogus have suggested that [186]Re would be an excellent isotope for RIT [47]. The half-life of [186]Re is 3.7 days. [186]Re has an ideal γ-emission for imaging. The energy (β; E_{max}, 1,07 MeV) and path length (r_{90} = 1.8 mm) make [186]Re an excellent candidate radionuclide for RIT in patients with minimal disease. Several methods for the labeling of [186]Re have been described.

Using a labeling procedure in which the chelating agent N,N,N,N,-tetrakis(2-mercaptoethyl)ethylenediamine (N_2S_4) was used to conjugate MAbs with [186]Re, Najafi et al. describe partial and complete remissions of tumors in RIT experiments after 1 or 2 injections of 500 μCi [125]. Unfortunately, no biodistribution data were avai-

Table 3. Radionuclides presently under investigation for (pre)clinical RIT studies

Radionuclide	Emission	Energy (keV)[a]	Energy frequency (%)	Half-life (hr)
Iodine-131	beta	606	89	193
	gamma	364	81	
Yttrium-90	beta	2284	100	64
Rhenium-186	beta	1077	71	91
	beta	939	21	
	gamma	137	10	
Rhenium-188	beta	2120	71	17
	beta	1965	25	
	gamma	155	15	
Copper-67	beta	390	57	61
	beta	482	22	
	beta	575	20	
	gamma	185	49	
Samarium-153	beta	632	34	47
	beta	702	44	
	beta	805	21	
	gamma	103	28	
Luthetium-177	beta	497	79	161
	beta	176	12	
	gamma	208	11	
Astatine-211	alpha	5867	42	7
	alpha[b]	7450	58	
Bismuth-212	alpha	6050	25	1
	alpha	6090	10	
	beta	2246	48	
	gamma	727	12	
Iodine-125	gamma	35	7	1440

[a] For ß-emission, an approximation of the average energy is $E_{max}/3$, [b] α-particle from ^{211}Po, to which ^{211}At decays for 58.3%.

lable to determine accumulated doses in tumor and normal tissues. A single-vial direct labeling procedure has been developed by John et al, using reduced antibody for direct conjugation of $^{186}ReO_4^-$ (rheniumperrhenate) to the antibody [126]. Fritzberg et al. succeeded to develop a specific and stable labeling of MAbs with this nuclide using the diamide-dimercaptide preformed chelate

approach [127]. This group recently demonstrated significant antitumor responses with [186]Re RIT of small cell lung carcinoma xenografts in nude mice, especially when treating small tumors [128]. Unfortunately, in these studies [186]Re-labeled MAbs were not compared with [131]I- or ^{90}Y-labeled MAbs for treatment of xenografts [129,130]. [186]Re-immunoconjugates are currently investigated in clinical trials. A good tumor targeting and general lack of retention in normal organs such as liver, spleen and bone has been observed [131]. Recently, the first results of phase I clinical trials with [186]Re-labeled MAbs have been reported [95]. However, the *in vivo* instability observed of the radioimmunoconjugates obtained with the above mentioned methods needs, in our view, further investigation. In addition, as was also stressed by Goldenberg and Griffiths [132], it remains doubtfull that when using commercially available [186]Re these methods will yield conjugates with specific activities high enough to allow patient studies. Since [186]Re can only be obtained as a carrier added radionuclide, the applicabiltity of the labeling procedure should not be restricted by the low specific activity of [186]Re.

The validity of the nude mouse model for the evaluation of radioimmunoconjugates

Most experimental studies for RIS and RIT have been conducted using human tumors xenografted into nude mice. These animals are immunodeprived due to the absence of a thymus. Thus, they allow the growth of human tumors transplanted either subcutaneously, intraperitoneally, in the gut, lung, liver or spleen or into the cerebral hemisphere. As such, the nude mouse model is widely accepted as a model for the preclinical evaluation of various anti-cancer agents [133]. However, as is the case with most *in vivo* models, there are intrinsic advantages and disadvantages to this model. The latter must most certainly be kept in mind when extrapolating experimental results to the situation in the clinic.

A first advantage is the potential of human tumor xenografts to retain original characteristics like histology, chemosensitivity and radiation sensitivity. A second advantage is the reproducibility under controlled conditions. Thirdly, a good agreement with clinical results has been observed with respect to the general normal tissue toxicity data in animals [134]. Finally, a reasonable but limited correlation with human trials, depending to the type of neoplasm, has been shown with respect to the tumor growth delay [135,136].

With respect to the limitations of the model, the first disadvantage is the absence of normal tissues expressing the human antigen to which the MAb under investigation was initially raised. In this model, these antigens can be truly regarded as tumor specific antigens. In man, in almost all cases there is at least a slight positive reaction with some normal tissues. Obviously, this will be of influence on parameters like pharmacokinetics and biodistribution of the radioimmunoconjugate. Most xenografted tumors do not show any metastasizing capacity in nude mice, thus oversimplifying the human situation. As a consequence, this lack of metastasizing potential unfortunately prevents the evaluation of RIT for the treatment of micrometastases in this model. The differences between men and mice in Fcγ-mediated functions and Fcγ-dependent antibody-induced immune responses furthermore limit the extrapolation of experimental results to the situation in the clinic. Other factors that are most likely to show differ-

ences between the experimental and clinical situation are tumor vascularity, lymphatic drainage, fibrotic reactions, encapsulation of the tumor and the presence or absence of oxygen depleted areas. These factors will most certainly be of influence on the efficiency of radiation. A final reason for discrepancies between experimental and clinical RIT is the size of the tumor compared to body weight and blood volume. The relative mass of a xenografted tumor (0.1-2.0 g) in a nude mouse (15-30 g) is in the range of 0.3-15%. In the clinical situation, the relative volume of a tumor (2-10 g) in a patient (70 kg) is in the range of 0.003-0.01%. Taking into accout that man can tolerate a higher dose of radioactivity, the absolute amount of conjugate localizing in tumors of patients is in general at least ten-fold lower than in mice. In addition, the larger blood volume in patients can lead to lower initial MAb concentrations thus reducing the turnover of MAb in the blood pool and the net uptake in the tumor. In conclusion, the model may be of use for the following studies of importance for the evaluation of RIT: (1) initial screening of a radioimmuno-conjugate, (2) comparison of different antibody types and fragments, (3) preliminary efficacy studies for target/nontarget specificity, (4) suitability of the radionuclide of choice, (5) toxicity studies, (6) comparing the efficacy of different radionuclides, and (7), basic dosimetry comparisons using animal target/ nontarget ratios extrapolated to humans.

Aim of the study

In spite of the increase in the locoregional control of head and neck squamous cell carcinoma, this has not resulted in an improved 5-year survival of patients. Due to improved surgery and radiotherapy, more patients advance to a stage in which they are exposed to the risk of developing distant metastases and "second primary" tumors. Since at present no adequate the-rapy is available for patients with distant metastases, there is a need for a more effective adjuvant systemic therapy. To achieve this long term goal, the development of MAbs with specificity for head and neck cancer for RIT was started several years ago. MAbs with this specificity were developed, and biodistribution and imaging studies with tracer amounts of ^{131}I-labeled MAb E48 IgG, K984 IgG and recently U36 have demonstrated the capacity of these MAbs for specific delivery of radioisotopes to HNSCC xenografts. At the start of this dissertation, MAb E48 was shown to be the most promising MAb available. The work presented in this thesis was aimed at further investigating the suitability of MAb E48 IgG and its F(ab')$_2$ fragment for RIT of head and neck cancer. Furthermore, studies initiated to characterize the antigen recognized by MAb E48 were continued.

With respect to the characterization of the MAb E48 defined antigen (E48 Ag), the subcellular localization of the E48 Ag was investigated by means of immunoelectron microscopy. In vitro experiments were performed to investigate the possible involvement of the E48 Ag in cell-cell adhesion (**Chapter 2**).

Based upon the tissue distribution profile of this antigen, experiments were performed to assess the biodistribution and pharmacokinetics of MAb E48 IgG and its F(ab')$_2$ fragment in nude mice bearing squamous cell carcinoma xenografts of the head and neck and of the vulva (**Chapter 3**).

Results obtained from the studies described in Chapter 3 warranted the start of a phase I trial in

patients, evaluating the safety and diagnostic accuracy of ^{99m}Tc-labeled MAb E48 IgG and its F(ab')$_2$ fragment in patients with head and neck cancer. In these studies, ^{99m}Tc-labeled MAb E48 IgG as well as its F(ab')$_2$ fragment were shown to be highly capable of detecting metastatic and recurrent disease. These observations were reason to start RIT experiments with ^{131}I in nude mice bearing relatively large head and neck squamous cell carcinoma xenografts. The efficacy or RIT in this model was compared with the efficacy of a number of clinically used conventional and experimental chemotherapeutic agents. Biodistribution experiments with therapeutic doses were performed to obtain data for dosimetric estimations (**Chapter 4**).

Because of the rapid *in vivo* dehalogenation of ^{131}I-labeled MAbs and the high percentage toxic γ-radiation it is recognized that ^{131}I is not the isotope of choice for RIT. Therefor a technical protocol for the labeling of MAbs with a more appropriate isotope, ^{186}Re, was developed (**Chapter 5**).

Subsequently, the therapeutic efficay of MAb E48, labeled with ^{186}Re according to the technical protocol described in Chapter 5, was evaluated in the nude mouse model. Biodistribution experiments were performed to investigate the biodistribution characteristics of the ^{186}Re-labeled MAb and to obtain data for dosimetric estimations (**Chapter 6**).

Finally, the biodistribution characteristics of ^{131}I-labeled MAb E48 IgG and ^{186}Re-labeled MAb E48 IgG were compared directly by simultaneous injection of the two radioimmunoconjugates. Furthermore, the therapeutic efficacy of ^{186}Re-labeled MAb E48 IgG for eradicating small tumor xenografts was investigated. The biodistribution data were used for dosimetric estimations (**Addendum**).

References

1. Leemans CR. The value of neck dissection in head and neck cancer: a therapeutic and staging procedure. Free University, *Academic thesis*, Elinkwijk, Utrecht, 1992.

2. Merino OR, Lindberg RD, Fletcher GH. An analysis of distant metastases from squamous cell cancer of the upper respiratory and digestive tracts. *Cancer* 40:145-151, 1970.

3. Jesse RH, Barkey HT, Lindberg RD, Fletcher GH. Cancer of the oral cavity: is elective neck dissection beneficial? *Am J Surg* 120:505-508, 1970.

4. Snow GB. Surgical management in the next decade. In: Fee WE, Goepfert H, Johns ME, Strong EW, Wards PH (Eds). *Head and neck cancer vol 2, Proceedings of the International Conference*, Boston Mass. 1988 Toronto: BC Dekker Inc, 17-23, 1990.

5. Schuller DE, Metch B, Mattox D, Stein DW, McCracken JD. Preoperative chemotherapy in advanced resectable head and neck cancer. Final report of the Southwest Oncology Group. *Laryngoscope* 98:1205-1211, 1988.

6. Head and Neck Contracts Program. Adjuvant chemotherapy for advanced head and neck squamous carcinoma. *Cancer* 60:301-311, 1987.

7. Vokes EE, Panje WR, Mick R, Kozloff MF, Sutton HG, Goldman MD, Tybor AG, Weichselbaum RR. A randomized study comparing two regimans of neoadjuvant and adjuvant chemotherapy in multimodal therapy for locally advanced head and neck cancer. *Cancer* 66:206-213, 1990.

8. Stell PM, Rawson NSB. Adjuvant chemotherapy in head and neck cancer. *Br J Cancer* 61:779-787, 1990.

9. Köhler G, Milstein C. Continuous cultures of fused cells secreting antibody of predefined specificity. *Nature* 256: 495-497, 1975.

10. Himmelweit B, (Ed.). The collected papers of Paul Ehrlich. Pergamon Press, Elmsford, New York, 1975.

11. Wessels BW, Harisiadis L, Carabell SC. Dosimetry and radiobiological efficacy of clinical radioimmunotherapy. *J Nucl Med* 30:827, 1989.

12. Zenner HP, Hermann IW. Monoclonal antibodies against surface antigens of laryngeal carcinoma cells. *Arch Otorhinolaryngol* 233:161-172, 1981

13. Zenner HP. Selective killing of laryngeal carcinoma cells by a monoclonal immunotoxin. *Ann Otol Rhinol Laryngol* 95:115-120, 1985.

14. Carey TE, Kimmel KA, Schwartz DR, Richter DE, Baker SR, Krause CJ. Antibodies to human squamous cell carcinoma. *Otolaryngol / Head Neck Surg* 91:482-491, 1983,

15. Kimmel KA, Carey TE, Judd WJ, McClatchey D. Monoclonal antibody (G10) to a common antigen of human squamous cell carcinoma: Binding of the antibody to the H type 2 blood group determinant. *J Natl Cancer Inst* 70:9-19, 1986.

16. Kimmel KA, Carey TE. Altered expression in squamous carcinoma cells of an orientation-restricted epithelial antigen detected by monoclonal antibody A9. *Cancer Res* 46:2614-2623, 1986.

17. Carey TE, Wolf GT, Hsu S, Poore J, Peterson K, McClatchey KD. Expression of A9 antigen and loss of blood group antigens as determinants of survival in patients with head and neck squamous carcinoma. *Otolaryngol / Head Neck Surg* 96:221-230, 1987

18. Van Waes C, Kozarsky KF, Warren AB, Kidd L, Paugh D, Liebert M, Carey TE. The A9 antigen associated with aggressive human squamous carcinoma is structurally and functionally similar to the newly defined integrin $\alpha^6\beta_4$. *Cancer Res* 1991, 51:2395-2402.

19. Boeheim K, Speak JA, Frei E, Bernal SD. SQM1 antibody defines a surface antigen in squamous carcinoma of the head and neck . *Int J Cancer*, 36:137-142, 1985.

20. Ranken R, White CF, Gottfried TG, Yonkovich, Blazek BE, Moss MS, Fee WE, Victor Liu Y-S. Reactivity of monoclonal antibody 17.13 with human squamous cell carcinoma and its application to tumor diagnosis. *Cancer Res* 47:5684-5690, 1987.

21. Ranken R, Kaplan MJ, Gottfried TG, Fee WE, Boles R, Silverman S, White C, Yonkovich S, Liu V. A monoclonal antibody to squamous cell carcinoma. *Laryngoscope* 97:657-

662, 1987.

22. Samuel J, Noujaim AA, Willans DJ, Brzezinska GS, Haines DH, Longenecker BM. A novel marker of basal (stem) cells of mammalian stratified squamous epithelia and squamous cell carcinomas. *Cancer Res* 48:2465-2470, 1989.

23. Myoken Y, Moroyama T, Miyauchi S, Takada K, Namba M. Monoclonal antibodies against human oral squamous cell carcinoma reacting with keratin proteins. *Cancer* 60:2927-2937, 1987.

24. Quak JJ. Monoclonal antibodies to squamous cell carcinomas of the head and neck. *Academic thesis*, Free University, Bariet-Ruinen, 1989.

25. Yanagawa T, Hayashi Y, Nishida T, Yoshida H, Yura Y, Azuma M, Sato M. Immunohistochemical demonstration of carcinoembryonic antigen on tissue sections from squamous cell head and neck cancer and plasma CEA levels of the patients. *Int J Oral Maxillofac Surg* 15:296-306, 1986.

26. Henzen-Logmans SC, Balm AJM, van der Waal I, Mullink H, Snow GB, Meijer CJLM. The expression of intermediate filaments and MAM-6 antigen in relation to the degree of morphological differentiation of carcinomas of the head and neck: diagnostic implications. *Otolaryngol / Head Neck Surg* 99:539-547, 1988.

27. Cowley G, Smith JA, Gusterson BA. Increased EGF receptors on squamous carcinoma cell lines. *Br J Cancer* 53:223-229, 1986.

28. Ozanne B, Schum A, Richards CS. Evidence for an increase of EGF receptors in epidermoid malignancies. In: *Cancer cells, growth factor and transformation*. Cold Spring Harbor Laboratory, NY 3, 41-49, 1985.

29. Soo KC, Ward M, Roberts KR, Keeling F, Carter RL, McGready VR, Ott RJ, Powell E, Ozanne B, Westwood JH. Radioimmunoscintigraphy of squamous carcinomas of the head and neck. *Head Neck Surg* 9:349-352, 1987.

30. Kairemo KJA, Hopsu EVM. Imaging of pharyngeal and laryngeal carcinomas with Indium-111-labeled monoclonal anti-CEA antibodies. *Laryngoscope* 100:1077-1082, 1990.

31. Kairemo KJA, Hopsu EVM. Imaging of tumours in the parotid region with Indium-111-labeled monoclonal antibody reacting with carcinoembryonic antigen. *Acta Oncologica* 29:539-543, 1990.

32. Quak JJ, Brakkee JGP, Scheper RJ, Snow GB, Balm AJM. A comparative study on the production of monoclonal antibodies to head and neck cancer. In: Wolf GT, Carey TE (Eds). *Head and Neck Oncology Research*. Kugler Publ Amsterdam, Berkley, 133-139, 1988.

33. Quak JJ, Balm AJM, Brakkee JGP, Scheper RJ, Meijer CJLM, Snow GB. Production of monoclonal antibodies to squamous cell carcinoma antigens. *Arch Otolaryngol / Head Neck Surg* 116:181-185, 1990.

34. Quak JJ, Balm AJM, van Dongen GAMS, Brakkee JGP, Scheper RJ, Snow GB, CJLM Meijer. A 22-kDa surface antigen detected by monoclonal antibody E48 is exclusively expressed in stratified and transitional epithelia. *Am J Pathol* 136:191-197, 1990.

35. Schrijvers AHGJ, Quak JJ, Uyterlinde AM, van Walsum M, Meijer CJLM, Snow GB, van Dongen GAMS. MAb U36, a novel monoclonal antibody successful in immunotargeting squamous cell carcinoma of the head and neck. Submitted.

36. Quak JJ, Schrijvers AHGJ, Brakkee JGP, Davis HD, Scheper RJ, Balm AJM, Meijer CJLM, Snow GB, van Dongen GAMS. Expression and characterization of two differentiation antigens in stratified squamous epithelia and carcinomas. *Int J Cancer* 50:507-513, 1992.

37. Takahashi H, Wilson B, Ozturk M, Motte P, Straus W, Isselbacher KJ, Wands JR. In vivo localization of human colorectal carcinoma by monoclonal antibody binding to a highly expressed cell surface antigen. *Cancer Res* 48:6573-6579, 1988.

38. Quak JJ, van Dongen GAMS, Gerretsen M, Hayashida D, Balm AJM, Brakkee JGP, Snow GB, Meijer CJLM. Production of monoclonal antibody (K931) to a squamous cell carcinoma antigen identified as the 17-1A antigen. *Hybridoma* 9:377-387, 1990.

39. Koprowski H, Steplewski Z, Mitchell K, Herlyn M, Herlyn D, Fuhrer P. Colorectal carcinoma antigens detected by

hybridoma antibodies. *Somat Cell Genet* 5:957-972, 1979.

40. Press OW, Eary JF, Badger CC, Martin PJ, Appelbaum FR, Levy R, Miller R, Brown S, Nelp WB, Krohn KA, Fisher D, DeSantes K, Porter B, Kidd P, Thomas ED, Bernstein ID. Treatment of refractory non-Hodgkin's lymphoma with radiolabeled MB-1 (anti-CD37) antibody. *J Clin Oncol* 7:1027-1038, 1989.

41. Britton KE, Buraggi GL, Bares R, Bischof-Delaloye A, Buell U, Emrich D, Granowska M. A brief guide to the pratice of radioimmunoscintigraphy and radioimmunotherapy in cancer. Report of the European Association of Nuclear Medicine Task Group on the clinical utility of radiolabeled antibodies. *Int J Biol Markers* 4:106-118, 1989.

42. Stewart JSW, Hird V, Snook D, Sullivan M, Hooker G, Courtenay-Luck N, Sivolapenko G, Griffiths M, Myers MJ, Lambert HE, Munro AJ, Epenetos AA. Intraperitoneal radioimmunotherapy for ovarian cancer: pharmacokinetics, toxicity, and efficacy of I-131 labeled monoclonal antibodies. *Int J Radiation Oncology Biol Phys* 16:405-413, 1989.

43. Order SE, Stillwagon GB, Klein JL, Leichner PK, Siegelman SS, Fishman EK, Ettinger DS, Haulk T, Kopher K, Finney K, Surdyke M, Self S, Leibel S. Iodine 131 antiferritin, a new treatment modality in hepatoma: A radiation therapy oncology group study. *J Clin Oncol* 3:1573-1582, 1985.

44. Chatal J-F, Saccavini J-C, Thedrez P, Curtet C, Kremer M, Guerreau D, Nolibe D, Fumoleau P, Guillard Y. Biodistribution of Indium-111-labeled OC125 monoclonal antibody intraperitoneally injected into patients operated on for ovarian carcinoma. *Cancer Res* 49:3087-3094, 1989.

45. Vaughan ATM, Anderson P, Dykes PW, Chapman CE, Bradwell AR. Limitations to the killing of tumours using radiolabelled antibodies. *Br J Radiol* 60:567-578, 1987.

46. Epenetos AA, Snook D, Durbin H, Johnson PM, Taylor-Papadimitriou. Limitations of radiolabeled monoclonal antibodies for localization in human neoplasms. *Cancer Res* 46:3183-3191, 1986.

47. Wessels BW, Rogus RD. Radionuclide selection and model absorbed dose calculations for radiolabeled tumor associated antibodies. *Med Phys* 11:638-645, 1984.

48. Howell RW, Rao D, Sastry KSR. Macroscopic dosimetry for radioimmunotherapy: nonuniform activity distributions in solid tumors. *Med Phys* 16:66-74, 1989.

49. Myers MJ. Dosimetry for radiolabelled antibodies - macro or micro? *Int J Cancer* 42:71s-73s, 1988.

50. Leichner PK, Klein JL, Fishman EK, Siegelmann SS, Ettinger DS, Order SE. Comparative tumor dose from ^{131}I-labeled polyclonal anti-ferritin, anti-AFP, and anti-CEA in primary liver cancers. *Cancer Drug Delivery* 1:321-328, 1984.

51. Nias AHW. Fractionated radiotherapy. In: *An introduction to radiobiology*. Chichester, England: Wiley and Sons, 256-276, 1990.

52. DeNardo SJ, DeNardo GL, O'Grady LF. Pilot studies of radioimmunotherapy of B0cell lymphoma and leukemia using ^{131}I LYM-1 monoclonal antibody. *Antib Immunoconjug Radiopharm* 1:17-33, 1988.

53. Schlom J, Molinolo A, Simpson JF, Siler K, Roselli M, Hinkle G, Houchens DP, Colcher D. Advantage of dose fractionation in monoclonal antibody-targeted radioimmunotherapy. *JNCI* 82:763-771, 1990

54. Buchsbaum DJ, Ten Haken RK, Heidorn DB, Lawrence TS, Glatfelter AA, Terry VH, Guilbault DM, Steplewski Z, Lichter AS. A comparison of ^{131}I-labeled monoclonal antibody 17-1A treatment to external beam irradiation on the growth of LS174T human colon carcinoma xenografts. *Int J Rad Oncol Biol Phys* 18:1033-1041, 1990.

55. Schlom J, Siler K, Milenic DE, Eggensperger D, Colcher D, Miller LS, Houchens D, Cheng R, Kaplan D, Goeckeler W. Monoclonal antibody-based therapy of a human tumor xenograft with a [177]Lutetium-labeled immunoconjugate. *Cancer Res* 51:2889-2896, 1991.

56. Marin LA, Smith CE, Langston MY, Quashie D, Dillehay LE. Response of glioblastoma cell lines to low dose rate irradiation. *Int J Radiat Oncol Biol Phys* 21:397-402, 1991.

57. Begent RHJ, Ledermann JA, Green AJ, Bagshawe KD, Riggs SJ, Searle F, Keep PA, Adam T, Dale RG, Glaser MG. Antibody distribution and dosimetry in patients receiving

radiolabelled antibody therapy for colorectal cancer. *Br J Cancer* 60:406-412, 1989.

58.   Riggs SJ, Green AJ, Begent RHJ, Bagshawe KD. Quantitation in ^{131}I-radioimmunotherapy using SPECT. *Int J Cancer* 42:95s-98s, 1988.

59.   Wilson CB, Snook DE, Dhokia B, Taylor CVJ, Watson IA, Lammertsma AA, Lambrecht R, Waxman J, Jones T, Epenetos AA. Quantitative measurement of monoclonal antibody distribution and blood flow using positron emission tomography and 124 Iodine in patients with breast cancer. *Int J Cancer* 47:344-347, 1991.

60.   Garg PK, Garg S, Bigner DD, Zalutsky MR. Localization of Fluorine-18-labeled Mel-14 monoclonal antibody F(ab')2 fragment in a subcutaneous xenograft model. *Cancer Res* 52:5054-5060, 1992.

61.   Larson SM, Pentlow KS, Volkow ND, Wolf AP, Finn RD, Lambrecht RM, Graham MC, Di Resta G, Bendriem B, Daghighian F, Yeh SDJ, Wang G-J, Cheung NKV. PET scanning of Iodine-124-3F9 as an approach to tumor dosimetry during treatment planning for radioimmunotherapy in a child with neuroblastoma. *J Nucl Med* 33:2020-2023, 1992.

62.   Epenetos AA, Hammersmith Hospital Oncology Group and Imperial Cancer Research Fund. Antibody-guided irradiation of malignant lesions: three cases illustrating a new method of treatment. *Lancet* ii:1441-1443, 1984.

63.   Epenetos AA, Hooker G, Krausz T, Snook D, Bodmer WF, Taylor-Papadimitriou J. Antibody-guided irradiation of malignant ascites in ovarian cancer: A new therapeutic method possessing specificity against cancer cells. *Obstet Gynecol* 68:71s-74s, 1986.

64.   Ward B, Mather S, Shepherd J, Crowther M, Hawkins L, Britton KE, Slevin ML. The treatment of intraperitoneal malignant disease with monoclonal antibody guided ^{131}I radiotherapy. *Br J Cancer* 58:658-662, 1988.

65.   Epenetos AA, Munro AJ, Stewart JSW, Rampling R, Lambert HE, McKenzie CG, Souter P, Rahemtulla A, Hooker G, Sivalopenko GB, Snook D, Courtenay-Luck N, Dhokia B, Krauk T, Bodmer WF. Antibody-guided irradiation of

advanced ovarian cancer with intraperitoneally administered radiolabeled monoclonal antibodies. *J Clin Oncol* 5:1890-1899, 1987.

66.   Crowther ME, Ward BG, Granowska M, Mather S, Britton KE, Shepherd JH, Slevin ML. Therapeutic considerations in the use of intraperitoneal radiolabelled monoclonal antibodies in ovarian carcinoma. *Nucl Med Comm* 10:149-159, 1989.

67.   Riva P, Marangolo M, Lazzari S, Agostini M, Sarti G, Moscatelli G, Franceschi G, Spinelli A, Vecchietti G. Locoregional immunotherapy of human ovarian cancer: preliminary results. *Int J Radiat Appl Instrum Part B* 16:659-666, 1989.

68.   Marks A, Buckman R, Kwok C-S, Kerr I, Shaw P, Michaels H, De Angelis C, Reed R, Reilly R, Mills G, Law J, Baumal R. Preclinical and clinical studies of radioiodinated monoclonal antibody 2G3 for therapy of intraperitoneal effusions associated with carcinoma of breast and ovary. *Antib Immunoconjug Radiopharm* 2:83-92, 1989.

69.   Buraggi GL, Grippa F, Gasparini M, Seregni E, Gavoni N, Marini A. Radioimmunotherapy of ovarian cancer with I-131 MOv18: preliminary results. *Proceedings of the 4th annual symposium on the current status and future directions of immunoconjugates: diagnostic and therapeutic applications in benign and malignant disorders*, Key Biscane, Florida, 98, 1992.

70.   Stewart JSW, Hird V, Sullivan M, Snook, Epenetos AA. Intraperitoneal radioimmunotherapy for ovarian cancer. *Br J Obstet Gynaecol* 96:529-536, 1989.

71.   Riva P, Marangolo M, Tison V, Moscatelli G, Franceschi G, Spinelli A, Rosti G, Morigi P, Riva N, Tirindelli D. Radioimmunotherapy trials in germ testicular carcinoma: a phase I study. *Int J Biol Markers* 5:188-194, 1990.

72.   Lenhard Jr RE, Order SE, Spunberg JJ, Asbell SO, Leibel SA. Isotopic immunoglobulin: A new systemic therapy for advanced Hodgkin's disease. *J Clin Oncol* 3:1296-1300, 1985.

73.   Vriesendorp HM, Herpst JM, Leichner PK, Klein JL, Order SE. Polyclonal [90]Yttrium labeled antiferritin for refractory

Hodgkin's disease. *Int J Radiation Oncology Biol Phys* 17:815-821, 1989.

74. DeNardo SJ, DeNardo GL, O'Grady LFO, Macey DJ, Mills SL, Epstein AL, Peng J-S, McGahan JP. Treatment of a patient with B cell lymphoma by I-131 LYM-1 monoclonal antibodies. *Int J Biol Markers* 2:49-53, 1987.

75. DeNardo GL, DeNardo SJ, O'Grady LFO, Levy NB, Adams GP, Mills SL. Fractionated radioimmunotherapy of B-cell malignancies with ^{131}I-Lym-1. *Cancer Res* 50:1014s-1016s, 1990.

76. Parker BA, Vassos AB, Halpern SE, Miller RA, Hupf H, Amox DG, Simoni JL, Starr RJ, Green MR, Royston I. Radioimmunotherapy of human B-cell lymphoma with ^{90}Y-conjugated antiidiotype monoclonal antibody. *Cancer Res* 50:1022s-1028s, 1990.

77. Kaminski MS, Fig LM, Zasadny KR, Koral KF, DelRosario RB, Francis IR, Hanson CA, Normolle DP, Mudgett E, Liu CP, Moon S, Scott P, Miller RA, Wahl RL. Imaging, dosimetry, and radioimmunotherapy with iodine 131-labeled anti-CD37 antibody in B-cell lymphoma. *J Clin Oncol* 10:1696-1711, 1992.

78. DeNardo SJ, DeNardo GL, O'Grady LFO, Hu E, Sytsma VM, Mills SL, Levy NB, Macey DJ, Miller CH, Epstein EL. Treatment of B cell malignancies with [131]I Lym-1 monoclonal antibodies. *Int J Cancer* supplement 3:96-101, 1988.

79. Goldenberg DM, Sharkey RM, Hall TC, Murthy S, Siegel JA, Izon DO, Swayne LC, Lake D, Hansen HJ, Pinsky CM. Radioimmunotherapy of B-cell lymphomas with ^{131}I-labeled LL2 (EPB-2) monoclonal antibody. *Antib Immunoconjug Radiopharm* 4:763-769, 1991.

80. Goldenberg DM, Horowitz JA, Sharkey RM, Hall TC, Murthy S, Goldenberg H, Lee RE, Stein R, Siegel JA, Izon DO, Burger K, Swayne LC, Belisle E, Hansen HJ, Pinsky CM. Targeting, dosimetry, and radioimmunotherapy of B-cell lymphomas with iodine-131-labeled LL2 monoclonal antibody. *J Clin Oncol* 9:548-564, 1991.

81. Czuczman MS, Divgi CR, Straus DJ, Lovett DR, Garin-Chesa P, Yeh S, Feirt N, Graham M, Leibel S, Gee TS, Myers J,

Pentlow K, Finn R, Schwartz M, Oettgen HF, Larson SM, Old LJ, Scheinberg DA. ^{131}I-labeled monoclonal antibody therapy of acute myelogenous leukemia and B cell lymphoma. *Antib Immunoconjug Radiopharm* 4:787-793, 1991.

82. Rosen ST, Zimmer AM, Goldman-Leikin R, Gordon LI, Kazikiewicz JM, Kaplan EH, Variakojis D, Marder RJ, Dykewicz MS, Piergies A, Silverstein EA, Roenigk Jr HH, Spies SM. Radioimmunodetection and radioimmunotherapy of cutaneous T cell lymphomas using an ^{131}I-labeled monoclonal antibody: An Illinois cancer council study. *J Clin Oncol* 5:562-573, 1987.

83. Rosen ST, Zimmer AM, Goldman-Leikin R, Kazikiewicz JM, Dykewicz MS, Silverstein EA, Spies SM, Kaplan EH. Progress in the treatment of cutaneous T cell lymphomas with radiolabeled monoclonal antibodies. *Int J Radiat Appl Instrum Part B* 16:667-668, 1989.

84. Zimmer AM, Rosen ST, Spies SM, Goldman-Leikin R, Kazikiewicz JM, Silverstein EA, Kaplan EH. Radioimmunotherapy of patients with cutaneous T-cell lymphoma using an iodine-131-labeled monoclonal antibody: Analysis of retreatment following plasmapheresis. *J Nucl Med* 29:174-180, 1988.

85. Schwartz MA, Lovett DR, Redner A, Divgi CR, Graham MC, Finn R, Gee TS, Andreeff M, Oettgen HF, Larson SM, Old LJ, Scheinberg DA. Leukemia cytoreduction and marrow ablation after therapy with ^{131}I-labeled monoclonal antibody M195 for acute myelogenous leukemia. *Proceedings of ASCO* 10:230, 1991.

86. Stillwagon GB, Order SE, Klein JL, Leichner PK, Leibel SA, Siegelman SS, Fishman EK, Ettinger DS, Haulk T, Kopher K, Brown SM, Finney K. Multi-modality treatment of primary nonresectable intrahepatic cholangiocarcinoma with ^{131}I anti-CEA: a radiation therapy oncology group study. *Int J Radiation Biol Phys* 13:687-695, 1987.

87. Fan Z, Tang Z, Liu K, Zhou D, Lu J, Yuan A, Zhao H. Radioiodinated anti-hepatocellular carcinoma (HCC) ferritin. *J Cancer Res Clin Oncol* 118:371-376, 1992.

88. Liu K-D, Tang Z-Y, Bao Y-M, Lu J-Z, Qian F, Yuan A-N,

Zhao H-Y. Radioimmunotherapy for hepatocellular carcinoma (HCC) using ^{131}I-anti HCC isoferritin IgG: Preliminary results of experimental and clinical studies. *Int J Radiation Oncology Biol Phys* 16:319-323, 1989.

89. Tang Z-Y, Liu K-D, Bao Y-M, Lu J-Z, Yu Y-Q, Ma Z-C, Zhou X-D, Yang R, Gan Y-H, Lin Z-Y, Fan Z, Hou Z. Radioimmunotherapy in the multimodality treatment of hepatocellular carcinoma with reference to second-look resection. *Cancer* 65:211-215, 1990.

90. Sitzmann JV, Order SE, Klein JL, Leichner PK, Fishman EK, Smith GW. Conversion by new treatment modalities of nonresectable to resectable hepatocellular cancer. *J Clin Oncol* 5:1566-1573, 1987.

91. Order SE, Vriesendorp HM, Leichner PK. A phase I study of [90]Yttrium antiferritin: dose escalation and tumor dose. *Antib Immunoconjug Radiopharm* 1:163-168, 1988.

92. Epenetos AA, Courtenay-Luck N, Dhokia B, Snook D, Hooker G, Lavender JP, Hemmingway A, Carr D, Paraharalambous M, Bosslet K. Antibody-guided irradiation of hepatic metastases using intrahepatically administered radiolabelled anti-CEA antibodies with simultaneous hepatic blood flow stasis using biodegradable starch microspheres. *Nucl Med Commun* 8:1047-1058, 1987.

93. Riva P, Marangolo M, Tison V, Armaroli L, Moscatelli G, Franceschi G, Spinelli A, Vecchietti G, Morigi P, Tassini R, Riva N, Tirindelli D. Treatment of metastatic colorectal cancer by means of specific monoclonal antibodies conjugated with iodine-131: a phase II study. *Int J Radiat Appl Instrum Part B* 18:109-119, 1991.

94. Meredith RF, Khazaeli MB, Liu T, Plott G, Wheeler RH, Russell C, Colcher D, Schlom J, Shochat D, LoBuglio AF. Dose fractionation of radiolabeled antibodies in patients with metastatic colon cancer. *J Nucl Med* 33:1648-1653, 1992.

95. Breitz HB, Weiden PL, Vanderheyden J-L, Appelbaum JW, Bjorn MJ, Fer MF, Wolf SB, Ratliff BA, Seiler CA, Foisie DC, Fisher DR, Schroff RW, Fritzberg AR, Abrams PG. Clinical experience with rhenium-186-labeled monoclonal antibodies for radioimmunotherapy: results of phase I trials. *J*

Nucl Med 33:1099-1112, 1992.

96. Montz R, Klapdor R, Rothe B, Heller M. Immunoscintigraphy and radioimmunotherapy in patients with pancreatic carcinoma. *Nuklearmedizin* 25:239-244, 1986.

97. Lashford L, Jones D, Pritchard J, Gordon I, Breatnach F, Kemshead JT. Therapeutic application of radiolabeled monoclonal antibody UJ13A in children with disseminated neuroblastoma. *NCI Monograms* 3:53-57, 1987.

98. Cheung NKV, Miraldi FD. Ganglioside G_{D_2}-specific antibodies in the diagnosis and therapy of human neuroblastoma. In: Kemshead JT (Ed). *Monoclonal antibodies in the diagnosis of childhood solid tumors*. Florida, CRC, 1987.

99. Epenetos AA, Courtenay-Luck N, Pickering D, Hooker G, Durbin H, Lavender JP, McKenzie CG. Antibody guided irradiation of brain glioma by arterial infusion of radioactive monoclonal antibody against epidermal growth factor receptor and blood group A antigen. *Br Med J* 200:1463-1466, 1985.

100. Kalofonos HP, Pawlikowska TR, Hemingway A, Courtenay-Luck N, Dhokia B, Snook D, Sivalopenko GB, Hooker GR, McKenzie CG, Lavender PJ, Thomas DGT, Epenetos AA. Antibody guided diagnosis and therapy of brain gliomas using radiolabeled monoclonal antibodies against epidermal growth factor receptor and placental alkaline phosphatase. *J Nucl Med* 30:1636-1645, 1989.

101. Brady LW, Woo DV, Markoe A, Dadparvar S, Karlsson U, Rackover M, Peyster R, Emrich J, Miyamoto C, Steplewski Z, Koprowski H. Treatment of malignant gliomas with ^{125}I labeled monoclonal antibody against epidermal growth factor receptor. *Antib Immunoconjug Radiopharm* 3:169-179, 1990.

102. Riva P, Arista A, Sturiale C, Moscatelli G, Tison V, Mariani M, Seccamani E, Lazzari S, Fagioli L, Franceschi G, Sarti G, Riva N, Natali PG, Zardi L, Scassellati GA. Treatment of intracranial human glioblastoma by direct intratumoral administration of ^{131}I-labeled anti-tenascin monoclonal antibody BC-2. *Int J Cancer* 51:7-13, 1992.

103. Papanastassiou V, Pizer BL, Coakham HB, Bullimore J, Zananiri T, Kemshead JT. Treatment of recurrent and cystic malignant gliomas by a single intracavity injection of [131]I

monoclonal antibody: feasibility, pharamacokinetics and dosimetry. *Br J Cancer* 67:144-151, 1993.

104. Carrasquillo JA, Krohn KA, Beaumier P, McGuffin RW, Brown JP, Hellström KE, Hellström I, Larson SM. Diagnosis and therapy for solid tumors with radiolabelled antibodies and immune fragments. *Cancer Treat Rep* 68:317-328, 1984.

105. Larson SM, Carrasquillo JA, Reynolds JC, Hellström I, Hellström KE, Mulshine JL, Mattis LE. Therapeutic applications of radiolabelled antibodies: current situation and prospects. *Nucl Med Biol* 13:207-213, 1986.

106. Smith DB, Mosely RP, Begent RHJ, Coakham HB, Glaser MG, Dewhurst S, Kelly A, Bagshawe KD. Quantitative distribution of ^{131}I-labelled monoclonal antibodies administered by the intra-ventricular route. *Eur J Cancer* 26:129-136, 1990.

107. Moseley RP, Davies AG, Richardson RB, Zalutsky M, Carrell S, Fabre J, Slack N, Bullimore J, Pizer B, Papanastassiou V, Kemshead JT, Coakham HB, Lashford LS. Intrathecal administration of ^{131}I radiolabelled monoclonal antibody as a treatment for neoplastic meningitis. *Br J Cancer* 62:637-642, 1990.

108. Lashford LS, Davies AG, Richardson RB, Bourne SP, Bullimore JA, Eckert H, Kemshead JT, Coakham HB. A pilot study of ^{131}I monoclonal antibodies in the therapy of leptomeningeal tumors. *Cancer* 61:857-868, 1988.

109. Pizer BL, Papanastassiou V, Moseley R, Tzanis S, Hancock JP, Kemshead JT, Coakham HB. Meningeal leukemia and medulloblastoma: preliminary experience with intrathecal radioimmunotherapy. *Antib Immunoconjug Radiopharm* 4:753-761, 1991.

110. Pizer B, Papanastassiou V, Hancock J, Cassano W, Coakham H, Kemshead J. A pilot study of monoclonal antibody targeted radiotherapy in the treatment of central nervous system leukemia in children. *Br J Haematol* 77:466-472, 1991.

111. DeNardo SJ. Treatment of breast cancer with biologically active chimeric monoclonal antibodies. *Proceedings of the 4th annual symposium on the current status and future directions of immunoconjugates: diagnostic and therapeutic applications in benign and malignant disorders*, Key Biscane, Florida, 34,

1992.

112. Reilly RM. Radioimmunotherapy of malignancies. *Clin Pharm* 10:359-375, 1991.

113. Simpkin DJ, Mackie TR. EGS4 Monte Carlo determination of the beta dose kernel in water. *Med Phys* 17:179-186, 1990.

114. Bhargava KK, Acharya SA. Labeling of monoclonal antibodies with radionuclides. *Semin Nucl Med* 19:187-192, 1989.

115. Zalutsky MR, Noska MA, Colapinto EV, Garg PK, Bigner DD. Enhanced tumor localization and in vivo stability of a monoclonal antibody radioiodinated using N-succimidyl-3-(tri-n-butylstannyl)benzoate. *Cancer Res* 49:5543-5549, 1989.

116. Wilbur DS, Hadley SW, Hylarides MD, Abrams PG, Morgan Jr AC, Reno JM, Fritzberg AR. Development of a stable radioiodinating reagent to label monoclonal antibodies for radiotherapy of cancer. *J Nucl Med* 30:216-226, 1989.

117. Vaughan ATM, Keeling A, Yankuba SCS. The production and biological distribution of yttrium-90-labeled antibodies. *Int J Appl Radiat Isot* 36:803-806, 1985.

118. Sharkey RM, Kaltovich FA, Shih LB, Fand I, Govelitz G, Goldenberg DM. Radioimmunotherapy of human colonic cancer xenografts with ^{90}Y-labeled monoclonal antibodies to carcinoembryonic antigen. *Cancer Res* 48:3270-3275, 1988.

119. Meares CF, Moi MK, Diril H, Kukis DL, McCall MJ, Deshpande SV, DeNardo SJ, Snook D, Epenetos AA. Macrocyclic chelates of radiometals for diagnosis and therapy. *Br J Cancer* 62:21-26, 1990.

120. Kosmas C, Snook D, Gooden CS, Courtenay-Luck NS, McCall MJ, Meares CF, Epenetos AA. Development of humoral immune responses against a macrocyclic chelating agent (DOTA) in cancer patients receiving radioimmunoconjugates for imaging and therapy. *Cancer Res* 52:904-911, 1992.

121. Deshpande SV, DeNardo SJ, Meares CF, McCall MJ, Adams GP, Moi MK, DeNardo GL. Copper-67 labeled monoclonal antibody Lym-1, a potential radiopharmaceutical for cancer therapy; labeling and biodistribution RAJI tumored mice. *J Nucl Med* 29:217-225, 1988.

122. Boniface GR, Izard ME, Walker KZ, McKay DR, Sorby PJ,

Turner HJ, Morris JG. Labeling of monoclonal antibodies with Samarium-153 for combined radioimmunoscintigraphy and radioimmunotherapy. *J Nucl Med* 30:683-691, 1989.

123. Goldrosen MH, Biddle WC, Pancook J, Bakshi S, Vanderheyden J-L, Fritzberg AR, Morgan Jr AC, Koon KA. Biodistribution, pharmacokinetics and imaging studies with [186]Re-labeled NR-LU-10 whole antibody in LS174T colonic tumor-bearing mice. *Cancer Res* 50:7973-7978, 1990.

124. Griffiths GL, Goldenberg DM, Knapp Jr FF, Callahan AP, Chang CH, Hansen HJ. Direct labeling of monoclonal antibodies with generator-produced rhenium-188 for radioimmunotherapy: labeling and animal biodistribution studies. *Cancer Res* 51:4594-4602, 1991.

125. Najafi A, Alauddin MM, Sosa A, Ma GQ, Chen DCP, Epstein AL, Siegel ME. The evaluation of [186]Re-labeled antibodies using N_2S_4 chelate *in vitro* and *in vivo* using tumor-bearing nude mice. *Nucl Med Biol* 19:205-212, 1992.

126. John E, Thakur ML, DeFulvio J, McDevitt MR, Damjanov I. Rhenium-186-labeled monoclonal antibodies for radioimmunotherapy: preparation and evaluation. *J Nucl Med* 34:260-267, 1993.

127. Fritzberg AR, Abrams PG, Beaumier PL, Kasina S, Morgan Jr AC, Rao TN, Sanderson JA, Srinivasan A, Wilbur D, Vanderheyden J-L. Specific and stable labeling of antibodies with technetium-99m with a diamide dithiolate chelating agent. *Proc Natl Acad Sci USA* 85:4025-4029, 1988.

128. Beaumier PL, Venkatesan P, Vanderheyden J-L, Burgua WD, Kunz LL, Fritzberg AR, Abrams PG, Morgan Jr Ac. [186]Re radioimmunotherapy of small cell lung carcinoma xenografts in nude mice. *Cancer Res* 51:676-681, 1991.

129. Klein JL, Nguyen TH, Laroque P, Kopher KAS, Williams JR, Wessels BW, Dillehay LE, Frincke J, Order SE, Leichner PK. Yttrium-90 and iodine-131 radioimmunoglobulin therapy of an experimental human hepatoma. *Cancer Res* 49:6383-6389, 1989.

130. Sharkey RM, Motta-Henessey C, Pawlyk D, Siegel JA, Goldenberg DM. Biodistribution and radiation dose estimates for yttrium- and iodine-labeled monoclonal antibody IgG and fragments in nude mice bearing human colonic tumor xenografts. *Cancer Res* 50:2330-2336, 1990.

131. Schroff RW, Weiden PL, Appelbaum J, Fer MF, Breitz H, Vanderheyden J-L, Ratliff B, Fisher D, Foisie D, Hanelin LG, Morgan Jr AC, Fritzberg AR, Abrams PG. Rhenium-186 labeled antibody in patients with cancer: report of a pilot phase I study. *Antib Immunoconjug Radiopharm* 3:99-110, 1990.

132. Goldenberg DM, Griffiths GL. Radioimmunotherapy: arming the missiles. *J Nucl Med* 33:1110-1112, 1992.

133. Boven E, Winograd B (Eds). *The nude mouse in oncology*. CRC Press, Florida, 1991.

134. Wessels BW. Current status of animal radioimmunotherapy. *Cancer Res* 50:970s-973s, 1990.

135. Rofstadt R. Human tumor xenografts in radiotherapeutic research. *Radiother Oncol* 3:35-46, 1985.

136. Moulder JE, Dutreix J, Rockwell S, Siemann DW. Applicability of animal tumor data to cancer therapy in humans. *Int J Radiat Oncol Biol Phys* 14:913-927, 1988.

Chapter 2

Evidence for a role of the monoclonal antibody E48 defined antigen in cell-cell adhesion in squamous epithelia and head and neck squamous cell carcinoma

Ad H.G.J. Schrijvers[1], Martijn Gerretsen[1], Jan M. Fritz[2],
Marijke van Walsum[1], Jasper J. Quak[1], Gordon B. Snow[1]
and Guus A.M.S. van Dongen[1].

Departments of Otolaryngology / Head and Neck Surgery[1] and Pathology[2],
Free University Hospital, Amsterdam, the Netherlands.

Summary

Monoclonal antibody (MAb) E48 recognizes a 20-22 kDa antigen expressed by human squamous and transitional epithelia and their neoplastic counterparts. Histochemical examination of these tissues revealed distinct surface labeling with MAb E48 [1]. To investigate the subcellular localization of the E48 antigen we have performed electron microscopical analysis. In cells of normal oral mucosa, the E48 antigen was expressed on the plasmalemma, particularly associated with desmosomes, suggesting involvement of the E48 antigen in intercellular adhesion. Furthermore, the level of expression of the E48 antigen appeared to be influenced by the cellular organization. In squamous cell carcinoma (SCC) cell lines grown in vitro as subconfluent monolayer cultures, the E48 antigen expression was low. However, E48 antigen expression increased when SCC cells were grown to confluency. E48 antigen expression was similarly high when SCC cell lines were cultured under conditions promoting 3-D growth either as colonies within floating collagen gels, or as xenograft in tumor bearing nude mice. Further evidence for the involvement of the E48 antigen in cell-cell adhesion was found when SCC cells were grown within collagen gels in the presence of MAb E48: no spherical colonies were formed, but cells grew out to colonies comprising of single cells. Moreover, in this culture system the percentage of SCC cells growing out to colony decreased by the presence of MAb E48. These findings indicate that the E48 antigen is involved in the structural organization of squamous tissue and might have a role in intercellular adhesion.

Introduction.

Squamous cell carcinoma (SCC) represents the major histological type of cancers arising from the head and neck (upper aero-digestive tract), lung, cervix, oesophagus and skin [2]. Identification and characterization of molecular markers is an important approach for improvement of diagnosis and therapy of SCC and for understanding the biological mechanisms in this type of cancer. Monoclonal antibodies (MAb's) can serve as molecular and functional probes to identify and characterize SCC markers.

Recently we developed a panel of MAb's with a high affinity to membrane antigens expressed on SCC cells [3,4]. One of these is MAb E48, which was found to be selectively reactive with human squamous and transitional epithelia and their neoplastic counterparts [1]. Stratified squamous epithelia of guinea pig, rat or bovine origin did not bind the MAb E48, indicating lack of interspecies cross-reactivity. MAb E48 showed reactivity with squamous cell carcinomas (SCC) of distinct sites of origin: head and neck, lung, cervix and skin. MAb E48 recognizes a 20-22 kDa polypeptide. Histochemical examination revealed distinct surface labeling with MAb E48[1]. Previous data from our laboratory [5,6] show that the E48 antigen may serve as a suitable target for diagnosis and therapy of squamous cell carcinoma. In fact, recently a phase I/II trial has been initiated to evaluate the safety and preliminary diagnostic accuracy of i.v. administered ^{99m}Tc-labeled MAb E48 F(ab')$_2$ fragments for the detection of lymph node metastases in patients with SCC of the head and neck.

Ongoing investigations concern the elucidation of the precise function of the E48 antigen and its

impact on the biological behaviour of SCC. To this end we have investigated the subcellular distribution of the E48 antigen, showing localization along the cell membrane and to a large extent on desmosomes. Furthermore, we used MAb E48, in an *in vitro* collagen gel culture system, to examine the possible involvement of the E48 antigen in intercellular adhesion.

Material and methods

MAb E48

Production and selection of MAb E48 were performed as previously described [3,4]. In short, a surgically removed metastasis of a moderately differentiated squamous cell carcinoma from the larynx (T3N1M+) was used as immunogen. After an intrasplenic booster, lymphocytes from the spleen were isolated and fused with Sp2/0 myeloma cells. Producing hybridomas were screened for lack of reactivity with blood cells and further screened for SCC specificity on tissue sections. MAb E48 (IgG$_1$) was one of the selected high affinity MAb's as revealed by Scatchard analysis ($K_a = 1.5 \times 10^{10} M^{-1}$).
MAb E48 was supplied by Centocor Inc., Leiden, The Netherlands, as a sterile, non-pyrogenic preparation.

Tissue and cell line
Human oral mucosa tissue was used for immunoelectron microscopical experiments. The SCC line UM-SCC-22B used in these studies was obtained from Dr. T.E. Carey, Ann Arbor, MI. UM-SCC-22B originates from a well-differentiated tumor of the hypopharynx [7]. Cells were routinely grown as subconfluent monolayers in culture flasks. The culture medium consisted of Dulbecco's modified Eagle's medium (DMEM) buffered with 15 mM HEPES and 16 mM NaHCO$_3$, 3% CO$_2$, pH 7.5 and supplemented with 10% foetal calf serum (FCS, Flow Laboratories, Herts, U.K.). UM-SCC-22B could also be established as xenografts in athymic nude mice. To this end, 2-5x10^6 cells were bilaterally injected subcutanously in the thoracic region of the mice [8].

Immunoelectron microscopy

Pre-embedding labeling: Unfixed oral mucosa tissue was frozen in liquid nitrogen, and cryostat-sections (10 μm thick) were prepared and mounted on poly-L-lysine (PLL, Sigma, St.Louis, MO, USA) coated glass slides. Sections were immediately fixed by a combination of 1% paraformaldehyde and 0.1% glutaraldehyde in PBS for 20 min. at 4°C. Subsequently, free aldehyde-groups were blocked with PBS + 2% BSA and sections were washed with PBS + 1% BSA and incubated overnight with undiluted supernatant of MAb E48 or control antibody JSB-1 at 4°C. The latter isotype-matched antibody is directed against the P-glycoprotein associated with multidrug resistance and not present in oral mucosa [9]. Next, sections were incubated with horseradish peroxidase conjugated rabbit anti-mouse immunoglobulins (RAM-HRP, DAKO-PATTS, Copenhagen, Denmark) for 3 hours at room temperature. After subsequent washing with PBS, 3,3'-diaminobenzidine (DAB, Sigma, St. Louis, MO, USA) in 0.1 M Tris-HCl + 0.03% H$_2$O$_2$ was added as substrate. After thorough washing with distilled water, slides were fixed in 1% OsO$_4$ in 0.1 M cacodylate buffer, pH 8.2 and further processed for electron microscopical

examination according to routine procedures.

Post-embedding labeling: Fixation, dehydration and embedding were adapted in such manner to optimize the preservation of antigenicity and ultrastructure, with special emphasis on membrane preservation. Several fixations were tested, with respect to preservation of antigenicity, using a previously described cell-ELISA system [1,4] (fixations tested were; acetone/methanol (9:1), 2% or 4% paraformaldehyde and 2% paraformaldehyde in combination with either 0.1%, 0.2% or 0.5% glutaraldehyde). Since 2% paraformaldehyde fixation was found to be optimal for the preservation of antigenicity in this system, we have used this fixation in further post-embedding experiments. Tissue processing and embedding procedures were performed essentially as described by Berryman and Rodewald [10]. Human oral mucosa was immediately fixed in 2% paraformaldehyde in PBS. After primary fixation the tissue specimens (± 2 mm^3) were washed three times with 0.1 M maleate buffer + 3.5% sucrose, pH 6.5 (further use of phosphate-ions was avoided in order to reduce the otherwise observed small granular precipitation in the final preparation) and subsequently stained *en-block*, for 2 hours at 4°C, with 2% uranylacetate in the same buffer, pH 6.0. This latter step was included in order to improve ultrastructural preservation of the cell membranes. Tissue samples were then partially dehydrated in graded series of acetone (50-80%), impregnated with several changes of LR-White® resin (Soft grade, Bio-Rad Labs., Veenendaal, NL) and polymerized for 24 hours at 50°C. Ultrathin sections (50-100 nm) were collected on formvar coated nickel grids (100 mesh) and incubated with MAb E48 in 0.1M Tris-buffered saline (TBS) for 2-4 hours at room temperature. After several washes with TBS, grids were incubated with colloidal gold (10 nm) conjugated goat anti-mouse immunoglobulins (GAM-IgG-G10, Janssen Life Science Products, Olen, Belgium). Subsequently, grids were washed with TBS and distilled water, contrasted with Reynold's lead citrate and examined with a Philips EM400 or a Zeiss EM 109.

Colony formation inhibition experiments

Collagen gels were populated as follows: UM-SCC-22B cells were harvested by trypsinization and the number of cells was determined. Cell suspensions were diluted to the desired concentration. A mixture of 0.5 ml collagen stock solution (concentration 3.5 mg/ml), 0.25 ml 0.032 N NaOH and 0.75 ml twice concentrated DMEM supplemented with 20% FCS was prepared on ice and further mixed with 0.5 ml cell suspension in DMEM supplemented with 10% FCS. This mixture was then poured in a 8 cm^2 dish (Greiner) and placed on a 37°C heating table, resulting in the formation of a gel within 1 minute. After two weeks, populated gels were fixed with 0.1% glutaraldehyde and cells were stained with Giemsa. The morphology was monitored and the number of colonies consisting of more than 20 cells was counted by phase contrast microscopy using an inverted microscope. Plating efficiency was defined as the percentage of plated cells grown out to a colony. Experimental conditions: Trypsinized cells were plated into collagen gels either immediately, or after preincubation with MAb E48 for 2 or 4 hours. Cell concentration during preincubation was 10^5 cells/ml. Antibody concentrations during preincubation were 0, 10,

25 or 100 μg/ml and remained unchanged after transfer of cells into collagen gels.

Results

Expression of the E48 antigen on SCC cells

Membrane binding of MAb E48 to viable non-fixed cells has been assessed by means of a cell-ELISA technique [1]. Four different SCC cell lines (UM-SCC-14C, UM-SCC-22A, UM-SCC-22B and A431), were found to express the antigen in this assay. However, no reactivity was seen with UM-SCC-11B, a cell line derived from a laryngeal SCC [1]. In the present study it was observed that the E48 antigen expression by UM-SCC-22B cells grown in vitro is low during the first days after plating (not shown). However, when cells were grown to confluency, groups of cells showed increased E48 antigen expression (Fig. 1a). The proportion of cells with high E48 antigen expression increased dramatically during subsequent days of culturing (Fig. 1b). Antigen expression was also high when cells were grown as colonies within floating collagen-gels (Fig. 1c), a culture system which permits an in vivo-like growth [11] of this cell type, or as xenografts in athymic nude mice (Fig. 1d). These data indicate that E48 antigen expression is influenced by spatial configuration of SCC cells.

Immunoelectron microscopy: Pre-embedding labeling with MAb E48

Immunoperoxidase labeling of oral mucosa at the ultrastructural level showed MAb E48 reactivity with desmosomal structures as well as along the cell membrane (Fig. 2a,b). No reactivity was observed when using the isotype matched control antibody JSB-1 (not shown). Since desmosomal areas are possible sites of heterogenous nucleation, and the possibility of inhomogeneous penetration of antibodies cannot be excluded, we have also developed a post-embedding procedure for the labeling of the E48 antigen. In this way more quantitative experiments on E48 expression can be performed.

Immunoelectron microscopy: Post-embedding labeling with MAb E48

Similar results were obtained using the post-embedding immunolabeling procedure. It was demonstrated even more clearly that the E48 antigen is to a large extent associated with desmosomes, desmosomal cores in particular, and is also expressed on the plasmalemma (Fig. 3a,b). Furthermore, labeling was not seen on the basement membrane nor on nuclear or cytoplasmic components.

MAb E48 used as a functional probe in collagen culture system

Since the E48 antigen is expressed on the outer cell surface and to a large extent seems to be associated with desmosomes we considered whether MAb E48 could interfere with cell-cell interaction. This was tested in vitro by growing UM-SCC-22B cells within 3D-collagen gels in the presence or absence of MAb E48. When UM-SCC-22B cells were cultured within these gels for 2 weeks it was observed that 75% of the plated cells grew out to a colony: 88% of these colonies had a spherical appearance (Fig. 4a), while 12% of the clusters consisted of dispersed single cells
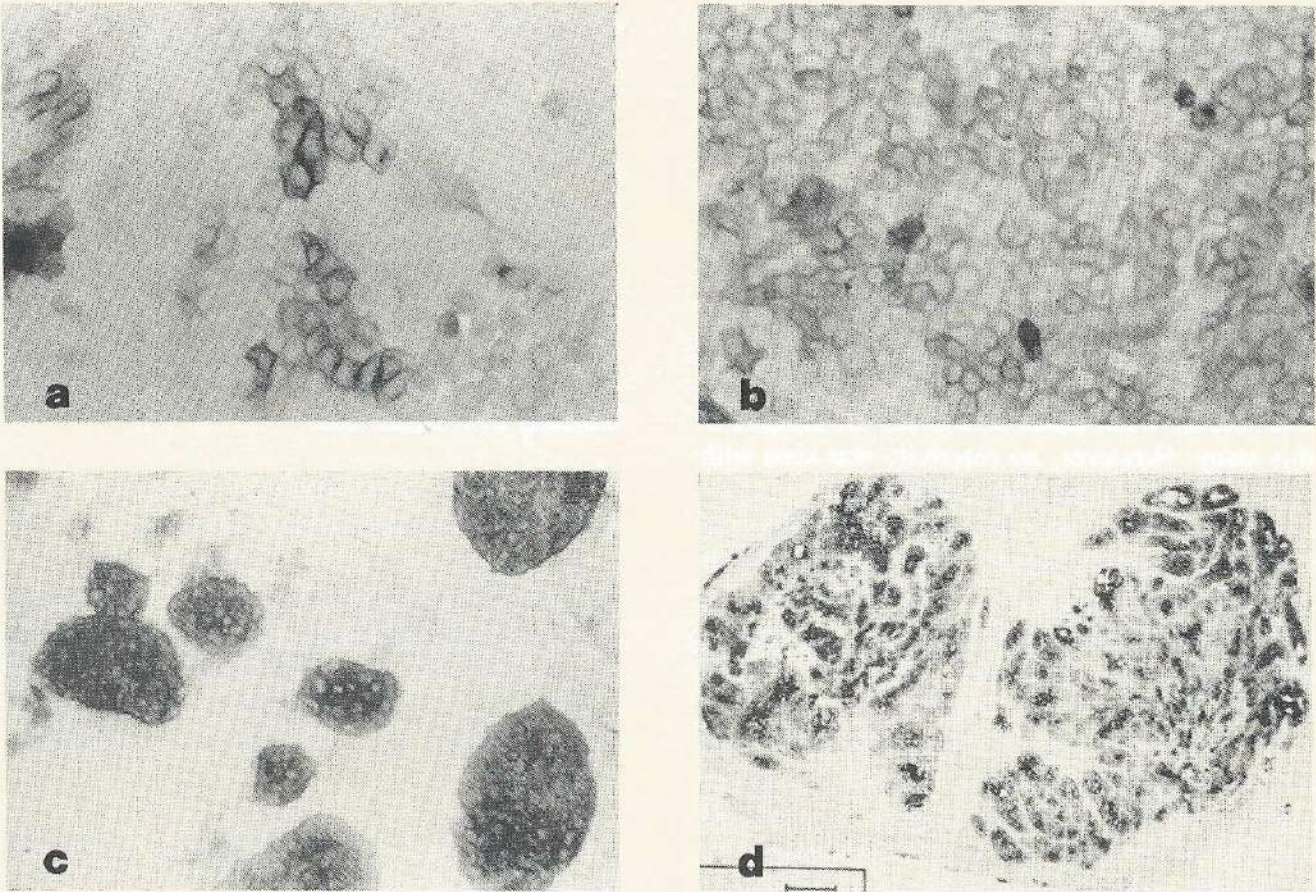
Figure 1. Indirect immunoperoxidase labeling of E48 antigen on squamous cell carcinoma (UM-SCC-22B) cells cultured in vitro as monolayers (2% paraformaldehyde fixation). (a) When cultured until confluency is reached (6-8 days after seeding) only some cells show a high E48 antigen expression. (b) After continued growth of confluent monolayers (12-14 days) the majority of cells have high E48 antigen expression. (c) When grown as spherical colonies in 3D-collagen gels all cells have a high E48 antigen expression. (d) Indirect immunoperoxidase labeling, using biotinylated MAb E48, revealed a high E48 antigen expression on UM-SCC-22B cells grown as xenografts in athymic nude mice, no labeling is observed on the mouse stroma.

(Fig. 4b). The presence of MAb E48 during culturing affected both the plating efficiency as well as the structural organization of the colonies in a concentration dependent way (Table 1). When cells were additionally preincubated with MAb E48 before being brought into the gel, the effects on colony formation were even more profound: plating efficiency decreased dramatically, while the ratio of dispersed cell-clusters versus spherical colonies increased. Under the same conditions there were no effects on growth using the isotype matched MAb K931 directed to the

17-1A antigen, which also binds to a high extent to the cell membrane of this cell line [12]. No effects on growth or colony formation were observed in this system when MAb E48 was administered after spherical colonies were already established (data not shown).

Discussion

Previous studies [1,5] indicated that MAb E48 is a high affinity antibody recognizing a membrane antigen along the cell membrane, to a large extent associated with desmosomes, and (2) the presence of MAb E48 during *in vitro* culturing of SCC was shown to prevent the formation of cell-cell contacts. Furthermore, expression of the E48 antigen was found to be increased when cells were grown under culture conditions which promote three-dimensional growth. These findings suggest that the E48 antigen serves as an adhesion molecule involved in the formation of cell-cell contacts. Hypothetically, binding of MAb E48 may disturb cellular interactions by sterically hindering the access of the E48 antigen. However, a similar hypothesis is valid when the E48 antigen is not an adhesion molecule itself, but just a molecule located closely adjacent to adhesion molecules. For this purpose the smaller monovalent E48 F(ab) fragment would have provided a more appropriate tool in the studies on colony forma-
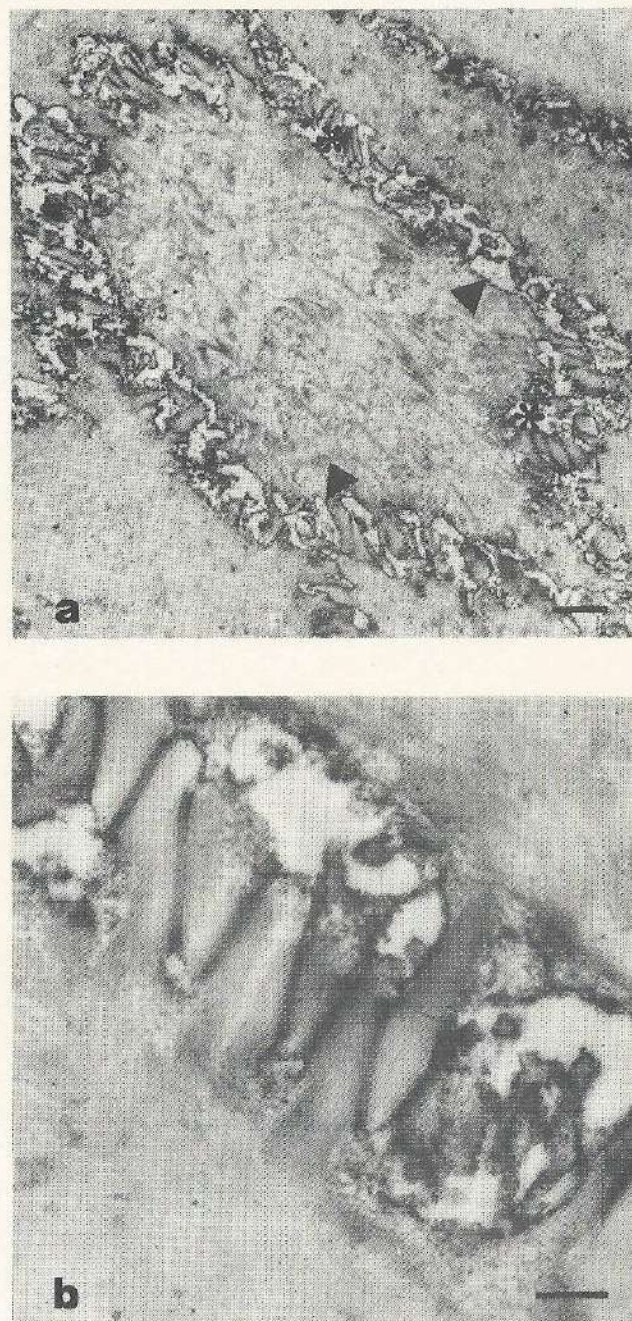
Figure 2. Ultrastructural immunolocalization of E48 antigen in human oral mucosa (1% paraformaldehyde + 0.1% glutaraldehyde fixation). (a) Preembedding labeling of MAb E48. Note continuous labeling along the cell surface (arrowhead) as well as associated with desmosomal structures (asterisk). Bar represents 1 μm. (b) High magnification detail of a desmosomal rich area, showing labeling of desmosomal cores. Bar represents 200 nm.
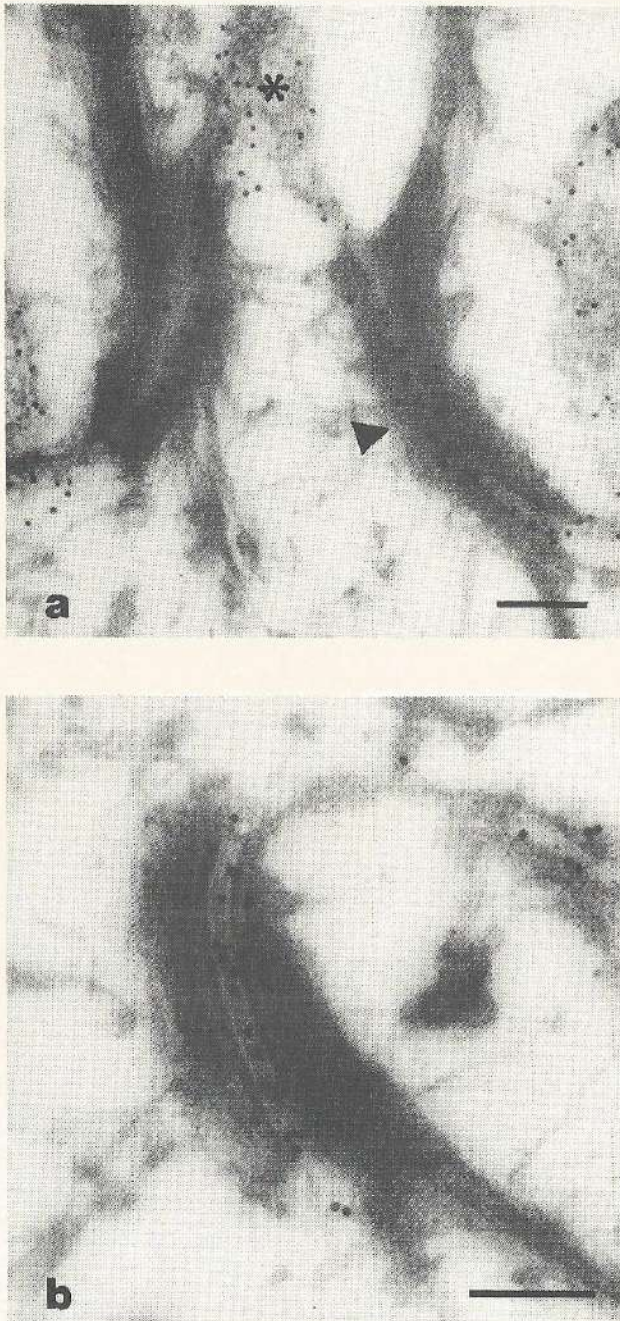
tion. Unfortunately, production of this entity
either by papain digestion of whole IgG or by
reduction of F(ab')$_2$ fragments, resulted in a
fragment without immunoreactivity.

Immunoelectron microscopical analysis indicate
that the E48 antigen is in part associated with
desmosomes (but not hemi-desmosomes) as
present in squamous epithelia. Desmosomes are
membrane specializations that anchor intermediate
filaments to the plasma membrane and link cells
together [13] and are therefore the principle junc-
tions involved in intercellular adhesion and tissue
organization [14]. Desmosomes are assembled
rapidly on the plasma membranes of adjacent
epithelial cells upon induction of cell-cell contact
[15-17]. The intercellular space between the two
desmosomal membranes is termed "midline" or
"desmoglea" and consists of electron dense
granular material, assumed to be formed by the
carbohydrate-rich portion of glycoproteins (des-
mogleins-DG), which are directly involved in
cell-cell adhesion [18,19]. Associated with the cyto-
plasmic sites of the two desmosomal membranes,
electron   dense   plaques,   the   "desmosomal
plaques", which are regions for attachment of
tonofilaments [20,21].

Biochemically, desmosomes consist of eight
major polypeptides [18,22,23]. The desmoplakins I and
II (DPI and DPII; Mr ≈ 265 kDa, 215 kDa),
plakoglobin (DPIII, Mr ≈ 82 kDa) and band 6
polypeptide (DPIV, Mr ≈ 76 kDa) are cytoplasmic
and are presumed to contribute to the membrane

Figure 3. Immunogold labeling of E48 antigen in human oral
mucosa (2% paraformaldehyde fixation). (a) Postembedding labeling
of MAb E48. Note immunogold localization along desmosomes
(arrowhead) as well as along the cell membrane (asterisk). (b)
Similar area of interest, note preferential labeling of desmosomal
cores. Bars represent 200 nm.
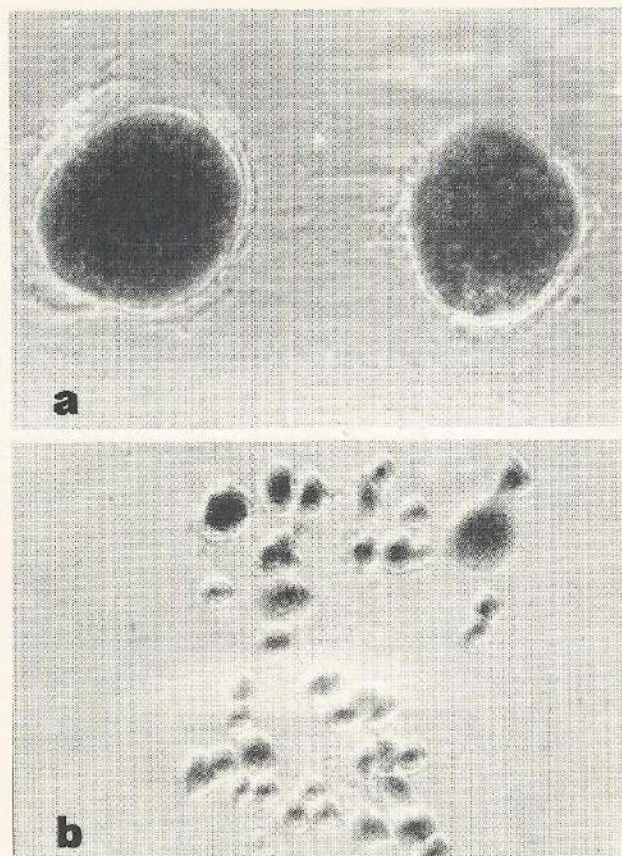
Figure 4. Effect of MAb E48 on colony formation of the squamous carcinoma cell line (UM-SCC-22B) grown in three-dimensional collagen gel. (a) The majority of plated cells formed spherical colonies under control growth conditions. (b) When grown in presence of 100 μg/ml MAb E48, the majority of cells grew out as clusters of dispersed single cells.

Table 1. Colony formation inhibition of MAb E48 on SCC cell line (UM-SCC 22B) grown in three-dimensional collagen gel.

	Plating efficiency (%)	Spherical colonies (%)	Dispersed colonies (%)
Without pretreatment[a]			
control	75	88	12
10 μg.ml⁻¹ MAb E48	74	81	19
25 μg.ml⁻¹ MAb E48	76	70	30
100 μg.ml⁻¹ MAb E48	51	18	82
2-h pretreatment[b]			
control	82	89	11
10 μg.ml⁻¹ MAb E48	80	78	11
25 μg.ml⁻¹ MAb E48	74	69	31
100 μg.ml⁻¹ MAb E48	23	0	100
4-h pretreatment[b]			
control	74	86	14
10 μg.ml⁻¹ MAb E48	74	75	25
25 μg.ml⁻¹ MAb E48	61	69	41
100 μg.ml⁻¹ MAb E48	0	0	0

Note. Values are the mean of three determinations, standard deviations were less than 10%.
Plating efficiency is the percentage of plated cells grown out to a colony.
[a] MAb E48 present from the moment the cells were brought into the gel, except for the controls which were grown in the absence of MAb E48 after plating.
[b] As a, but additionally before plating cells were preincubated with MAb E48 for the given time.

strengthening and filament binding properties [20,21,24,28]. Desmogleins I (DGI, Mr ≈ 165 kDa), desmocollins I and II (DGII and DGIII; Mr ≈ 130 kDa, 115 kDa) and a glycoprotein of Mr ≈ 22 kDa (DGIV) [18-20,25-27] are the integral membrane glycoproteins that are actively involved in cell-cell adhesion [18,19]. DGIV is believed to be a minor component of the desmoglea [20,28].

In its restricted pattern of occurrence in stratified squamous and transitional epithelia and in its localization on desmosomes, the E48 antigen resembles most closely desmoplakin II (215 kDa) [20,28] and the recently described band 6 protein (DPIV, 75 kDa) [21]. The heterogeneity in the pattern of occurrence for DGI, DGII and DGIII suggest differences of expression or glycosylation in cells of different types [28], e.g. certain epitopes of DGI are only expressed in desmosomes of stratified squamous epithelial tissues but not in desmosomes of other tissue types [29]. Moreover, the same tissue restriction has been observed for

DPIV [21]. These authors discuss that this basic protein is not an obligatory desmosomal constituent but an accessory component specific to the desmosomes of certain kinds of epithelial cells with stratified architecture, suggesting a cell-type-specific function. Interestingly, during the purification of this latter basic protein the 22 kDa glycoprotein (DGIV) has often been found to be co-purified [20,28], suggesting interaction of these molecules in squamous tissue.

The role of the 22 kDa desmosomal glycoprotein (DGIV) in intercellular adhesion is not clear. Untill now, it has not been possible to characterize this glycoprotein biochemically (personal communication Dr. W.W. Franke). It is tempting to speculate that the E48 antigen is identical to the 22 kDa desmosomal glycoprotein (DGIV).

In contrast to extensive data on immune and endothelial adhesion molecules, little information is available about epithelial adhesion molecules. Whether the E48 antigen is directly involved in organotypic intercellular adhesion is not yet known, although our *in vitro* data suggest that. To gain further insight in its molecular nature, initial experiments are performed (1) to purify the E48 antigen for chemical characterization and (2) to clone the gene coding for the E48 antigen.

References

1. Quak JJ, Balm AJM, van Dongen GAMS, Brakkee JGP, Scheper RJ, Snow GB, Meijer CJLM. A 22-kD surface antigen recognized by monoclonal antibody E48 is exclusively expressed in stratified squamous and transitional epithelia. *Am J Pathol* 136:191-197, 1990.

2. Zarbo RJ, Crissman JD. The surgical pathology of head and neck cancer. *Seminars in Oncol* 15:10-15, 1988.

3. Quak JJ, Balm AJM, Brakkee JGP, Scheper RJ, Meijer CJLM, Snow GB. Production of monoclonal antibodies to squamous cell carcinoma antigens. *Arch Otolaryngol* 116:181-185, 1990.

4. Quak JJ, Brakkee JGP, Scheper RJ, Snow GB, Balm AJM. A comparative study on the production of monoclonal antibodies to head and neck cancer. In: *Head and Neck Oncology Research*, edited by Wolf, G.T. and Carey, T.E. Amsterdam, Berkley: Kugler Publ., 1988, p. 133-139.

5. Quak JJ, Balm AJM, Brakkee JGP, Scheper RJ, Haisma HJ, Braakhuis BJM, Meijer CJLM, Snow GB. Localization and imaging of radiolabeled monoclonal antibody against squamous cell carcinoma of the head and neck in tumor bearing nude mice. *Int J Cancer* 44:534-538, 1989.

6. Gerretsen M, Quak JJ, Suh JS, van Walsum M, Meijer CJLM, Snow GB, van Dongen GAMS. Superior localisation and imaging of radiolabeled monoclonal antibody E48 F(ab')$_2$ fragment in xenografts of human squamous cell carcinoma of the head and neck and of the vulva as compared to monoclonal antibody IgG. *Br J Cancer* 63:37-44, 1991.

7. Carey TE. *Head and Neck Cancer*, New York:John Wiley and Sons, 1985. pp. 287-314.

8. Braakhuis BJM, van Dongen GAMS, Bagnay M, van Walsum M, Snow GB. Preclinical chemotherapy on human head and neck xenografts grown in athymic nude mice. *Head and Neck* 11:511-515, 1989.

9. Scheper RJ, Bulte JWM, Brakkee JGP, Quak JJ, van der Schoot E, Balm AJM, Meijer CJLM, Broxterman HJ, Kuiper CM, Lankelma J, Pinedo HM. Monoclonal antibody JSB-1 detects a highly conserved epitope on the P-glycoprotein

associated with multidrug resistance. *Int J Cancer* 42:389-394, 1988.

10. Berryman MA, Rodewald RD. An enhanced method for post-embedding immunocytochemical staining which preserves cell membranes. *J Histochem Cytochem* 38:159-170, 1990.

11. Boukamp P, Rupniak HTR, Fusenig NE. Environmental modulation of the expression of differentiation and malignancy in six human squamous cell carcinoma cell lines. *Cancer Res* 45:5582-5592, 1985.

12. Quak JJ, van Dongen GAMS, Gerretsen M, Hayashida D, Balm AJM, Brakkee JGP, Snow GB, Meijer CJLM. Production of monoclonal antibody (K931) to a squamous cell carcinoma antigen defined as the 17-1A antigen. *Hybridoma* 9:377-387, 1990.

13. Fahrquhar MG, Palade GE. Junctional complexes in various epithelia. *J Cell Biol* 17:375-412, 1963.

14. Kam E, Watt FM, Pitts JD. Patterns of junctional communication in skin: studies on cultured keratinocytes. *Exp Cell Res* 173:431-438, 1987.

15. Kelly DE, Shienvold FL. The desmosome: fine structural studies with freeze-fracture replication and tannic acid staining of sectioned epidermis. *Cell Tissue Res* 172:309-323, 1976.

16. Overton J. Development of cell junctions of the adhaerens type. *Curr Topics Dev Biol* 10:1-32, 1975.

17. Pasdar M, Nelson WJ. Kinetics of desmosome assembly in Madin-Darby canine kidney epithelial cells: temporal and spatial regulation of desmoplakin organization and stabilization upon cell-cell contact. I. biochemical analysis. *J Cell Biol* 106:677-685, 1988.

18. Gorbsky G, Steinberg MS. Isolation of the intercellular glycoproteins of desmosomes. *J Cell Biol* 90:243-248, 1981.

19. Cowin P, Mattey D, Garrod D. Identification of desmosomal surface components (desmocollins) and inhibition of desmosome formation by specific Fab'. *J Cell Science* 70:41-60, 1984.

20. Cowin P, Kapprell H-P, Franke WW. The complement of desmosomal plaque proteins in different cell types. *J Cell Biol* 101:1442-1454, 1985.

21. Kapprell H-P, Owaribe K, Franke WW. Identification of a basic protein of Mr 75,000 as an accessory desmosomal plaque protein in stratified and complex epithelia. *J Cell Biol* 106:1679-1691, 1988.

22. Skerrow CJ, Matoltsky AG. Isolation of epidermal desmosomes. *J Cell Biol* 3:515-524, 1974.

23. Franke WW, Schmid E, Grund C, Mueller H, Engelbrecht I, Moll R, Stadler J, Jarasch J-D. Antibodies to high molecular weight polypeptides of desmosomes: specific localization of a class of junctional proteins in cells and tissues. *Differentiation* 20:217-241, 1981.

24. Green K, Parry DAD, Steinert PM, Virata MLA, Wagner RM, Angst BD, Nilles LA. TITLE . *J Biol Chem* 265:2603-2612, 1990.

25. Schmelz M, Duden R, Cowin P, Franke WW. A constitutive transmembrane glycoprotein of M_r 165 000 (desmoglein) in epidermal and non-epidermal desmosomes. I. Biochemical identification of the polypeptide. *Eur J Cell Biol* 42:177-183, 1986.

26. Pasdar M, Nelson WJ. Regulation of desmosome assembly in epithelial cells: Kinetics of synthesis, transport, and stabilization of desmoglein I, a major protein of the membrane core domain. *J Cell Biol* 109:163-177, 1989.

27. Cohen SM, Gorbsky G, Steinberg MS. Immunochemical characterization of related families of glycoproteins in desmosomes. *J Biol Chem* 258:2621-2627, 1983.

28. Moll R, Cowin P, Kapprell H-P, Franke WW. Biology of disease. Desmosomal proteins: New markers for identification and classification of tumors. *Lab Invest* 54:4-25, 1985.

29. Jones JCR, Vikstrom KL, Goldman RD. Evidence for heterogeneity in the $160/165x10^3$ M_r glycoprotein components of desmosomes. *J Cell Science* 88:513-520, 1987.

Chapter 3

Superior localization and imaging of radiolabeled monoclonal antibody E48 F(ab')$_2$ fragment in xenografts of human squamous cell carcinoma of the head and neck and of the vulva as compared to monoclonal antibody E48 IgG.

Martijn Gerretsen[1], Jasper J.Quak[1], Jang S.Suh[1], Marijke van Walsum[1],
Chris J.L.M.Meijer[2], Gordon B.Snow[1]
and Guus A.M.S.van Dongen[1].

Departments of Otolaryngology / Head and Neck Surgery[1] and Pathology[2],
Free University Hospital, Amsterdam, The Netherlands.

Summary

Monoclonal antibody (MAb) E48 and its F(ab')$_2$ fragment, radiolabeled with ^{131}I, were tested for tumor localization and imaging in nude mice bearing a squamous cell carcinoma xenograft line derived from a head and neck carcinoma (HNX-HN) or from a vulva carcinoma (VX-A431). MAb IgG or F(ab')$_2$ fragments were injected in parallel and at day 1, 2, 3, and 6 or 7, mice were either scanned with a gamma camera or dissected for determination of isotope biodistribution. In HNX-HN bearing mice, E48 IgG as well as F(ab')$_2$ showed highly specific localization in tumor tissue. The mean tumor uptake (n=4) expressed as the percentage of the injected dose per gram of tumor tissue (percentage ID.g^{-1}) of IgG was 11.9% at day 1 and increased to 14.6% at day 6 whereas percentage ID.g^{-1} of F(ab')$_2$ was 7.2% at day 1 and decreased during subsequent days. Tumor to blood ratios (T/B) at day 1 were 1.2 for IgG and 13.6 for F(ab')$_2$ and reached a maximum at day 6 with values of 6.4 and 54.2 respectively. In VX-A431 bearing mice, only E48 F(ab')$_2$ showed preferential localization in tumor tissue. At day 1, percentage ID.g^{-1} of IgG was 3.7 and T/B was 0.3, while percentage ID.g^{-1} of F(ab')$_2$ was 2.4 and T/B was 3.2. percentage ID.g^{-1} decreased after day 1 while T/B increased. In these experiments no preferential localization of either isotype matched ^{125}I-labeled control IgG or F(ab')$_2$ was observed. In F(ab')$_2$ injected HNX-HN bearing mice as well as VX-A431 bearing mice, tumors could be visualized at day 1 and 2 without any appreciable. background activity. With MAb IgG this was also possible in HNX-HN bearing mice (but not in VX-A431 bearing mice) but only at day 3 and 6. These findings suggest that the superior tumor to non-tumor ratios render the E48 F(ab')$_2$ fragment more qualified for specific targeting of radioisotopes to tumor xenografts in this experimental setting.

Introduction

Of all human neoplasms, squamous cell carcinoma (SCC) is one of the most common tumor types and represents the major histological type of neoplasm arising from head and neck, cervix, skin, and lung. The relative sensitivity of head and neck SCC for radiation therapy has led us to investigate the possibility of using monoclonal antibodies (MAb's) directed against tumor associated antigens (TAA's) to specifically target radioisotopes to SCC tumors.

So far, only a limited number of MAb's to SCC have been described [1-12]. Most of these antibodies show considerable cross reactivity with normal tissues or only show reactivity with SCC of distinct sites of origin. Among the few MAb's reacting with SCC originating from various organs are MAb 17.13 [10], an IgM isotype antibody and thus less suited for in vivo immunolocalization studies ; MAb 174H.64 [11], reacting with a cytoskeletal protein, which possibly contains extracellulair domains, and MAb 3F8E3 [12], which is a low affinity antibody.

We have developed a MAb designated E48, raised against a SCC of the larynx, which shows strong and selective reactivity to squamous epithelia and their neoplastic derivatives of various tissue sites [13]. Recently, we described the capacity of MAb E48 IgG for highly specific delivery of radioisotopes in nude mice carrying human head and neck SCC xenografts [14]. How-

ever, F(ab')$_2$ fragments have been demonstrated to have better tumor to non-tumor ratios in nude mice bearing xenografts due to a more rapid clearance from the blood [15-18]. These superior tumor to non-tumor ratios resulted in much lower background levels and improved tumor images.

In this investigation, we have compared the characteristics of E48 IgG and E48 F(ab')$_2$ fragment with regard to biodistribution and imaging in nude mice bearing SCC xenografts. Two xenograft lines, the head and neck SCC xenograft line HNX-HN and the vulva SCC xenograft line VX-A431, were selected from a panel of xenograft lines based on the E48 antigen expression. These tumors represent the heterogeneity of the E48 immunohistochemical reaction pattern as observed in 92 human tumors and 8 SCC xenograft lines available at our laboratory. Immunohistochemical examination of E48 expression in the HNX-HN line revealed strong homogenous membrane bound expression and to a lesser extent cytoplasmatic expression while the E48 expression pattern in the VX-A431 line was shown to be moderate and diffuse.

Material and methods

MAb IgG and F(ab')$_2$ fragments

MAb E48 (IgG1) detects a 22 kDa surface antigen which, in normal tissues, is exclusively expressed in stratified squamous epithelia and transitional epithelia [13]. So far tested, MAb E48 reacted with 91 out of 93 SCC of head and neck, lung, cervix and skin, while out of 42 non-SCC tumors, 40 showed no binding. The isotype-matched control antibody JSB-1, directed against the P-glycoprotein related to multidrug resistance and not reactive with the xenografts in our study, has been described in detail elsewhere [19]. Hybridomas were grown either in tissue culture or as ascites in BALB/c mice. To purify the antibodies, the ascites was filtered through a 0.22 μm filter and loaded on a protein A column (Pharmacia, Uppsala Sweden). Eluted fractions were tested for immunoreactivity and dialysed against 0.9% sodium chloride. Protein concentration was determined in the BioRad (Richmond, Ca) micro assay procedure.

Purified MAb E48 and JSB-1 were digested with 4% (w/w) pepsin (Pierce) for 18 hours at 37°C temperature in 25 mM sodium acetate buffer (pH 4.0). The reaction was terminated by addition of 2 M Tris to bring the pH at 8.0. After extensive dialysis versus 0.9% sodium chloride, the F(ab')$_2$ fragments were further purified by Protein A Sepharose column chromatography followed by elution with 300 mM sodium chloride in 20 mM phosphate buffer (pH 7.4), over a Sephacryl S-200 column (Pharmacia). After dialysis versus 0.9% sodium chloride and concentrating of the protein preparation, the protein concentration was determined. Purity of MAb and F(ab')$_2$ preparations was evaluated by SDS polyacrylamide gel electrophoresis under non-reducing conditions and appeared to be more than 95%.

Nude mice xenografts

Female nude mice (NMRI, 25-32 g Harlan Olac CPB, Zeist, the Netherlands) were 8-10 weeks old at the time of the experiments. The head and neck SCC xenograft line HNX-HN was established by subcutaneous implantation of tumor

fragments measuring 3x3x1 mm, in the lateral thoracic region on both sides of nude mice. The head and neck xenograft line was established from a T4N2 squamous cell carcinoma of the base of the tongue from a 54-year-old female patient. The vulva xenograft line VX-A431 was established by injecting in vitro cultured A431 cells subcutaneously. The A431 cell line was kindly provided by Dr.B. Defize, Hubrecht laboratorium Utrecht, the Netherlands. Both xenograft lines were maintained by serial s.c. transplantation.

Radioiodination

Iodination of IgG and F(ab')$_2$ fragments was performed essentially as described by Haisma et al.[20]. 500 μg of IgG or F(ab')$_2$ fragment was mixed with 1 mCi ^{125}I or ^{131}I and specific activity of the conjugate was determined. After removing excess unbound iodine, percentage of incorporated radioactivity was determined.

MAb IgG and F(ab')$_2$ in vitro binding assays

The binding characteristics of radiolabeled MAb E48 and E48 F(ab')$_2$ were analyzed by immunoreactivity and affinity assays. The immunoreactivity assay was performed essentially as described by Lindmo et al.[21]. In short, A431 cells were fixed in 0.1% glutaraldehyde and six serial dilutions, ranging from 5 x 10^6 cells per tube to 3.1 x 10^5 cells per tube, were made with 1% bovine serum albumin (BSA) in PBS. To the tubes, 10,000 cpm of the labeled MAb or F(ab')$_2$ fragment were added and incubated overnight at room temperature. To the last sample, excess unlabeled MAb or F(ab')$_2$ fragment was added to

determine non-specific binding. Cells were spun down and radioactivity in the pellet and supernatant was determined in a gamma counter and the percentage bound and free radiolabeled MAb was calculated (LKB-Wallac 1218 Compu-Gamma). Data were graphically analyzed in a modified Lineweaver Burk plot and the immunoreactive fraction was determined by linear extrapolation to conditions representing infinite antigen excess.

The affinity assay was performed essentially as described by Badger et al.[22]. In short, 5 x 10^6 fixed A431 cells in PBS containing 1% BSA were incubated overnight at room temperature with 5000 cpm of the labeled MAb or F(ab')$_2$ fragment and a serial dilution of unlabeled MAb or F(ab')$_2$ fragment. The concentration of the unlabeled MAb or F(ab')$_2$ fragment was chosen several times higher and several times lower than the concentration of labeled MAb or F(ab')$_2$ as calculated from the specific activity. Cells were spun down and radioactivity in the pellet and supernatant was determined in a gamma counter. Data were graphically analyzed by Scatchard analysis and affinity constant and number of antigenic sites per cell was determined. Both the immunoreactivity assay and the affinity assay were performed in triplo.

Biodistribution

In vivo tissue distribution was studied in nude mice bearing human squamous cell carcinoma xenografts of the head and neck (HNX-HN) or of the vulva (VX-A431), following i.v. administration of 10 μCi [131]I E48 IgG and 10 μCi ^{125}I JSB-1 IgG or 10 μCi [131]I E48 F(ab')$_2$ fragment and 10 μCi ^{125}I JSB-1 F(ab')$_2$ fragment. Mice

were bled, killed and dissected 1,2,3 and 6 days after i.v. injection (HNX-HN mice) or 1,2,3 and 7 days after i.v. injection (VX-A431 mice). For each day, 3 or 4 mice were used. Organs were immediately removed, placed in 5 ml plastic tubes and weighed. Samples were taken from blood, urine, tumor, liver, spleen, kidney, heart, stomach, jejunum, colon, bladder, sternum, muscle, lung, skin and tongue. After weighing, all organs and tumors were counted in a dual isotope gamma counter. The antibody uptake in the tumor and other tissues was calculated as the percentage of the injected dose per gram of tissue (percentage ID.g^{-1}). The specific localization index (SLI) was calculated by dividing the uptake of the specific MAb or F(ab')$_2$ fragment (E48) by the uptake of the non-specific MAb or F(ab')$_2$ fragment (JSB-1) into the tumor.

Radioimmunoscintigraphy

Mice were killed by cervical dislocation and placed under the camera. Two mice were scanned simultaneously with an Ohio gamma camera (Sigma 410 S); 100,000 cpm were obtained and data were stored in a computer (PDP 1134 computer system) for further analysis and production of colour images.

Immunohistochemistry

Expression of the E48 antigen in the xenografts was assessed on frozen tissue sections by the biotin-avidin peroxidase technique. Therefore, the E48 MAb was labeled with biotin. Biotin-N-hydroxysuccimide in DMF was added to a solution of protein-A purified antibody in 0.1 M bicarbonate buffer (pH 8.5) in a ratio of 1:10

(w/w). After mixing, the solution was gently stirred at room temperature for 1 hour and finally dialysed against several changes of PBS. After incubating frozen sections with biotinylated MAb, the sections were washed three times with PBS and incubated with a preformed biotin-avidin peroxidase complex (Vectastain ABC kit, Vector, Burkingame, CA). The peroxidase label was developed with diaminobenzidinetetrahydrochloride (DAB, Sigma) plus H$_2$O$_2$.

Results

Immunohistochemistry

The expression of the E48 antigen in the xenograft lines HNX-HN and VX-A431 was assessed by the biotin-avidin peroxidase technique. Frozen xenograft sections were incubated with protein-A purified biotinylated E48 and JSB-1. E48 showed strong membrane and to a lesser extent cytoplasmatic staining on frozen sections of the HNX-HN xenograft (fig.1). On sections of the VX-A431 xenograft E48 showed a moderate and diffuse binding pattern (fig.2). No reactivity was observed with JSB-1 with either xenograft.

Radiolabeling of MAb and F(ab')$_2$ fragments

In the experiment with HNX-HN mice as well as VX-A431 mice, labeling of 500 μg E48 IgG with 1 mCi ^{131}I resulted in a specific activity of 0.82 μCi/μg. Labeling of 500 μg E48 F(ab')$_2$ fragment with 1 mCi ^{131}I resulted in a specific activity of 0.68 μCi/μg in case of the experiment with HNX-HN, while labeling of 290 μg E48 F(ab')$_2$ fragment with 1 mCi ^{131}I resulted in a
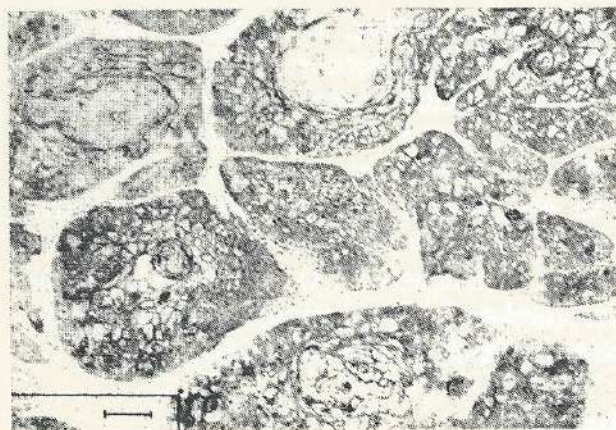
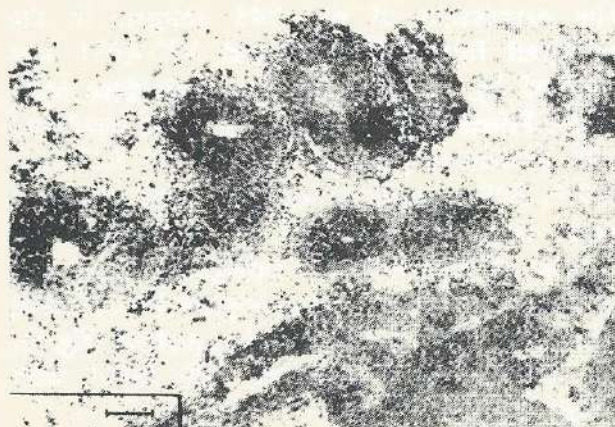Fig. 1. Section of xenograft HNX-HN, stained with biotinylated MAb E48 by indirect immunoperoxidase method.

Fig. 2. Section of xenograft VX-A431, stained with biotinylated MAb E48 by indirect immunoperoxidase method.

specific activity of 1.13 μCi/μg in case of the experiment with VX-A431. Labeling of 500 μg control MAb JSB-1 IgG or control JSB-1 F(ab')$_2$ fragment with 1 mCi ^{125}I resulted in specific activities of 0.81 μCi/μg and 0.75 μCi/μg, respectively. More than 98% of the iodine was bound, as revealed by TCA precipitation.

In vitro immunoreactivity and affinity assays

As determined by the modified Lineweaver-Burke plot, the immunoreactive fractions of E48 IgG and E48 F(ab')$_2$ fragments at infinite antigen excess were > 0.95 in all experiments. The affi-
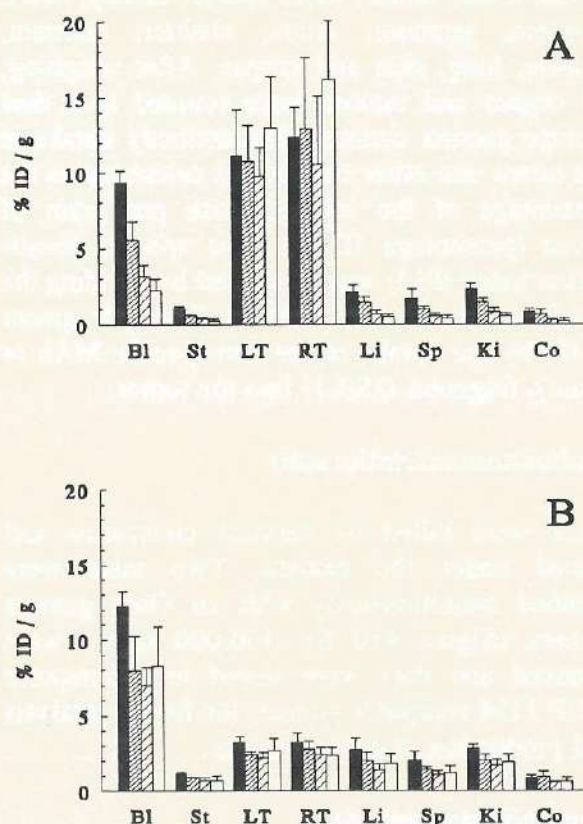
Fig.3. Biodistribution data for (A) 10 μCi ^{131}I-labeled E48 IgG and (B) 10 μCi ^{125}I-labeled JSB-1 IgG in athymic mice bearing HNX-HN xenografts. At 1 (black), 2 (thick hatched), 3 (thin hatched) and 6 (open) days following i.v. injection tissues were dissected and counted and the percentage injected dose per gram (percentage ID.g^{-1}) was calculated. Each day 3-4 mice were dissected Bl=blood; St=sternum; LT=left tumor; RT=right tumor; Li=liver; Sp=spleen; Ki=kidney; Co=colon.

Fig. 4. Biodistribution data for (A) 10 μCi ^{131}I-labeled E48 F(ab')$_2$ and (B) 10 μCi ^{125}I-labeled JSB-1 F(ab')$_2$ in athymic mice bearing HNX-HN xenografts. At 1 (black), 2 (thick hatched), 3 (thin hatched) and 6 (open) days following i.v. injection tissues were dissected and counted and the percentage injected dose per gram (percentage ID.g^{-1}) was calculated. Each day 3-4 mice were dissected. Bl=blood; St=sternum; LT=left tumor; RT=right tumor; Li=liver; Sp=spleen; Ki=kidney; Co=colon.

nity constants were 1.5 x 10^{10} M^{-1} for E48 IgG and 1.2 x 10^{10} M^{-1} for E48 F(ab')$_2$ fragment as determined by the Scatchard plot. A431 cells expressed 3.3 x 10^4 binding sites/cell. Binding of control IgG and F(ab')$_2$ fragment to A431 cells was <2% of the input doses.

Pharmacokinetics of MAb and F(ab')$_2$ fragments

At day 1,2,3 and 6 (HNX-HN) or 1,2,3 and 7 (VX-A431), serum samples were collected to determine free iodine. Less than 5% free iodine was present as revealed by TCA precipitation. At day 1 after injecting the labeled MAb IgG and F(ab')$_2$, 9.32 to 11.66% ID.g^{-1} E48 IgG and 12.11 to 12.21% ID.g^{-1} JSB-1 IgG was present in the blood, whereas 0.53 to 0.74% ID.g^{-1} E48 F(ab')$_2$ fragment and 0.83 to 1.30% ID.g^{-1} JSB-1 F(ab')$_2$ was present in the blood, indicating a much faster clearance of F(ab')$_2$ fragments from the blood as as compared to whole IgG.

Biodistribution

Tumor uptake of E48 IgG and F(ab')$_2$ fragment in HNX-HN bearing mice:
The amount of ^{131}I-E48 IgG and ^{131}I-E48 F(ab')$_2$ fragment in the xenografts and various organs, expressed as the average percentage of radioactivity of the injected dose per gram of tissue (percentage ID.g^{-1}), is shown in Fig. 3A and Fig. 4A. Table IA and IB show the tumor to tissue ratios of E48 IgG and E48 F(ab')$_2$ fragment as well as of control IgG and control F(ab')$_2$, calculated by dividing the percentage ID.g^{-1} of tumor tissue by the percentage ID.g^{-1} of various non-tumor tissues. At day 1,2,3 and 6, the percentage ID.g^{-1} in tumors of ^{131}I E48 IgG injected mice was 11.9 (mean tumor weight ± standard error of the mean (mtw ± sem): 352.6 ± 207.5), 11.9 (mtw ± sem: 487.3 ± 238.0), 10.2 (mtw ± sem: 398,6 ± 181.8) and 14.6 (mtw ± sem: 326.8 ± 268.4) respectively (Fig.3A), whereas percentage ID.g^{-1} in tumors of

Table Ia Tumor to tissue ratio of E48 and JSB-1 IgG in HNX-HN bearing mice

Tumor to tissue ratio of E48 IgG

	Day 1	Day 2	Day 3	Day 6
Blood	1.2±0.4	2.1±0.3	3.3±1.0	6.4±2.4
Sternum	11.7±4.1	17.2±6.2	28.5±9.9	68.3±38.8
Liver	5.7±3.3	7.8±2.4	16.0±6.6	26.0±9.2
Spleen	7.9±4.1	10.0±2.2	20.5±10.1	40.7±22.0
Kidney	4.9±1.8	7.2±2.1	13.0±5.2	25.8±10.0
Colon	15.9±5.4	15.2±6.0	36.5±15.2	72.3±39.7

Tumor to tissue ratio of JSB-1 IgG

	Day 1	Day 2	Day 3	Day 6
Blood	0.3±0.1	0.4±0.1	0.9±0.5	0.3±0.1
Sternum	2.8±0.3	3.0±0.3	7.5±7.1	3.4±0.6
Liver	1.3±0.5	1.4±0.4	4.1±4.0	1.5±0.4
Spleen	1.7±0.5	1.8±0.1	4.7±3.7	2.3±0.4
Kidney	1.1±0.1	1.3±0.2	3.3±3.0	1.4±0.3
Colon	3.8±0.2	3.2±1.1	9.9±9.2	4.6±1.0

Table Ib Tumor to tissue ratio of E48 and JSB-1 F(ab')$_2$ in HNX-HN bearing mice

Tumor to tissue ratio of E48 F(ab')$_2$

	Day 1	Day 2	Day 3	Day 6
Blood	13.6±5.0	29.4±6.8	49.4±22.2	54.2±8.9
Sternum	71.4±36.8	231.1±68.8	329.4±115.1	172.5±46.2
Liver	32.5±16.0	93.8±13.9	134.8±51.2	141.2±16.5
Spleen	33.8±16.6	105.6±20.6	143.2±59.1	176.2±34.2
Kidney	15.3±7.7	60.4±8.1	76.9±25.9	93.8±4.9
Colon	82.9±40.0	220.6±62.7	297.0±104.3	225.1±50.3

Tumor to tissue ratio of JSB-1 F(ab')$_2$

	Day 1	Day 2	Day 3	Day 6
Blood	0.5±0.1	0.6±0.1	1.1±0.4	0.5±0.1
Sternum	4.2±0.8	5.7±0.4	7.9±2.8	4.3±0.8
Liver	1.9±0.6	2.8±0.8	3.3±1.4	1.4±0.8
Spleen	1.9±0.4	3.1±0.4	3.9±1.6	2.9±0.4
Kidney	0.7±0.3	2.0±0.6	2.6±1.4	1.8±0.2
Colon	5.3±1.3	6.8±1.5	9.5±3.4	6.9±0.4

Table IIa Specific localization index of E48 IgG in HNX-HN bearing mice

Day 1	Day 2	Day 3	Day 6
3.65	4.52	4.35	5.79

Table IIb Specific localization index of E48 F(ab')$_2$ in HNX-HN bearing mice

Day 1	Day 2	Day 3	Day 6
9.03	6.66	18.45	28.40

^{131}I E48 F(ab')$_2$ injected mice decreased after day 7.2 (mtw ± sem: 277.4 ± 185.3) to 4.4 (mtw ± sem: 368.5 ± 256.2) at day 2, 3.7 (mtw ± sem: 510.8 ± 316.5) at day 3 and 2.0 (mtw ± sem: 336.7 ± 203.0) at day 6 (fig.4A). To exclude the possibility that uptake might be due to non-specific protein trapping, an isotype matched antibody and its F(ab')$_2$ fragment were included as a control. The control IgG and control F(ab')$_2$ did not show any specific accumulation, neither in the tumors nor in any organ (Fig. 3B and 4B). Table IIA and IIB show the specific localization index (SLI) of E48 IgG and E48 F(ab')$_2$ fragment, calculated by dividing the percentage ID.g^{-1} of speific IgG or F(ab')$_2$ fragment (E48) in the tumor by the percentage ID.g^{-1} of control IgG or F(ab')$_2$ frag-ment (JSB-1). In the course of the experiment, SLI of E48 IgG did not change significantly (3.7 at day 1 to 5.8 at day 6), whereas SLI of E48 F(ab')$_2$ fragment reached a maximum of 28.4 at day 6.

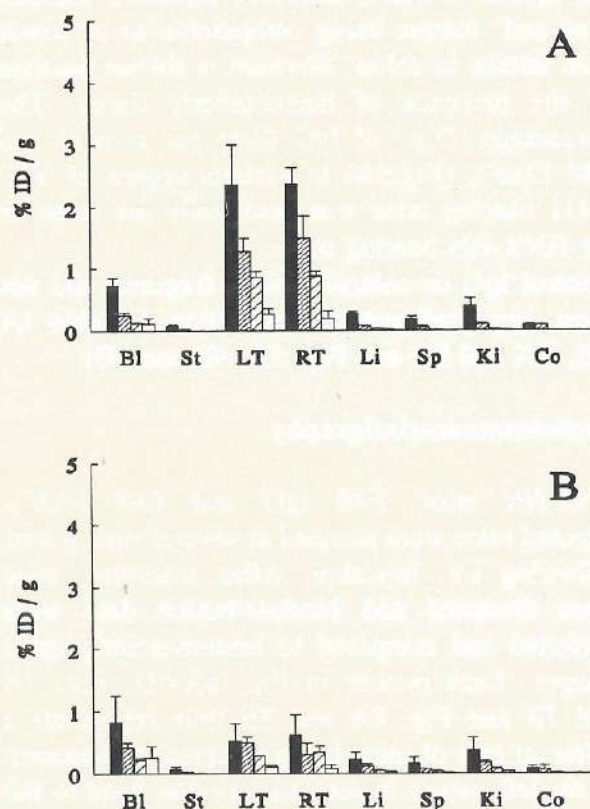*Tumor uptake of E48 IgG and E48 F(ab')$_2$ fragment in VX-A431 bearing mice:*
The percentage ID.g^{-1} of ^{131}I-E48 IgG and ^{131}I-

Fig. 5. Biodistribution data for (A) 10 μCi ^{131}I-labeled E48 F(ab')$_2$ and (B) 10 μCi ^{125}I-labeled JSB-1 F(ab')$_2$ in athymic mice bearing VX-A431 xenografts. At 1 (black), 2 (thick hatched), 3 (thin hatched) and 7 (open) days following i.v. injection tissues were dissected and counted and the percentage injected dose per gram (percentage ID.g^{-1}) was calculated. Each day 3-4 mice were dissected. Bl=blood; LT=left tumor; RT=right tumor; Li=liver; Sp=spleen; Ki=kidney; Co=colon.

E48 F(ab')$_2$ fragment in xenografts and various organs was determined as above. Table IIIA and IIIB show the tumor to tissue ratios of E48 IgG and E48 F(ab')$_2$ fragment. At day 1,2,3 and 7, the percentage ID.g^{-1} in tumors of E48 IgG injected mice was 3.7 (mtw ± sem: 370.3 ±

Table IIIa   Tumor to tissue ratio of E48 and JSB-1 IgG in VX-A431 bearing mice

| | Tumor to tissue ratio of E48 IgG | | | |
	Day 1	Day 2	Day 3	Day 6
Blood	0.3±0.1	0.3±0.1	0.6±0.1	1.5±0.6
Sternum	3.3±0.9	3.6±0.8	5.9±0.8	12.2±4.0
Liver	1.3±0.3	1.5±0.5	2.2±0.4	6.6±2.5
Spleen	1.8±0.4	1.9±0.3	3.0±0.3	10.0±4.6
Kidney	1.3±0.1	1.4±0.3	2.1±0.5	6.5±4.1
Colon	4.0±0.4	4.2±1.3	6.3±1.1	15.6±7.0

| | Tumor to tissue ratio of JSB-1 IgG | | | |
	Day 1	Day 2	Day 3	Day 6
Blood	0.4±0.3	0.3±0.1	0.4±0.1	0.7±0.2
Sternum	4.6±3.9	3.7±0.7	4.9±1.0	6.5±1.1
Liver	1.7±1.1	1.5±0.2	1.8±0.5	3.7±0.9
Spleen	2.5±2.2	1.9±0.3	2.3±0.3	5.5±1.9
Kidney	1.9±1.5	1.3±0.1	1.7±0.5	3.5±1.2
Colon	5.2±3.8	4.9±1.1	5.3±1.2	9.0±2.8

Table IIIb   Tumor to tissue ratio of E48 and JSB-1 F(ab')$_2$ in VX-A431 bearing mice

| | Tumor to tissue ratio of E48 F(ab')$_2$ | | | |
	Day 1	Day 2	Day 3	Day 6
Blood	3.2±0.4	5.7±2.0	7.3±0.6	3.5±3.0
Sternum	28.9±3.7	51.1±16.5	72.7±15.2	39.1±23.8
Liver	8.8±1.7	16.8±6.1	24.7±2.2	12.9±9.9
Spleen	12.7±1.6	25.3±5.2	38.9±5.8	17.2±8.7
Kidney	6.4±1.6	13.5±5.0	20.4±2.4	11.6±6.9
Colon	25.7±4.9	43.4±24.2	75.2±11.6	42.6±20.3

| | Tumor to tissue ratio of JSB-1 F(ab')$_2$ | | | |
	Day 1	Day 2	Day 3	Day 6
Blood	0.7±0.1	1.1±0.2	1.5±0.4	0.6±0.4
Sternum	8.7±1.6	12.3±2.4	17.1±5.3	6.5±3.6
Liver	2.5±0.2	4.2±0.9	6.2±1.3	2.8±1.8
Spleen	3.4±0.3	5.9±1.2	8.8±2.7	3.5±1.4
Kidney	1.5±0.4	2.6±0.5	4.0±0.9	2.1±0.9
Colon	7.8±2.2	10.8±5.5	19.7±6.9	6.7±3.5

Table IVa	Specific localization index of E48 IgG in VX-A431 bearing mice		
Day 1	Day 2	Day 3	Day 7
1.71	1.14	1.20	1.03

Table IVb	Specific localization index of E48 IgG in VX-A431 bearing mice		
Day 1	Day 2	Day 3	Day 7
4.10	3.48	2.84	2.30

247.2), 3.3 (mtw ± sem: 525.3 ± 237.5), 3.5 (mtw ± sem: 409.3 ± 142.9) and 3.0 (mtw ± sem: 356.3 ± 248.1), respectively (data not shown), whereas percentage ID.g^{-1} in E48 F(-ab')$_2$ injected mice decreased steadily after day 1, from 2.4 (mtw ± sem: 640.4 ± 573.6) to 1.4 (mtw ± sem: 621.2 ± 05.6), 0.9 (mtw ± sem: 274.6 ± 145.9) and 0.2 (mtw ± sem: 290.8 ± 135.0), respectively (Fig.5A). Table IVA and IVB show the SLI of E48 IgG and E48 F(ab')$_2$ fragment. E48 IgG did not show a pronounced specific localization in the tumor xenografts, as reflected by the low SLI of E48 IgG (Table IVA). E48 F(ab')$_2$ however did show appreciable specific localization (Table IVB), with SLI being 4.1 at its maximum at day 1. The control IgG (data not shown) and control F(ab')$_2$ (Fig.5B) did not show any specific accumulation in the tumors nor in any organ.

Uptake in other organs:
The percentage ID.g^{-1} of E48 IgG and E48 F(-ab')$_2$ fragment in various organs of HNX-HN bearing mice is presented in Fig. 3A and Fig. 4A. Only the most relevant organs are shown,

the uptake in heart, stomach, jejunum, muscle, lung and tongue being comparable to or lower than uptake in colon. Sternum is shown because of the presence of haemopoietic tissue. The percentage ID.g^{-1} of IgG (data not shown) and E48 F(ab')$_2$ (Fig.5A) in various organs of VX-A431 bearing mice was essentially the same as for HNX-HN bearing mice.
Control IgG or control F(ab')$_2$ fragment did not show any preferential localization (Table IA ,IB, IIA and IIB and Fig. 3B, 4B and 5B).

Radioimmunoscintigraphy

HNX-HN mice. E48 IgG and E48 F(ab')$_2$ injected mice were scanned at several time points following i.v. injection. After scanning, mice were dissected and biodistribution data were collected and compared to immunoscintigraphic images. Each picture in Fig. 6A-6D, Fig. 7A and 7B and Fig. 8A and 8B thus represents a different pair of mice being scanned. Orientation of the left mouse in each picture was head to tail from top to bottom, orientation of the right mouse was tail to head from top to bottom. Fig. 6A represents two mice, scanned 1 day after injection of 10 μCi ^{131}I-labeled E48 IgG per mouse. The percentage ID.g^{-1} of the xenografts was 10.13, 8.69, 11.87 and 10.49 from left to right respectively. High blood pool activity, most prominent in the thoracic cavity, hampered distinction of xenografts on day 1 (Fig.6A) as well as day 2 (Fig.6B). This background activity only markedly decreased 2 days after injection, after which timepoint xenografts could be visualized without appreciable background disturbance (Fig.6C, Fig.6D). Fig. 7A and 7B represent mice being scanned 1 day and 2 days after injec-
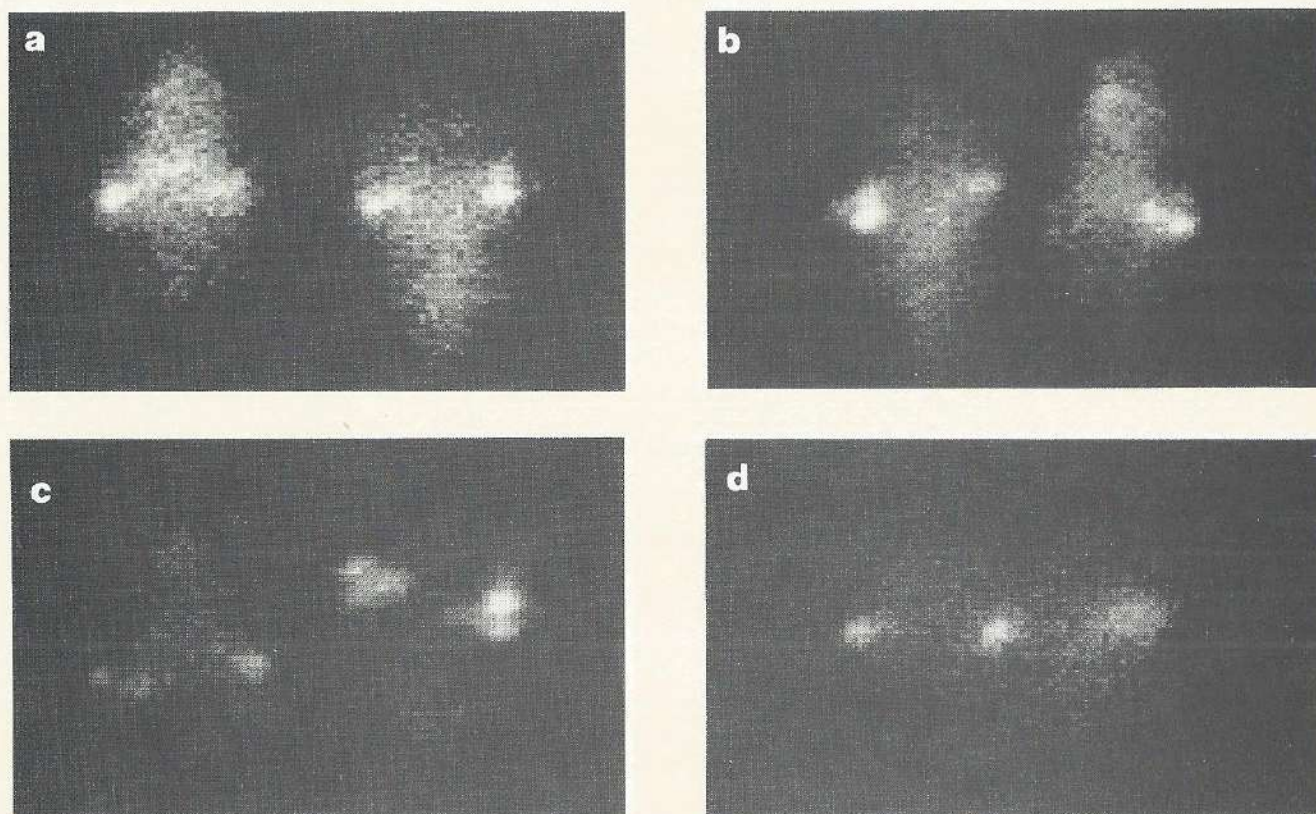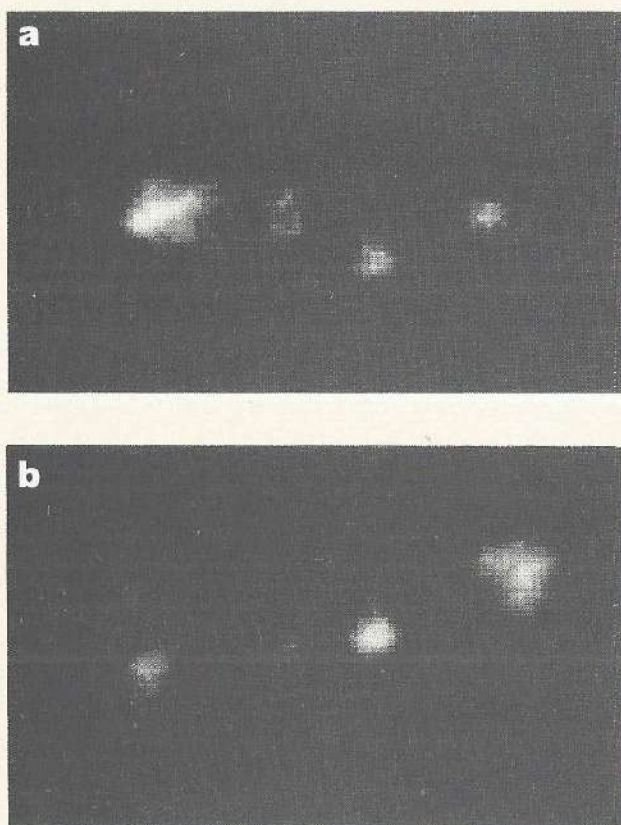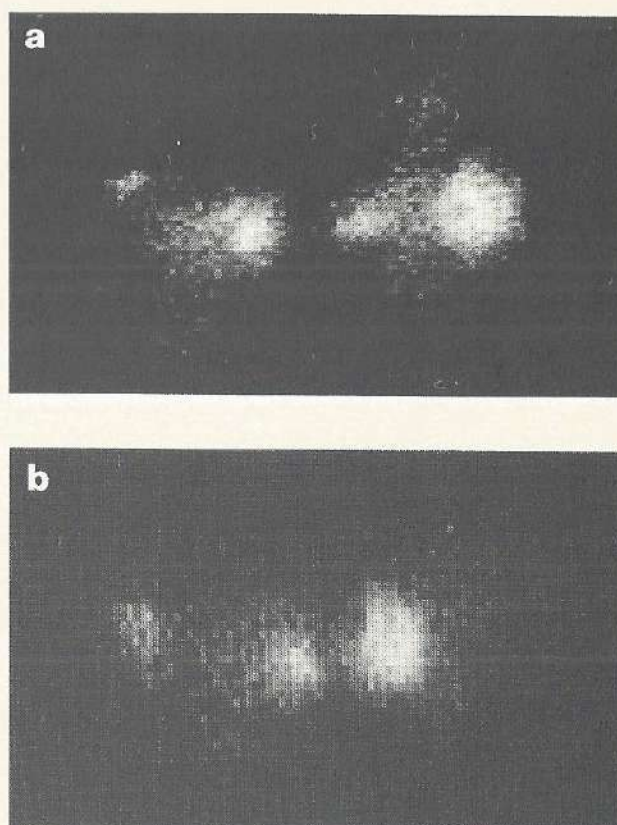
Fig. 6. Whole body scintigraphic images of pairs of athymic mice each bearing one or two subcutaneous HNX-HN xenografts given an injection of 10 μCi ^{131}I-E48 IgG. Images were taken at day 1 (A), day 2 (B), day 3 (C) and day 6 (D). Weight of xenografts in mg from left to right: A: 577, 575, 463, 464; B: 772, 211, 148, 341; C: 297, 472, 255, 694; D: 252, 379, NX , 766 (NX = no xenograft present)

tion of 10 μCi ^{131}I labeled E48 F(ab')$_2$ fragment per mouse. The percentage ID.g^{-1} at day 1 was of 6.09, 6.12, 8.28 and 9.03 from left to right, respectively (Fig.7A), and at day 2 the percentage ID.g^{-1} was 4.28, 6.11, 3.24 and 2.89 from left to right, respectively (Fig.7B). No background activity could be detected, resulting in images showing only xenograft localization of radioisotope.

VX-A431 mice. Images of mice injected with 10 μCi ^{131}I-labeled E48 IgG did not result in identi-fication of xenografts at any timepoint after injection, due to consistent high blood pool activity (images not shown). Images of mice injected with 10 μCi ^{131}I-labeled E48 F(ab')$_2$ however, 1 day (Fig. 8A) and 2 days (Fig. 8B) after injection, did show xenografts depicted without significant background disturbance. The percentage ID.g^{-1} at day 1 was 2.41, 1.72, 2.16 and 2.08 from left to right, respectively (fig.8A) and at day 2 the percentage ID.g^{-1} was 1.06, 1.11 and 1.03, respectively (Fig.8B).

Fig. 7. Whole body scintigraphic images of pairs of athymic mice each bearing one or two subcutaneous HNX-HN xenografts given an injection of 10 μCi ^{131}I-E48 F(ab')$_2$. Images were taken at day 1(A) and day 2(B). Weight of xenografts in mg from left to right: A: 314, 294, 205, 705; B: 895, 353, 585, 167.

Fig. 8. Whole body scintigraphic images of pairs of athymic mice each bearing one or two subcutaneous VX-A431 xenografts given an injection of 10 μCi ^{131}I-E48 F(ab')$_2$. Images were taken at day 1(A) and day 2(B). Weight of xenografts in mg from left to right: A: 283, 1399, 442, 1810; B: 862, 698, 1677, NX.

Discussion

Conjugates of radioisotopes and immunoglobulins or their fragments are attractive agents for tumor diagnosis and therapy. However, fragments are cleared more rapidly from the blood than whole IgG [15-18], resulting in lower background activity and reducing the radiation dose

to normal tissues. Moreover, fragments lack the Fc region responsible for nonspecific tissue uptake by Fc receptor binding and may be less immunogenic in humans [23]. Finally, the smaller size of fragments should allow better tumor penetration than whole IgG. Although these phenomena hold true for both Fab and F(ab')$_2$, reports dealing with studies on tumor uptake of

whole IgG, F(ab')$_2$ and Fab often show a strong decrease in tumor uptake of F(ab')$_2$ and Fab when compared to whole IgG and a strong decrease in tumor to normal tissue ratios of Fab when compared to F(ab')$_2$, most likely the result of increased clearance from the blood and a decreased affinity inherent in the generation of univalent Fab fragments [16-18,24]. In this investigation we compared the characteristics of E48 IgG and E48 F(ab')$_2$ with regard to biodistribution and imaging parameters in nude mice bearing SCC xenografts. In a previous study we reported the production of MAb E48 recognizing a 22 kDa antigen exclusively expressed in stratified squamous epithelia and transitional epithelium of the bladder [13,25]. In neoplastic tissues, reactivity with MAb E48 is restricted to squamous cell carcinoma of head and neck, lung, cervix and skin and to urinary bladder carcinoma. Reactivity was observed mainly on the membrane and to a lesser extent within the cytoplasm. Based on immunohistochemical examination, two xenograft lines were selected from 8 SCC lines available at our laboratory. The head and neck xenograft line SCC HNX-HN revealed strong and homogenous membrane binding of the antibody and showed a well organized tumor structure with separated tumor nests in well developed stroma, representing a pattern displayed by the majority of human tumors investigated so far. The vulva SCC xenograft line VX-A431 revealed a moderate and diffuse binding pattern of the antibody and displayed a much less organized tumor tissue structure. These two tumors represent the extremes of immunohistochemical reaction patterns as observed in 92 human HNSCC tumors immunohistochemically stained with MAb E48. In a previous study, we already

demonstrated the capacity of E48 IgG for specific delivery of radioisotopes to tumors in nude mice bearing a SCC xenograft line [14,25]. In nude mice bearing the HNX-HN xenograft line, the use of the F(ab')$_2$ fragment of E48 strongly improved tumor uptake ratios and localization specificity when compared directly with IgG. Although the digestion of IgG for the generation of F(ab')$_2$ did not significantly alter the affinity of the radiolabeled conjugate, F(ab')$_2$ did show a decrease in the percentage ID.g^{-1} tumor tissue as compared to IgG. Differences in pharmacokinetics of the conjugates are likely to be the major factors leading to this decrease. However, the improved tumor uptake ratios and specificity of localization resulted in images without background disturbance at day 1 for F(ab')$_2$, whereas IgG did not give comparable images until day 3. In nude mice bearing the xenograft line VX-A431, E48 IgG uptake in tumors did not differ from control IgG, thus failing to reach tumor to non tumor ratios enabling visualization of tumor xenografts at any time point. E48 F(ab')$_2$ fragments however did show specific localization in tumor tissue, and although the percentage ID.g^{-1} was almost one third of the percentage ID.g^{-1} of E48 F(ab')$_2$ in HNX-HN bearing mice and the SLI of F(ab')$_2$ in VX-A431 bearing mice was less than half the SLI of F(ab')$_2$ in HNX-HN bearing mice, tumors could still be well visualized at day 1. These differences in percentage ID.g^{-1} and specificity of localization between the HNX-HN and VX-A431 xenograft lines might be due to such variables as vascularization, blood vessel morphology and permeability, tumor microcirculation, necrosis, composition of extracellular matrix and intratumoral hydrostatic pressure, parameters likely to be of considerable

influence on the efficacy of non-surgical modalities [26-31]. Additionally, differences in number and exposition of antigenic sites cannot be ruled out to be a major factor in causing the differences in localization of the radiolabeled conjugates between the two xenograft lines. A lower number of exposed antigenic sites per cell in the VX-A431 xenograft line as compared to the HNX-HN xenograft line combined with the higher penetration capacities of the smaller E48 F(ab')$_2$ fragment as compared to E48 IgG might very well explain the inability of E48 IgG to specifically localize in the VX-A431 xenograft line. In this perspective, the differences in localization characteristics between the HNX-HN and the VX-A431 xenograft lines might reflect the heterogeneity of expression and accessibility of antigenic sites in human tumors in the clinical situation.

In normal tissues, neither E48 IgG nor E48 F(ab')$_2$ showed any non specific accumulation in vital organs, including the radiation sensitive reticuloendothelial system (liver, spleen and bone marrow). The overall tumor to non-tumor ratios of F(ab')$_2$ however were several times higher than tumor to non-tumor ratios of IgG. Tumor to non-tumor ratios of F(ab')$_2$ in VX-A431 bearing mice were still higher than tumor to non-tumor ratios of IgG in HNX-HN bearing mice.

Sofar, only a limited number of MAb's reacting with human squamous cell carcinoma have been described. Most of these antibodies show considerable cross reactivity with other tissues or only show reactivity with SCC of distinct sites of tissue origin. Additionally, features of these antibodies as isotype, cytoplasmatic localization of the antigen and relatively low affinity of the antibody render them less suited for in vivo localization studies or application in a clinical setting.

Within the limitations of our experiments, we have shown the E48 F(ab')$_2$ fragment to be a promising candidate for immunodiagnostic application in a clinical setting. Preparations for a phase I / II clinical study are currently in progress.

References

1. Carey TE, Kimmel KA, Schwartz DR, Richter DE, Baker SR, Krause CJ. Antibodies to human squamous cell carcinoma. *Otolaryngol Head Neck Surg* 91:482-491, 1983.

2. Zenner HP, Hermann IW. Monoclonal antibodies against surface antigens of laryngeal carcinoma cells. *Arch Otorhinolaryngol* 233:161-172, 1981.

3. Boeheim K, Speak JA, Frei E, Bernal SD. SQM1 antibody defines a surface membrane antigen in squamous carcinoma of the head and neck. *Int J Cancer* 36:137-142, 1985.

4. Kimmel KA, Carey TE. Altered expression in squamous carcinoma cells of an orientation restricted epithelial antigen detected by monoclonal antibody A9. *Cancer Res* 46:3614-3623, 1986.

5. Fernsten PD, Pekny KW, Reisfeld RA, Walker LE. Antigens associated with human squamous cell lung carcinoma defined by murine mononclonal antibodies. *Cancer* 46:2970-2977, 1986.

6. Koprowska I, Zipfel S, Ross AH, Herlyn M. Development of monoclonal antibodies that recognize antigens associated with human cervical carcinoma. *Acta Cytol* 30:207-213, 1986.

7. Brenner BG, Jothy S, Shuster J, Fuks A. Monoclonal antibodies to human lung tumor antigens demonstrated by immunofluorescence and immunoprecipitation. *Cancer Res* 42:3187-3192, 1982.

8. Kyoizumi S, Akiyama M, Kouno N, Kobuke K, Hakoda M, Jones SL, Yamakido M. Monoclonal antibodies to human squamous cell carcinoma of the lung and their application to tumor diagnosis. *Cancer Res* 45:3274-3281, 1985.

9. Myoken Y, Moroyama T, Miyauchi S, Takada K, Namba M. Monoclonal antibodies against human oral squamous cell carcinoma reacting with keratin proteins. *Cancer* 60:2927-2937, 1987.

10. Ranken R, White CF, Gottfried TG, Yonkovich SJ, Blazek BE, Moss MS, Fee Jr WE, Liu YS. Reactivity of monoclonal antibody 17.13 with human squamous cell carcinoma and its application to tumor diagnosis. *Cancer Res* 47:5684-5690, 1987.

11. Samuel J, Noujaim AA, Willans DJ, Brzezinska GS, Haines DM, Longenecker BM. A novel marker for basal (stem) cells of mammalian stratified squamous epithelia and squamous cell carcinomas. *Cancer Res* 49:2465-2470, 1989.

12. Tatake RJ, Amin KM, Maniar HS, Jambhekar NA, Srikhande SS, Gangal SG. Monoclonal antibody against human squamous-cell-carcinoma-associated antigen. *Int J Cancer* 44:840-845, 1989.

13. Quak JJ, Balm AJM, van Dongen GAMS, Brakkee JGP, Scheper RJ, Snow GB, Meijer CJLM. A 22-kd surface antigen detected by monoclonal antibody E 48 is exclusively expressed in stratified squamous and transitional epithelia. *Am J Pathol* 136:191-197, 1990.

14. Quak JJ, Balm AJM, Brakkee JGP, Scheper RJ, Haisma HJ, Braakhuis BJM, Meijer CJLM, Snow GB. Localization and imaging of radiolabeled monoclonal antibody against squamous-cell carcinoma of the head and neck in tumor-bearing nude mice. *Int J Cancer* 44:534-538, 1989.

15. Pervez S, Paganelli G, Epenetos AA, Mooi WJ, Evans DJ, Krausz T. Localization of monoclonal antibody AUA1 and its F(ab')₂ fragment in human tumor xenografts: an autoradiographic and immunohistochemical study. *Int J Cancer* 3:30s-33s, 1988.

16. Colapinto EV, Humphrey PA, Zalutsky MR, Groothuis DR, Friedman HS, de Tribolet N, Carrel S, Bigner DD. Comparative localization of murine monoclonal antibody MEL-14 F(ab')2 fragment and whole IgG2a in human glioma xenografts. *Cancer Res* 48:5701-5707, 1988.

17. Buchegger F, Mach JP, Leonnard P, Carrel S. Selective tumor localization of radiolabeled anti-human melanoma monoclonal antibody fragment demonstrated in the nude mouse model. *Cancer* 58:655-662, 1986.

18. Endo K, Kamma H, Ogata T. Radiolabeled monoclonal antibody 15 and its fragment for localization and imaging of xenografts of human lung cancer. *J Natl Cancer Inst* 80:835-840, 1988.

19. Scheper RJ, Bulte JWM, Brakkee JGP, Quak JJ, van der

Schoot E, Balm AJM, Meijer CJLM, Broxterman HJ, Kuiper CM, Lankelma J, Pinedo H. Monoclonal antibody JSB-1 detects a highly conserved epitope on the P-glycoprotein associated with multidrug resistance. *Int J Cancer* 42:389-394, 1988.

20. Haisma HJ, Hilgers J, Zurawski Jr VR. Iodination of monoclonal antibodies for diagnosis and radiotherapy using a convenient one vial method. *J Nucl Med* 27:1890-1895, 1986.

21. Lindmo T, Boven E, Luttita F, Fedorko J, Bunn Jr PA. Determination of the immunoreactive fraction of radiolabeled monoclonal antibodies by linear extrapolation to binding at infinite antigen excess. *J Immunol Methods* 72:77-89, 1984.

22. Badger CC, Krohn KA, Bernstein ID. In vitro measurement of avidity of radioiodinated antibodies. *Int J Rad Appl Instrum* 14:605-610, 1987.

23. Smith TW, Lloyd BL, Spicer N, Haber E. Immunogenicity and kinetics of distribution and elimination of sheep digoxin-specific IgG and Fab fragments in the rabbit and baboon. *Clin Exp Immunol* 36:384-396, 1979.

24. Wahl RL, Parker CW, Philpott GW. Improved radioimaging and tumor localization with monoclonal F(ab')₂. *J Nucl Med* 24:316-325, 1983.

25. Quak JJ, Gerretsen M, Schrijvers AHGJ, Meijer CJLM, van Dongen GAMS, Snow GB. Detection of squamous cell carcinoma xenografts in nude mice by radiolabeled monoclonal antibody E48. *Arch Otolaryngol Head and Neck Surg* 117:1287-1291, 1991.

26. Sands H, Jones PL, Shah SA, Palme D, Vessella RL, Gallagher BM. Correlation of vascular permeability and blood flow with monoclonal antibody uptake by human Clouser and renal cell xenografts. *Cancer Res* 48:188-193, 1988.

27. Cobb LM. Intratumour factors influencing the access of antibody to tumour cells. *Cancer Immunol Immunother* 28:235-240, 1989.

28. Kallinowski F, Schlenger KH, Runkel S, Kloes M, Stohrer M, Okunieff P, Vaupel P. Blood flow, metabolism, cellular environment, and growth rate of human tumor xenografts. *Cancer Res* 49:3759-3764, 1989.

29. Jain RK, Wie J. Dynamics of drug transport in solid tumours: distributed parameter model. *J Bioeng* 1:3-10, 1977.

30. Sweet MB, Thonar EJ, Berson SD, Skikne MI, Immelman AR, Kerr WA. Biochemical studies of the matrix of craniovertebral chordoma and a metastasis. *Cancer* 44:652-660, 1979.

31. Hori K, Suzuki M, Saito AI. Increased tumour pressure in association with the growth rate of rat tumors. *Jpn J Cancer Res* 77:65-68, 1986.

Radioimmunotherapy of human head and neck squamous cell carcinoma xenografts with ^{131}I-labeled monoclonal antibody E48 IgG

Martijn Gerretsen[1], Ad H.G.J. Schrijvers[1], Marijke van Walsum[1],
Boudewijn J.M. Braakhuis[1], Jasper J. Quak,
Chris J.L.M. Meijer[2], Gordon B. Snow[1]
and Guus A.M.S. van Dongen[1].

Departments of Otolaryngology / Head and Neck Surgery[1] and Pathology[2],
Free University Hospital, Amsterdam, the Netherlands.

Summary

Monoclonal antibody (MAb) E48 reacts with a 22 kD antigen exclusively expressed in squamous and transitional epithelia and their neoplastic counterparts. Radiolabeled with ^{99m}Tc, MAb E48 is capable of targeting metastatic and recurrent disease in patients with head and neck cancer. In this study, the capacity of ^{131}I-labeled MAb E48 to eradicate xenografts of human squamous cell carcinoma of the head and neck (HNSCC) in nude mice was examined. Experimental groups received a single i.v. bolus injection of 400 μCi MAb E48 IgG (number of mice (n)=6, number of tumors (t)=9) or 800 μCi MAb E48 IgG (n=5, t=7), whereas control groups received either diluent (n=3, t=5), unlabeled MAb E48 IgG (n=4, t=5) or 800 μCi ^{131}I-labeled isotype-matched control MAb (n=6, t=9). A 4.1-fold increase in the median tumor volume doubling time and regression of 2 out of 10 tumors (20%) was observed in mice treated with 400 μCi. In mice treated with 800 μCi, 2 out of 7 tumors (29%) showed complete remission without regrowth during follow-up (>3 months). Median tumor volume doubling time in the remaining 5 tumors was increased 7.8-fold. No antitumor effects were observed in mice injected with diluent, unlabeled MAb E48 or ^{131}I-labeled control MAb. In the same xenograft model, chemotherapy with doxorubicin, 5-fluorouracil, cisplatin, bleomycin, methotrexate or 2'2'-difluorodeoxycytidine yielded a less profound effect on tumor volume doubling time. Increases in tumor volume doubling time with these chemotherapeutic agents were 4, 2.2, 2.1, 1.7, 0, and 2.6 respectively. Moreover, no cures were observed with any of these chemotherapeutic agents. From the tissue distribution of 800 μCi MAb E48, the absorbed cumulative radiation doses of tumor and various organs were calculated using the trapezoid integration method for the area under the curve. To tumor xenografts, 12,170 cGy was delivered, blood received 2,984 cGy, whereas in every other tissue the accumulated dose was less than 6% of the dose delivered to tumor. These data, describing the first radio-labeled MAb with therapeutic efficacy against HNSCC, suggest radioimmunotherapy with MAb E48 to be a potential therapeutic modality for the treatment of head and neck cancer.

Introduction

Despite an increase in the locoregional control of head and neck squamous cell carcinoma, due to improved surgery and radiotherapy, current therapy regimens have failed as yet to increase the 5-year survival rate of patients with head and neck cancer [1,2]. Whereas fewer patients tend to die because of uncontrolled locoregional disease, there is an increase in the number of distant metastases and second primary tumors. The role of chemotherapy in these patients is limited. Responses are often observed but enhancement of survival is not obtained. These facts justify the search for more specific and effective therapeutical methods. Since HNSCC have an intrinsic sensitivity for radiation [3], we focus on the use of monoclonal antibodies labeled with radioisotopes for radioimmunotherapy (RIT). RIT of human tumors in experimental and/or clinical settings has already been described for various types of cancer, including colorectal carcinomas [4-7], malignant gliomas [8-11], ovarian carcinoma [12,13], small cell lung carcinoma [14-16], mammary carcinoma [17],

renal cell carcinoma [18,19], and cutaneous T cell lymphoma [20,21]. Thusfar however, no HNSCC-specific MAbs have been available to test the efficacy of RIT to eradicate HNSCC xenografts in an experimental setting. Therefore, we have developed a panel of MAbs, among which MAb E48, raised against HNSCC [22-24]. MAb E48 recognizes a 20-22 kD antigen, on normal tissues selectively expressed on stratified squamous epithelia and transitional epithelium of the bladder. On tumors, reactivity is restricted to malignancies arising from these tissues. The MAb E48 defined antigen is involved in the structural organization of squamous epithelia, possibly at the level of cell-cell adhesion [25]. Biodistribution and imaging studies with tracer amounts of ^{131}I-labeled E48 IgG and F(ab')$_2$ fragments already demonstrated the capacity of MAb E48 for specific delivery of radioisotope to HNSCC xenografts [26,27]. Recent data from an ongoing phase I/II trial with intravenously administered ^{99m}Tc-labeled MAb E48 F(ab')$_2$ and IgG in patients with HNSCC indicate that MAb E48 is highly capable of detecting metastatic and recurrent disease [28]. In the present study we demonstrate a dose dependent growth delay, regression and complete remission of established tumors by injection of single doses ^{131}I-labeled MAb E48 in nude mice bearing HNSCC xenografts. In this experimental model, the efficacy of RIT was compared to the antitumor activity of a number of clinically used or experimental chemotherapeutic agents [29].

Material and methods

Monoclonal antibodies

Monoclonal antibody E48 was raised against a SCC of the larynx [22]. Affinity-purified MAb E48 IgG and control MAb Myoscint® IgG, raised against myosin, were obtained from Centocor Europe Inc., Leiden, The Netherlands. Both are murine MAbs of the IgG1 subclass.

Xenografts

Female nude mice (NMRI, 25-32 g Harlan Olac CPB, Zeist, the Netherlands) were 8-10 weeks old at the time of the experiments. The head and neck SCC xenograft line HNX-HN was established by subcutaneous implantation of tumor fragments measuring 3x3x1 mm, in the lateral thoracic region on both sides of nude mice. Thereafter, the xenograft line was maintained by serial transplanting [30]. The tumor from which the HNX-HN line originates was a T4N2M0 squamous cell carcinoma of the base of the tongue from a 54-year-old female patient. As determined by indirect immunoperoxidase staining, the expression pattern of the MAb E48 defined antigen in the HNX-HN line was comparable to the pattern of the majority of human HNSCC tumors [27]. During experiments, food and water, with potassium iodide added to the water to prevent thyroid accumulation of ^{131}I, were available *ad libitum*.

Iodine-131 labeling

Iodination of MAb IgG was performed essentially as described earlier [27,31]. MAb IgG in phosphate buffered saline, pH 7.4, and ^{131}I were mixed in a ratio of approximately 1 mg MAb : 10 mCi ^{131}I in a vial coated with Iodogen (Pierce). After 10 min incubation at room temperature, a sample was removed to determine the amount of incorporated

iodine. To the reaction mixture, 1 ml AG1-X-8 resin (BioRad) in PBS, 1% BSA was added to absorb free iodine. To remove the resin and to sterilize the product, the reaction mixture was filtered through a 0.22 μm filter.

Quality control of ^{131}I-labeled MAb E48 IgG

After labeling, the immunoreactive fraction was at least 85% in all experiments. Incorporated ^{131}I was higher than 90% in all experiments. Specific activity of the radioimmunoconjugate varied between 5 and 10 mCi.mg^{-1}.

MAb IgG *in vitro* binding assay

The binding characteristics of radiolabeled MAb E48 IgG were analyzed in an immunoreactivity assay, essentially as described earlier [27]. In short, cells of the squamous cell carcinoma cell line UM-SCC-22B, a gift from Dr.T.E. Carey (Ann Arbor, MI, USA) were fixed in 1% paraformaldehyde and five serial dilutions, ranging from 5×10^6 cells/tube to 3.1×10^5 cells/tube, were made with 1% bovine serum albumin (BSA) in 10 mM phosphate-buffered saline (PBS). To the tubes, 10,000 cpm of the labeled MAb IgG was added and incubated 120 min at room temperature. To a duplicate of the last sample, excess unlabeled MAb IgG was added to determine non-specific binding. Cells were spun down and radioactivity in the pellet and supernatant was determined in a gamma counter and the percentage bound and free radiolabeled MAb was calculated (LKB-Wallac 1218 CompuGamma). Data were graphically analyzed in a modified Lineweaver-Burke plot and the immunoreactive fraction was determined by linear extrapolation to conditions representing infinite antigen excess.

Toxicity Studies

The maximum tolerated dose of each of the chemotherapeutic agents, corresponding to a weight loss between 5 and 15%, was determined as described earlier [29,30]. In the same way, the maximum tolerated dose of ^{131}I-labeled MAb E48 was determined. Nude mice without xenografts were injected with diluent (PBS) or with increasing doses of ^{131}I-labeled MAb E48 IgG. Total body dose was determined in a dose calibrator. Total accumulated radiation dose was calculated as described in the section "Dosimetry calculations". The weight of the mice was measured daily over a period of 4 weeks, at which timepoint no radioactivity could be detected.

In vivo biodistribution studies

Biodistribution studies with tracer dose ^{131}I-labeled MAb E48 IgG in nude mice bearing HNX-HN xenografts have previously been described [26,27]. To compare the biodistribution of a therapeutical dose with a tracer dose, 28 mice bearing xenografts of a size comparable with the tracer dose study were injected i.v. with 800 μCi ^{131}I-labeled MAb E48 IgG. At the time of injection the estimated xenograft volume was 323 ± 244 mm^3 as determined by measuring the tumor in 3 dimensions with calipers ((LxWxH)/2) (versus 352 ± 207.5 in the tracer dose study). Mice were bled, killed and dissected 2, 5 and 8 hours and 1, 3, 7, 10, 14, 21, 28 and 35 days after i.v. injection. Organs were immediately removed, placed in 5 ml plastic tubes and

weighed. Samples were taken from blood, urine, tumor, liver, spleen, kidney, heart, stomach, ileum, colon, bladder, sternum, muscle, lung, skin and tongue. After weighing, radioactivity in all organs and tumors was counted in a gamma counter. The antibody uptake in the tumor and other tissues was calculated as the percentage of the injected dose per gram of tissue (% ID.g^{-1}).

Radioimmunotherapy

Mice bearing 1 or 2 xenografts with a volume between 50 and 250 mm^3 were given a single intravenous injection of 400 (n=6, t=9) or 800 (n=5, t=7) μCi ^{131}I-labeled MAb E48 IgG. Control groups were given diluent (n=3, t=5), unlabeled MAb E48 IgG (n=4, t=5; amount equivalent of 800 μCi ^{131}I-labeled MAb E48 IgG) or 800 μCi ^{131}I-labeled control MAb IgG (n=6, t=9). Groups were randomized for initial tumor volume, for diluent 90 ± 68 (mean ± s.e.m.), for unlabeled MAb E48 96 ± 26, for 800 μCi ^{131}I-labeled control MAb 122 ± 106, for 400 μCi ^{131}I-labeled MAb E48 93 ± 40, and for 800 μCi ^{131}I-labeled MAb E48 118 ± 32. At day 1, 2, and 3, cages were cleaned to remove excreted radioactivity and thereafter this was done weekly. During the first week mice were weighed daily and tumor size was determined daily as described earlier. After the first week weight and tumor size were determined twice a week. At the same timepoints whole body dose was measured in a dose calibrator. Mice were sacrificed when tumor size exceeded 1000 mm^3.

Dosimetry calculations

Dosimetry calculations were performed using the data of the biodistribution of 800 μCi ^{131}I-labeled MAb E48 IgG. The absorbed cumulative radiation dose for tumor and various organs was calculated using the trapezoid integration method for the area under the curve [32]. Due to the therapeutic effect of the dose, tumors at day 35 had almost completely regressed and were thus not included in dosimetry calculations. The final segment of the area under the curve was calculated based on the biological halflife: dose of last segment = dose previous segment (day 21-day 28) x 0.693.(t½ in previous segment)$^{-1}$. cGy were further calculated by multiplying the μCi.h.g^{-1} by the g.cGy.(μCi.h)$^{-1}$ factor published by the Medical Internal Radiation Dose committee for ^{131}I of 0.4313 [33].

Chemotherapy

All drugs were injected at the maximum tolerated dose level (5-15% weight loss). Schedules were based on results of experiments performed in previous studies [29,30]. Mean number of mice and tumors in all schedules was 5 and 7, respectively. The volume of the tumors at the time of injection ranged between 50-150 mm^3. The following doses and injection schedules were applied: Doxorubicin (DOX, Farmitalia, Bournonville-Pharma, Almere, The Netherlands) at 8 mg.kg^{-1} i.v. at day 0 and 8; dFdC (2'2'-difluorodeoxycytidin, Gemcitabine, LY 188011, Lilly Research, Windlesham, Surrey, United Kingdom) at 120 mg.kg^{-1} i.p. at day 0, 3, 6 and 9; 5-FU (Fluorouracil Roche, Hoffman-La Roche, Mijdrecht, The Netherlands) at 125 mg.kg^{-1} i.p. at day 0 and 8; CDDP (Platinol, Bristol Meyers, Weesp, The Netherlands) at 5 mg.kg^{-1} i.v. at day 0, 8 and 15; Bleo (Bleomycin, Lundbeck, Amsterdam, The Netherlands) at 15

mg.kg^{-1} i.p. at day 0, 1, 2, 3 and 4, and methotrexate (Leder-trexate, Lederle, Etten-Leur, The Netherlands) at 1.8 mg.kg^{-1} i.p. at day 0, 1, 2, 3 and 4.

Evaluation of therapeutic efficacy

Tumor bearing mice were treated with RIT or chemotherapy when most tumors reached a volume of at least 50 mm^3 (range 50-250 mm^3). Tumors smaller than 50 mm^3 at the time of injection were not included in the determination of the tumor volume doubling time because of inaccuracy in measuring these tumors. Tumor growth was expressed as the tumor volume at each timepoint relative to the tumor volume at day 0. Efficacy of RIT as well as chemotherapy was expressed by means of the tumor growth delay factor (GDF), defined as (TD$_t$-TD$_c$)/TD$_c$ (TD$_t$ = median tumor volume doubling time of treated mice, TD$_c$ = median tumor volume doubling time of control mice). Prolonged survival (survival defined as the time period between day 0 and the timepoint of sacrifice, being when tumor size exceeded 1000 mm^3) was determined by comparing experimental groups with treatment groups using the Mann-Whitney U-test.

Results

Toxicity studies

The total cumulative whole body radiation dose for 220 μCi, 420 μCi, 670 μCi and 840 μCi ^{131}I-labeled MAb E48 IgG was 8,343, 11,673, 22,693 and 28,987 cGy, respectively. Besides loss of weight, no adverse reactions were observed. Loss of weight occurred immediately in
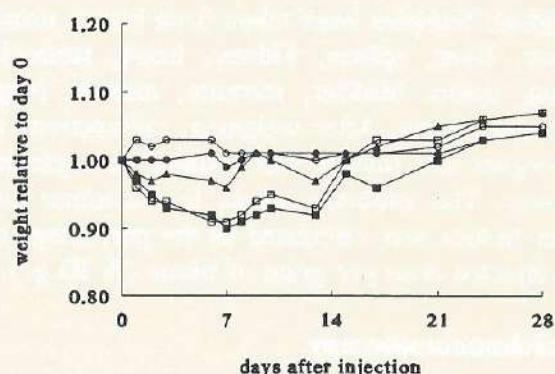
Fig.1. Toxicity of ^{131}I-labeled MAb E48 in nude mice without xenografts, monitored as the bodyweight relative to day 0, for diluent (○), 220 μCi (●), 420 μCi (▲), 670 μCi (□) and 840 μCi (■). Values are the mean of four mice per dose, standard deviations were less than 3%.

the 420, 670 and 840 μCi groups, and reached a maximum of 2.5, 10 and 10% respectively (Fig.1). Recovery of weight was observed for all mice from day 13 on and reached control values within 4 weeks. Based on these data, the maximum dose for therapy experiments was set at 800 μCi.

Biodistribution

The biodistribution of 800 μCi ^{131}I-labeled MAb E48 IgG is shown in Fig.2. Radioactivity measured in the blood is 23% ID.g^{-1} after 2 hours and is cleared with a T$_{1/2}\alpha$ of 14.3 hrs and a T$_{1/2}\beta$ of 127.7 hrs. Radioactivity accumulated rapidly in tumors and reached a maximum of 19.4 $\pm$ 2.9 % after 3 days. Activity is retained in the tumor up to 8.1 $\pm$ 3.5 %ID.g^{-1} at day 28. No specific accumulation is observed in any other tissue.
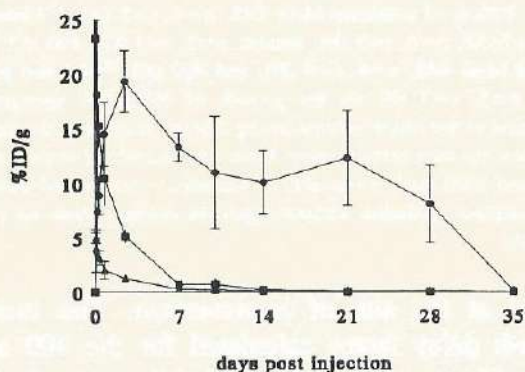
Fig.2. Biodistribution of 800 μCi ^{131}I-labeled MAb E48 in nude mice bearing HNX-HN xenografts. Mice were bled, killed and dissected 2, 5 and 8 hrs and 1, 3, 7, 10, 14, 21, 28 and 35 days after injection and the percentage injected dose per gram (%ID.g^{-1}) was calculated and plotted versus time. Tumor (●), blood (■) and lung (▲) are shown.

Dosimetry calculations

The absorbed cumulative radiation dose for tumor and various organs is shown in Fig.3. Based on the area under the curve of the biodistribution data of 800 μCi ^{131}I-labeled MAb E48 IgG the absorbed radiation dose to tumors in the group receiving 800 μCi was 12,170 cGy, whereas blood received only 2,984 cGy. Other tissues received the following dose: lung: 662 cGy; kidney: 607 cGy; spleen: 581 cGy; bladder: 571 cGy; heart: 543 cGy; colon: 424 cGy; ileum: 405 cGy; sternum: 405 cGy; liver: 403 cGy; muscle: 276 cGy; stomach: 251 cGy.

Evaluation of therapeutic efficacy

Tumor growth expressed as the tumor volume at each timepoint relative to the tumor volume at day 0 for control and treatment groups is shown
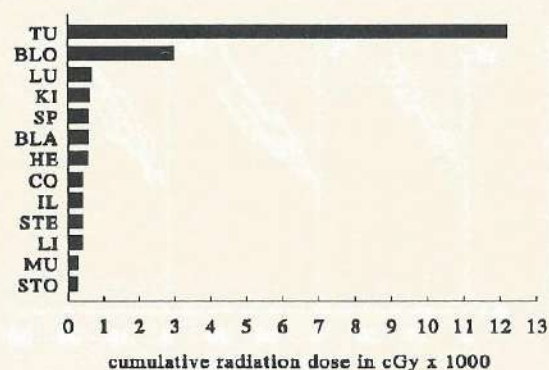
Fig.3. Total accumulated radiation dose in 10^3 cGy, calculated using the trapezoid integration method for the area under the curve. Tu, tumor; Blo, blood; Lu, lung; Ki, kidney; Sp, spleen; Bla, bladder; He, heart; Co, colon; Il, ileum; Ste, sternum; Li, liver; Mu, muscle; Sto, stomach.

in Fig.4. Tumors in the groups receiving unlabeled MAb E48 IgG (Fig.4A), 800 μCi ^{131}I-labeled control MAb IgG (Fig.4B) and diluent (Fig.4C) all showed exponential growth. Median tumor volume doubling times in the group receiving diluent or unlabeled MAb E48 IgG was 5.5 days. Median tumor volume doubling time in the group receiving 800 μCi ^{131}I-labeled control MAb showed a minimal, statistically insignificant increase. All tumors in the group receiving 400 μCi ^{131}I-labeled MAb E48 IgG (Fig.4D) showed delay of growth with a median tumor volume doubling time of 22.6 days, while 2 out of 9 tumors showed regression. All tumors in the group receiving 800 μCi ^{131}I-labeled MAb E48 IgG (Fig.4E) showed tumor regression, with a median tumor volume doubling time of 43 days. Moreover, in this group, 2 out of 7 tumors showed complete remission without regrowth during follow-up (> 3 months). After sacrificing these animals, no evidence of tumor could be de-
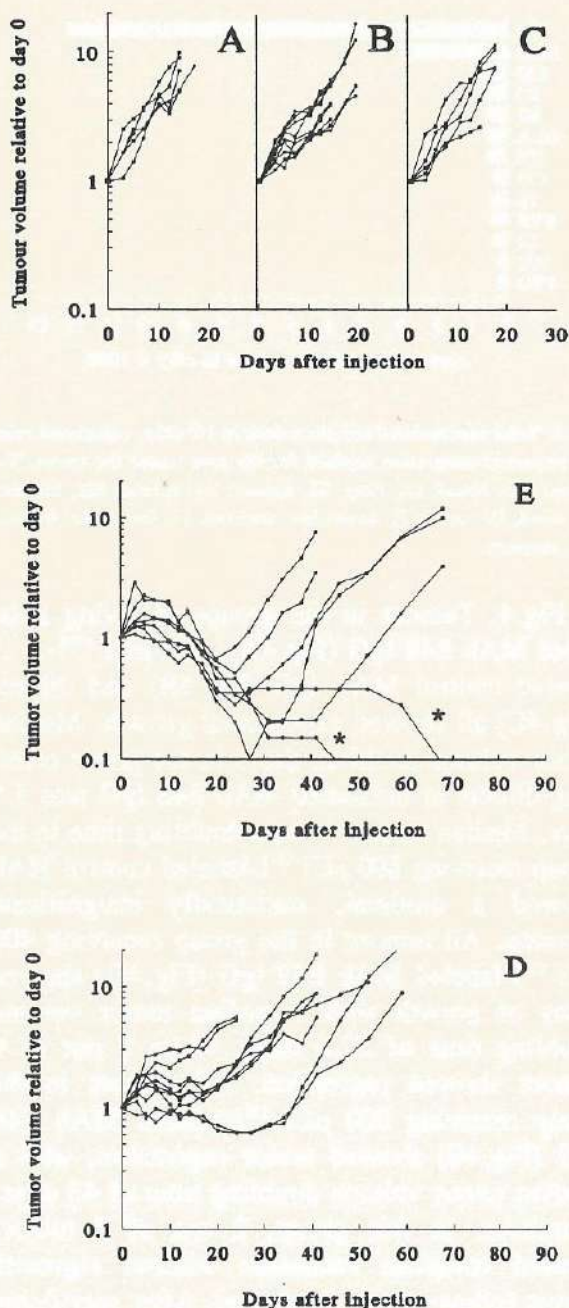
Fig.4. Effects of unlabeled MAb E48, n=4, t=5 (A), ^{131}I-labeled control MAb, n=6, t=9 (B), diluent, n=3, t=5 (C), 400 μCi ^{131}I-labeled MAb E48, n=6, t=9 (D), and 800 μCi ^{131}I-labeled MAb E48, n=5, t=7 (E) on the growth of HNX-HN xenografts, expressed as the tumor volume during therapy relative to the tumor volume at the start of the therapy. Mice were sacrificed when tumors exceeded 1000 mm^3, n=number of animals, t=number of tumors. *= complete remission without regrowth during follow up (>3 months).

tected at the site of implantation. The tumor growth delay factor calculated for the 400 and 800 μCi groups was 3.1 and 6.8, respectively. Weight loss in experimental groups did not exceed 15% at any timepoint. When compared with the tumor growth delay factor of chemotherapeutic agents like adriamycin (3.0), 5-fluorouracil (1.2), cisplatin (1.1), bleomycin (0.7), methotrexate (0) and 2'2'-difluorodeoxycytidine (1.6), established in the same HNX-HN xenograft, RIT shows a very high therapeutic efficacy (Fig.5). No cures were observed with chemotherapeutic agents. Prolonged survival, as determined by the Mann-Whitney U-test, was significant for both RIT groups as compared to control groups (p < 0.01).

Discussion

Therapeutic efficacy of radiolabeled MAbs in the nude mouse model has been described for several tumor types. Although clinical radioimmunoscintigraphy studies for the detection of HNSCC have been reported with ^{111}In-labeled anti-epidermal growth factor receptor [34] and with ^{111}In-labeled anti-carcinoembryonic antigen [35,36], no reports are available on therapy experiments of HNSCC xenografts with radiolabeled MAbs. Here we present the first data on RIT of HNSCC. As a first approach to assess the potential of radiolabe-
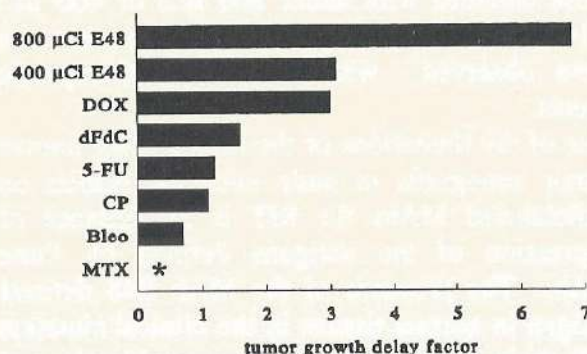
Fig.5. Antitumor effect of RIT in comparison with chemotherapy in HNX-HN xenografts. Antitumor effect was expressed as the tumor growth delay factor (see: Material and methods). DOX, doxorubicin; dFdC, 2'2'-difluorodeoxcytidine; 5-FU, 5-fluorouracil; CP, cisplatin; Bleo, bleomycin; MTX, methotrexate (* = 0)

led MAb E48 in eradicating HNSCC xeno-grafts, therapy experiments, consisting of single bolus injection of two different doses, were designed in a straightforward manner. Dosimetry calculations were based on the biodistribution of a therapeutic dose, since continued tumor growth in biodistribution experiments with tracer dose may well result in underestimation of the radiation dose up to 35-52% [5,32]. In our studies, no differences in biodistribution between tracer and therapeutic doses were observed. In tracer dose studies however, no data were available during the first 12 hours and after day 7, whereas in this study data were obtained from 2 hours p.i. up to 35 days, allowing more accurate dosimetry calculations. A remarkable good retention of MAb E48 was observed with 8.1 ± 3.5 %ID.g^{-1} at day 28 after injection.

Although numerous reports with ^{131}I-labeled MAb IgG or F(ab')$_2$ have been described with anti-tumor effects, only few studies achieve complete remissions after single bolus injections. Wessels

et al. reported complete remissions of renal cell carcinoma xenografts after single bolus injection of 600 μCi ^{131}I-labeled MAb IgG [18], whereas Sharkey et al. observed no regrowth of colon carcinoma xenografts after a single injection of 1 Mci MAb IgG [37]. Lee et al. obtained appa-rent cures of mice with intracranial glioma xeno-grafts after a single injection of 1.25 mCi MAb IgG [9]. Complete ablation of highly radiation sensitive neuroblastoma xenografts was achieved with a single injection of 1 mCi IgG by the group of Cheung et al. [38]. Buchegger et al. completely eradicated xenografts of colon carcinomas with single injections of 2,200-2,800 μCi, but instead of IgG, pooled F(ab')$_2$ fragments of three different anti-CEA MAbs were used [39]. Other successful studies applied fractionated protocols [15,17,39,40]. In our study, single injections of 400 or 800 μCi ^{131}I-labeled E48 MAb IgG showed pronounced anti-tumor effects, resulting in complete remissions of 2 out of 7 tumors in the group receiving 800 μCi ^{131}I-labeled MAb E48 IgG. No remnant tumor could be detected when mice were sacrificed after 3 months follow-up. These cures might very well be due to the intrinsic sensitivity of head and neck tumors for radiation [3]. In addition, the accumulated dose, 12,170 cGy, in tumor tissue as a result of a single bolus injection 800 μCi was very high, reflecting the excellent targeting and retention characteristics of MAb E48 in this experimental model.

Therapeutic efficacy of RIT has been found to be inversely correlated with tumor size [6,9,37]. Accordingly, RIT has the potential to be the most useful in adjuvant therapy when minimal disease is present [37,41]. In the case of head and neck cancer this would apply to patients with stage III and IV disease. In these patients local recurrences

occur in 50-60%, while 15-25% develop distant metastases after surgery and/or radiotherapy [1]. Unfortunately, no relevant metastatic model for HNSCC is available. In our study, the correlation between tumor size and therapeutic effect could not be determined due to the selected size range. In several studies, an increase in therapeutic efficacy combined with a decrease in toxicity has been observed when total dose was given in multiple fractions [8,15,39,40,42]. Therefore, the efficacy of RIT with MAb E48 with respect to growing, established HNX-HN xenografts will be further investigated comparing single injection regimen to multiple injection regimens. Furthermore, since ^{131}I is not the isotope of choice in clinical applications because of the low percentage therapeutic ß-emission (32%) and the high percentage damaging γ-radiation (66%), and because of the rapid dehalogenation of ^{131}I-labeled conjugates, we have developed a MAb E48 radioimmunoconjugate labeled with [186]Re, an isotope with a high percentage ß-emission (90%) and low percentage γ-emission (8%). MAbs labeled with this isotope have already been described in tumor localization and tumor therapy studies [16,43]. MAb E48 labeled with this isotope will be tested in the HNX-HN xenograft model.

Thusfar, clinical results with chemotherapy have been disappointing with respect to the effect on 5-year survival of patients, despite the number of trials over the past 10 years [1,44]. In our HNX-HN xenograft model, a number of conventional drugs, known to produce remissions in patients with head and neck cancer, and one experimental chemotherapeutic agent have been evaluated [29] (unpublished data). In the dose schedules described, none of the chemotherapeutic agents caused tumor growth delay factors higher than those obtained with either 800 μCi or 400 μCi ^{131}I-labeled MAb E48 IgG. Furthermore, no cures were observed with these chemotherapeutic agents.

One of the limitations of the model using human tumor xenografts in nude mice for studies on radiolabeled MAbs for RIT is the absence of expression of the antigens defined by these MAbs. The presence of the MAb E48 defined antigen in normal tissues in the clinical situation will obviously influence the pharmacokinetics and biodistribution of radiolabeled MAb E48. In clinical radioimmunoscintigraphy studies using ^{99m}Tc-labeled MAb E48 F(ab')$_2$ fragment we observed uptake of radioactivity in normal oral mucosa and adrenal glands [28]. Uptake in these tissues seems to be diminished when using whole IgG. Most clinical trials with radiolabeled MAb for diagnosis or therapy of solid neoplasms have reported MAb uptake in large tumors in the range of 0.001-0.01 %ID.g^{-1} [45,46]. Preliminary data on the localization of ^{99m}Tc-labeled MAb E48 IgG indicate accumulation of the conjugate in tumors of 0.5-4.0 cm diameter up to a mean % ID.g^{-1} of 0.03 at 44 hrs (range: 0.0143-0.0823, number of patients = 7). This looks very promising indeed, when taking into account the higher accumulation of MAbs in small tumor loads. Chatal *et al.* reported on the biodistribution of ^{111}In-labeled MAb OC125 intraperitoneally injected into patients with ovarian carcinoma, demonstrating low accumulation in large tumors (0.0014-0.0032 %ID.g^{-1}) but significantly higher accumulation in small tumor nodules (0.13 $\pm$ 0.08 %ID.g^{-1}) and malignant cell clusters (median 0.33 with a maximum of 4.16 %ID.g^{-1}) [47]. Assuming that this size correlation also applies for head and neck tumors and assuming that patients will tolerate a

dose of 100 mCi of ^{131}I-labeled MAb E48 (or an equivalent dose of [186]Re-labeled MAb E48) [13,20], achieving radiation doses in tumor tissue enabling elimination of minimal disease lies within reach. Our data, showing the capacity of a single bolus injection ^{131}I-labeled MAb E48 to eradicate HNSCC xenografts in nude mice, present the first successful RIT results for head and neck squamous cell carcinoma. Together with data from an ongoing phase I clinical trial in our hospital, showing the capacity of ^{99m}Tc-labeled MAb E48 F(ab')$_2$ fragment and IgG in detecting metastatic and recurrent disease, this indicates the potential of radiolabeled MAb E48 for radioimmunotherapy of patients with head and neck cancer.

Acknowledgement.

References

1. Choksi AJ, Dimery IW, Hong WK. Adjuvant chemotherapy of head and neck cancer: the past, the present and the future. *Seminars in oncology* 15:45s-49s, 1988.

2. Cognetti EV, Pinnaro P, Carlini P, Ruggeri EM, Impiobato FA, Rosario Del Vecchio M, Gianarelli D, Perrino A. Neoadjuvant chemotherapy in previously untreated patients with advanced head and neck squamous cell cancer. *Cancer* 62:251-261, 1988.

3. Wessels BW, Harisiadis L, Carabell SC. Dosimetry and radiobiological efficacy of clinical radioimmunotherapy. *J Nucl Med* 30:827, 1989.

4. Esteban JM, Hyams DM, Beatty BG, Merchant B, Beatty JD. Radioimmunotherapy of human colon carcinomatosis xenograft with 90Y-ZCE025 monoclonal antibody toxicity and tumour phenotype studies. *Cancer Res* 50:989s-992s, 1990.

5. Lee Y-CC, Washburn LC, Sun TT, Byrd BL, Crook JE, Holloway E.C, Steplewski Z. Radioimmunotherapy of human colorectal carcinoma xenografts using 90Y-labelled monoclonal antibody CO17-1A prepared by two bifunctional chelate techniques. *Cancer Res* 50:4546-4551, 1990.

6. Schlom J, Siler K, Milenic DE, Eggensperger D, Colcher D, Miller LS, Houchens D, Cheng R, Kaplan D, Goeckeler W. Monoclonal antibody-based therapy of a human tumour xenograft with a [177]Lutetium-labelled immunoconjugate. *Cancer Res* 51:2889-2896, 1991.

7. Blumenthal RD, Kashi R, Stephens R, Sharkey RM, Goldenberg DM. Improved radioimmunotherapy of colorectal cancer xenografts using antibody mixtures against carcinoembryonic antigen and colon-specific antigen-p. *Cancer Immunol Immunother* 32:303-310, 1991.

8. Colapinto EV, Zalutsky MR, Archer GE, Noska MA, Friedman HS, Carrel S, Bigner DD. Radioimmunotherapy of intracerebral human glioma xenografts with ^{131}I-labelled F(ab')$_2$ fragments of monoclonal antibody Mel-14. *Cancer Res* 50:1822-1827, 1990.

9. Lee Y, Bullard DE, Humphrey PA, Colapinto EV,

Friedmen HS, Zalutsky MR, Colem RE, Bigner DD. Treatment of intracranial human glioma xenografts with ^{131}I-labeled anti-tenascin monoclonal antibody 81C6. *Cancer Res* 48:2904-2910, 1988.

10. Lee Y-S, Bullard DE, Zalutsky MR, Coleman RE, Wikstrand CJ, Friedman HS, Colapinto EV, Bigner DD. Therapeutic efficacy of antiglioma mesenchymal extracellular matrix ^{131}I-labelled murine monoclonal antibody in a human glioma xenograft model. *Cancer Res* 48:559-566, 1988.

11. Williams JA, Wessels BW, Edwards JA, Kopher KA, Wanek PM, Wharam MD, Order SE, Klein JL. Targeting and therapy of human glioma xenografts *in vivo* utilizing radiolabeled antibodies. *Cancer Res* 50:974s-979s, 1990.

12. Stewart JSW, Hird V, Sullivan M, Snook D, Epenetos AA .Intraperitoneal radioimmunotherapy for ovarian cancer. *Br J Obstet Gynaecol* 96:529-536, 1989.

13. Ward B, Mather S, Shepherd J, Crowhter M, Hawkins L, Britton K, Slevin ML. The treatment of intraperitoneal malignant disease with monoclonal antibody guided ^{131}I radiotherapy. *Br J Cancer* 58:658-662, 1988.

14. Smith A, Groscurth P, Waibel R, Westera G, Stahel RA. Imaging and therapy of small cell carcinoma xenografts using ^{131}I-labeled monoclonal antibody SWA11. *Cancer Res* 50 (suppl.):980s-984s, 1990.

15. Smith A, Waibel R, Stahel RA. Selective immunotherapy of small cell cancer xenografts using ^{131}I-labelled SWA11 antibody. *Br J Cancer* 64:263-266, 1991.

16. Beaumier PL, Venkatesan P, Vanderheyden J-L, Burgua WD, Kunz LL, Fritzberg AR, Abrams PG, Morgan Jr AC. ^{186}Re Radioimmunotherapy of small cell lung carcinoma xenografts in nude mice. *Cancer Res* 51:676-681, 1991.

17. Senekowitsch R, Reidel G, Möllenstadt S, Kriegel H, Pabst H-W. Curative radioimmunotherapy of human mammary carcinoma xenografts with iodine-131-labeled monoclonal antibodies. *J Nucl Med* 30:531-537, 1989.

18. Wessels BW, Vessella RL, Palme II DF, Berkopec JM, Smith GK, Bradley EW. Radiobiological comparison of external beam irradiation and radioimmunotherapy in renal cell carcinoma xenografts. *Int J Radiat Oncol Biol Phys* 17:1257-1263, 1989.

19. Chiou RK, Vessella RL, Limas C, Shafer RB, Elson MK, Arfman EW, Lange PH. Monoclonal antibody-targeted radiotherapy of renal cell carcinoma using the nude mouse model. *Cancer* 61:1766-1775, 1988.

20. Rosen ST, Zimmer AM, Goldman-Leikin R, Gordon LI, Kazikiewicz JM, Kaplan EH, Variakojis D, Marder RJ, Dykewicz MS, Piergies A, Silverstein EA, Roenigk HH, Spies SM. Radioimmunodetection and radioimmunotherapy of cutaneous T cell lymphomas using an ^{131}I-labeled monoclonal antibody: an Illinois Cancer Council Study. *J Clin Oncol* 5:562-573, 1987.

21. Mulshine JL, Carrasquillo JA, Weinstein JN, Keenan AM, Reynolds JC, Herdt J, Bunn PA, Sausville E, Eddy J, Cotelingam JD, Perentesis P, Pinsky C, Larson SM. Direct intralymphatic injection of radiolabeled ^{111}I-T101 in patients with cutaneous T cell lymphoma. *Cancer Res* 51:688-695, 1991.

22. Quak JJ, Balm AJM, van Dongen GAMS, Brakkee JGP, Scheper RJ, Snow GB, Meijer CJLM. A 22-kd surface antigen detected by monoclonal antibody E 48 is exclusively expressed in stratified squamous and transitional epithelia. *Am J Pathol* 136:191-197, 1990.

23. Quak JJ, van Dongen GAMS, Gerretsen M, Hayashida D, Balm AJM, Brakkee JGP, Snow GB, Meijer CJLM. Production of a monoclonal antibody (K 931) to a squamous cell carcinoma associated antigen identified as the 17-1A antigen. *Hybridoma* 9:377-387, 1990.

24. Quak JJ, Schrijvers AHGJ, Brakkee JGP, Davis HD, Scheper RJ, Balm AJM, Meijer CJLM, Snow GB, van Dongen GAMS. Expression and characterization of two differentiation antigens in stratified epithelia and carcinomas. *Int J Cancer* 50:507-513, 1992.

25. Schrijvers AHGJ, Gerretsen M, Fritz JM, van Walsum M, Quak JJ, Snow GB, van Dongen GAMS. Evidence for a role of the monoclonal antibody E48 defined antigen in cell-cell adhesion in squamous epithelia and head and neck

squamous cell carcinoma. *Exp Cell Res* 196:264-269, 1991.

26. Quak JJ, Balm AJM, Brakkee JGP, Scheper RJ, Haisma HJ, Braakhuis BJM, Meijer CJLM, Snow GB. Localization and imaging of radiolabeled monoclonal antibody E48 against squamous cell carcinoma of the head and neck in tumor bearing nude mice. *Int J Cancer* 44:534-538, 1989.

27. Gerretsen M, Quak JJ, Suh JS, van Walsum M, Meijer CJLM, Snow GB, van Dongen GAMS. Superior localisation and imaging of radiolabelled monoclonal antibody E48 F(ab')₂ fragment in xenografts of human squamous cell carcinoma of the head and neck and of the vulva as compared to monoclonal antibody E48 IgG. *Br J Cancer* 63:37-44, 1991.

28. van Dongen GAMS, Leverstein H, Roos JC, Quak JJ, van den Brekel MWM, van Lingen A, Martens HJM, Castelijns JA, Visser GWM, Meijer CJLM, Snow GB. Radioimmunoscintigraphy of head and neck tumors using technetium-99m-labeled monoclonal antibody E48 F(ab')₂. *Cancer Res* 52:2569-2574, 1992.

29. Braakhuis BJM, van Dongen GAMS, Vermorken JB, Snow GB. Preclinical *in vivo* activity of 2'2'-difluoro-deoxycytidine (Gemcatibine) against human head and neck cancer. *Cancer Res* 51:211-214, 1991.

30. Braakhuis BJM, van Dongen GAMS, Bagnay M, van Walsum M, Snow GB. Preclinical chemotherapy on human head and neck xenografts grown in athymic nude mice. *Head and Neck* 11:511-515, 1989.

31. Haisma HJ, Hilgers J, Zurawski VR. Iodination of monoclonal antibodies for diagnosis and therapy using a convenient one vial method. *J Nucl Med* 27:1890-1895, 1986.

32. Badger CC, Krohn KA, Shulman H, Flournoy N, Bernstein ID. Experimental radioimmunotherapy of murine lymphoma with ¹³¹I-labeled anti-T cell antibodies. *Cancer Res* 46:6223-6228, 1986.

33. Dilman LT. Radionuclide decay schemes and nuclear parameters for use in radiation-dose estimation. In: *The Society of Nuclear medicine (MIRD Pamphlet No.4)*, New York, 1969.

34. Soo KC, Ward M, Roberts KR, Keeling F, Carter RL, McReady VR, Ott RJ, Powell E, Ozanne B, Westwood JH, Gusterson BA. Radioimmunoscintigraphy of squamous carcinomas of the head and neck. *Head and Neck Surgery* 9:349-352, 1987.

35. Kairemo KJA, Hopsu EVM. Imaging of pharyngeal and laryngeal carcinomas with Indium-111-labelled monclonal anti-CEA antibodies. *Laryngoscope* 100:1077-1082, 1990.

36. Kairemo KJA, Hopsu EVM. Imaging of tumours in the parotid region with Indium-111-labelled monoclonal antibody reacting with carcinoembryonic antigen. *Acta Oncologica* 29:539-543, 1990.

37. Sharkey RM, Pykett MJ, Siegel JA, Alger EA, Primus FJ, Goldenberg DM. Radioimmunotherapy of the GW-39 human colonic tumor xenograft with ¹³¹I-labeled murine monoclonal antibody to carcinoembryonic antigen. *Cancer Res* 47:5672-5677, 1987.

38. Cheung N-K, Landmeier B, Neely J, Nelson AD, Abramowsky C, Ellery S, Adams RB, Miraldi F. Complete tumor ablation with iodine-131-labeled disialoganglioside GD2-specific monoclonal antibody against human neuroblastoma xenografted in nude mice. *J Natl Cancer Inst* 77:739-745, 1986.

39. Buchegger F, Pfister C, Fournier K, Prevel F, Schreyer M, Carrel S, Mach J-P. Ablation of human colon carcinoma in nude mice by ¹³¹I-labeled monoclonal anti-carcinoembryonic antigen antibody F(ab')₂ fragments. *J Clin Invest* 83:1449-1456, 1989.

40. Schlom J, Molinolo A, Simpson JF, Siler K, Roselli M, Hinkle G, Houchens DP, Colcher D. Advantage of dose fractionation in monoclonal antibody-targeted radioimmuno-therapy. *J Natl Cancer Inst* 82:763-771, 1990.

41. Langmuir VK, Sutherland RM. Dosimetry models for radioimmunotherapy. *Med Phys* 15:867-873, 1988.

42. Buchegger F, Pelegrin A, Delaloye B, Bischof Delaloye A, Mach JP. Iodine-131-labeled MAb F(ab')₂ fragments are more efficient and less toxic than intact anti-CEA antibodies in radioimmunotherapy of large human colon carcinoma grafted in nude mice. *J Nucl Med* 31:1035-1044, 1990.

43. Goldrosen MH, Biddle WC, Pancook J, Bakshi S,

Vanderheyden J-L, Fritzberg AR, Morgan Jr AC, Foon KA. Biodistribution, pharmacokinetics, and imaging studies with [186]Re-labeled NR-LU-10 whole antibody in LS174T colonic tumor-bearing mice. *Cancer Res* 50:7973-7978, 1991.

44. Snow GB. Head and neck: Editorial overview. *Current Opinion in Oncology* 3:497-499, 1991.

45. Goldenberg DM. Challenges to the therapy of cancer with monoclonal antibodies. *J Natl Cancer Inst* 83:78-79, 1991.

46. Epenetos AA, Kosmas C. Monoclonal antibodies for imaging and therapy. *Br J Cancer* 59:152-155, 1989.

47. Chatal J-F, Saccavini J-C, Thedrez P, Curtet C. Kremer M, Guerreau D, Nolibe D, Fumoleau P, Guillard Y. Biodistribution of Indium-111-labeled OC125 monoclonal antibody intraperitoneally injected into patients operated on for ovarian carcinomas. *Cancer Res* 49:3087-3094, 1989.

Labeling of monoclonal antibodies with [186]Re using the MAG₃ chelate for radioimmunotherapy of cancer: a technical protocol.

Gerard W.M. Visser[1], Martijn Gerretsen[2], Jacobus D.M. Herscheid[1], Gordon B. Snow[2], and Guus A.M.S. van Dongen[2].

Radio-Nuclide-Center[1], Free University,
Department of Otolaryngology / Head and Neck Surgery[2],
Free University Hospital, Amsterdam, The Netherlands.

Summary

A detailed technical protocol is provided for reproducible and aseptical production of stable ^{186}Re-monoclonal-antibody conjugates. For evaluation, the labeling of MAb E48 IgG and its F(ab')$_2$ fragment, promising candidates for radioimmunotherapy of squamous cell carcinoma of the head and neck, was used. S-benzoyl-mercaptoacetyltriglycine (S-benzoyl-MAG$_3$) was used as a precursor. ^{186}Re-MAG$_3$ was prepared via an unique solid phase synthesis, whereafter known strategies for esterification and conjugation to MAb IgG/F(ab')$_2$ were applied. The biodistribution of ^{186}Re-E48 F(ab')$_2$ in tumor bearing nude mice was found to be comparable to that of analogously labeled ^{99m}Tc-E48 F(ab')$_2$ or to that of ^{131}I-E48 F(ab')$_2$, indicating that the intrinsic behavior of the antibody remains preserved when using this labeling technique. Radiolytic decomposition of ^{186}Re-E48 IgG/F(ab')$_2$ solutions of 10 mCi.ml^{-1} was effectively reduced by the antioxidant ascorbic acid. Upon increase of the Re-MAG$_3$ molar amount, a conjugation of seven to eight Re-MAG$_3$ molecules per MAb molecule was in general the maximum ratio that chemically could be obtained. Such a ratio did not impair the immunoreactivity or alter the in vivo biodistribution characteristics of the immunoconjugate, making this labeling procedure suitable for general clinical application.

Introduction

Tumor targeting with radiolabeled monoclonal antibodies might be a valuable approach for diagnosis and therapy of squamous cell carcinoma of the head and neck (HNSCC). Squamous cell carcinoma represent the vast majority of all malignant tumors of the head and neck. HNSCC have a proclivity to metastasize to regional lymph nodes in the neck rather than to spread hematogeneously. The status of the cervical nodes has been recognized as the single most important prognostic factor in HNSCC.

Most early stage HNSCC (stage I and II) can be safely cured with surgery and or radiation therapy. Less effective, however, is the treatment of stage III and IV disease: 50-60% of patients with resectable tumors develop locoregional recurrence, while 15-25% develop distant metastases. The role of chemotherapy in these patients is limited. Responses are often seen but enhancement of survival is minimal.

Radioimmunoconjugates may be benificial in assessment of tumor involvement in the lymph nodes. It can be expected that the relative superficial localization of the neck nodes allows accurate radioimmunodetection with a gamma camera. In addition, radioimmunoconjugates may also be of value for early detection and therapy of recurrent disease and distant metastases. A factor in favor of radioimmunotherapy is the intrinsic radiosensitivity of HNSCC. We recently tested a panel of monoclonal antibodies for targeting of HNSCC in preclinical and clinical studies. The most promising antibody, designated MAb E48, recognizes a 22 kDa surface antigen; this antigen is probably involved in cell-cell adhesion and is exclusively expressed by squamous and transitional epithelia and their malignant counterparts[1,2]. The capacity of MAb E48 IgG as well as F(ab')$_2$ for highly specific delivery of ^{131}I to human head and neck tumors has been demonstrated in xenografted nude mice [3,4]. Recently, we demonstrated a dose dependent growth delay, regression and

complete remissions of established tumors by injection of single doses ^{131}I-labeled MAb E48 IgG in nude mice bearing HNSCC xenografts [5]. As a first approach to test the capability of MAb E48 for tumor targeting in patients with head and neck cancer, we decided to evaluate MAb E48-F(ab')$_2$ for its accuracy in detection of lymph node metastases. To this end we used a [99mTc]-MAG$_3$-labeled conjugate of MAb E48 F(ab')$_2$ which appeared highly capable of detecting metastatic and recurrent disease [6]. Preliminary data indicate that MAb E48 IgG is also well suited for tumor targeting in patients: labeled with [99mTc], the percentage injected dose per gram of tissue was found to be ranging from 0.014-0.080% at 44 hr after injection. These data justify the further development of MAb E48 for therapeutic approaches. Sofar, most clinical experience with RIT has been obtained with ^{131}I-labeled immunoconjugates. ^{131}I-labeling of MAbs is easy, while the isotope has an appropriate half-life (8 days) and ß-particle energy (0.6 MeV) for utility in radioimmunotherapy (RIT). However, disadvantages are the reported instability of ^{131}I-labeled immunoconjugates and the γ-emission which represents 65% of the released energy. It has been hypothesized that [186]Re may be a better candidate isotope for radioimmunotherapy than [131]I [7]. With its half life of 3.7 days, its 9% γ-emission which has an ideal energy (137 KeV) for imaging, and its 71% ß-emission of 1.07 MeV and 21% ß-emission of 0.94 MeV [8], theoretically [186]Re seems to be better suited for RIT than [131]I. The physical properties of [99mTc] and [186]Re seem to be ideal for radioimmunoscintigraphy (RIS) and for RIT respectively and the chemical properties of [99mTc] and [186]Re are considered to be similar. Therefore, at our institute effort has been

put on the development of analogous [99mTc] and [186]Re labeling chemistry for MAbs directed to HNSCC, with the clinical option in mind to use [99mTc] imaging to identify [186]Re therapy candidates. In this concept it is clear that the biodistribution of the MAb should be the same irrespective whether labeled with [99mTc] or [186]Re. Consequently, because the specific activity of [186]Re is several orders of magnitude lower than that of [99mTc], the applicability of the labeling procedure should not be restricted by the low specific activity of [186]Re.

The approach which obviously gives the best chemical control over the labeling process, leading to highly stable conjugates without aggregate formation, has been described by Fritzberg et al.[9,10]. During this multistep procedure, an active ester of tetrafluorophenol and a N_2S_2-pentanoate or N_3S-butyrate carrying the radioisotope is prepared, which is subsequently conjugated to amino groups of the antibody. Either the ester is formed after prelabeling of the chelate in the presence of $S_2O_4^{2-}$ at pH=12, or the preformed active ester of the chelate is labeled via transchelation at pH=3 (the "pre-ester" method) [9-12]. The thus obtained conjugates were found to have retained their immunoreactivity and to be stable upon challenge by other chelating compounds [9].

Trying to apply this method using S-benzoyl-MAG$_3$, the precursor of [99mTc]-MAG$_3$ used for renal function measurement, we found that both methods were not suitable for coupling [186]Re to the antibody. [186]Re-MAG$_3$ was not formed with $S_2O_4^{2-}$ at pH = 12 during the prelabeling method, while for MAG$_3$ the pre-ester method failed due to severe hydrolysis of the esterbond, even in the presence of isopropanol.

In the present study we report on a solid phase synthesis of ^{186}Re-MAG$_3$. A detailed technical protocol is provided for reproducible and aseptical labeling leading to stable and sterile monoclonal antibody conjugates (either IgG or their fragments) with ^{186}Re to a high Re:MAb molar ratio. The chemical c.q. in vitro stability in connection with the radiolytic decomposition occurring when using strong ß-emitters, is described. From comparative studies in (HNSCC bearing) nude mice, biodistribution characteristics of ^{186}Re-labeled as well as from ^{99m}Tc- and ^{131}I-labeled E48 IgG and its F(ab')$_2$ fragment, are provided.

Material and methods

Materials

2,3,5,6-Tetrafluorophenol (TFP) and 1-ethyl-3-(3-dimethylaminopropyl)-carbodiimide (EDC) were purchased from Janssen Chimica. S-benzoyl-MAG$_3$ as a pure white solid, i.e. free from the presence of organic acids, not in "kit" form, was a gift from Mallinckrodt Medical, Petten, The Netherlands. S-benzoyl-MAG$_3$ was dissolved in MeCN:H$_2$O (9:1) at a concentration of 1 mg.ml^{-1} and this stock solution was found to be very stable especially with respect to loss of the sulphur protecting group. Upon HPLC analysis even after 3 months no detectable amounts of benzoic acid or other compounds were observed. Details on HPLC analysis: 15 cm C18 Novapak column (Waters), eluent 25% (vol/vol) EtOH/ 6.25 mM (n-Bu)$_4$NH$_2$PO$_4$; flow rate 1 ml.min^{-1}, R$_t$ S-benzoyl-MAG$_3$ = 14.5 min, R$_t$ benzoic acid = 5.3 min, detection at 210 and 254 nm.
^{186}Re was obtained as a [^{186}Re]ReO$_4^-$ solution from

Mallinckrodt Medical. Quantitative measurement of the ^{186}Re activities in solutions was performed in glass vessels with internal diameter 13.5 mm in a dose calibrator. It was found that the amount of radioactivity measured in the ^{99m}Tc 140 keV channel needed to be multiplied with a factor 2.5 to obtain the ^{186}Re activity.

The tube heater was made from a Cu/Zn block fitting to the glass vessel. Heating of the block was accomplished by a 240V/150W Watlow band element. Thermo-control was carried out by a West temperature controller (type PYZ4 TCY1), a solid state relais, and a PT 100 (Platinum Resistance Thermometer). The tube heater avoids the use of a water- or oilbath in the sterile flow hood. pH measurements were carried out with a small volume glass/Pt electrode (Schott CG837, Φ 3 mm).

For purification of the ester and the conjugate respectively, Sep-pak C$_{18}$ cartridges (Waters) and PD-10 Sephadex columns (Pharmacia) were used. For final sterilization of the radioimmunoconjugate, 0.22 μm Acrodisk filters (Gelman Sciences Inc.) were used.

All solutions were sterile and pyrogen-free and were made from 'water for injection'.

Analysis

HPLC analysis of the ^{186}Re- and ^{99m}Tc-labeled MAG$_3$ and their corresponding MAG$_3$-TFP esters was performed on a 25 cm Lichrosorb 10 RP 18 column (Chrompack) with a gradient elution. Solution A consisted of a 5:95 mixture of EtOH and a 0.01 M sodium phosphate buffer + 0.015 M sodium azide pH = 6 solution; solution B was a 9:1 mixture of MeOH and H$_2$O. Gradient (flow rate 1 ml.min^{-1}): 10 min 100% A, 10 min 100%

A → 100% B, 10 min 100% B. Radioactivity was detected continuously by an Ortec 406A single channel analyzer connected to a Drew 3040 Data collector (Betron Scientific) and fractions of 1 ml were collected on a LKB 2212 Helirac. Comparison of the injection standard with the total effluent from the HPLC column showed in all cases a quantitative recovery of the activity (>98%) from the HPLC column. The HPLC retention times were 3.0 min (most probably a low valent oxo-[186]Re species), 3.6 min ([186]ReO$_4^-$), 6.5 min ([186]Re-MAG$_3$), 23.0 min ([186]Re-MAG$_3$-TFP), 3.1 min (most probably a low valent oxo-^{99m}Tc species), 3.9 min ([99m]TcO$_4^-$), 9.4 min (^{99m}Tc-MAG$_3$), 23.4 min (^{99m}Tc-MAG$_3$-TFP).

Thin layer chromatography (TLC) of the labeled MAbs was performed on silicagel impregnated glass fiber sheets (Gelman Sciences Inc.), thickness 0.3 mm, length 10 cm, eluent 0.1 M citric acid pH = 7. After development (5 min.), the chromatograms were cut into 1 cm segments and counted in a LKB Wallac Compugamma. Rf MAbs = 0; Rf [[186]Re]ReO$_4^-$ = 1.

[186]Re-labeling protocol

A detailed protocol for labeling of MAbs with [186]Re by using the MAG$_3$ chelate is provided by Table 1.

[99m]Tc-labeling protocol

For the synthesis of ^{99m}Tc-MAG$_3$ simply heating at 100 °C for 10 minutes is sufficient (step 5, Table 1), while the presence of sulphite (step 2, Table 1) and step 7 (Table 1) are not necessary; consequently only 250 μl of 1 N H$_2$SO$_4$ is needed to bring the pH between 5.7-6.3 (step 8, Table
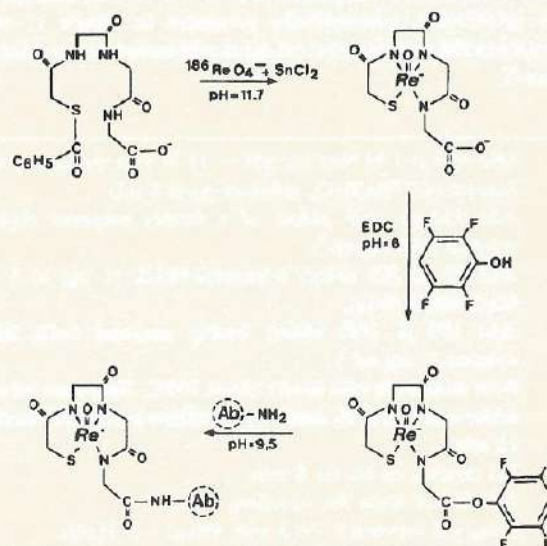
Fig.1.Schematic presentation of the solid phase synthesis of [186]Re-MAG$_3$, its esterification and conjugation to MAbs. For description of the synthesis routings see Table 1 and Fig.2.

1). As such, step 1-20 (Table 1) is the standard protocol for the ^{99m}Tc labeling of MAb E48 [1], 323A3 [13], K928 [14] and chimeric SF-25 (cSF-25)[15] IgG and F(ab')$_2$, which are currently being used in ongoing patient studies at our institute. Part of these clinical studies have been published recently[6]. In general 150-250 mCi ^{99m}Tc is used for labeling, but higher amounts (tested up to 900 mCi) were labeled equally effective. Also the volume in which the [99m]TcO$_4^-$ is added allows a great deal of flexibility. Reaction volumes up to 8 ml did not appear to be a problem. Using 2 mg MAb, ^{99m}Tc-MAb is thus obtained with a total yield of 40 ± 5% (decay corrected), and with a radiochemical purity >97%.

Table 1. Protocol for the preparation of ^{186}Re-MAG$_3$-conjugated MAb IgG/F(ab')$_2$ schematically presented in Figure 1, with reference to the experimental set-up as schematically provided by Figure 2*.

1	Mix 150 μl 1 M Na$_2$CO$_3$ (pH = 11.7) with the appropriate amount of [^{186}Re]ReO$_4^-$ solution (up to 8 ml).
2†	Add 150 μl (120 μMol) of a freshly prepared Na$_2$SO$_3$ solution (100 mg.ml^{-1}).
3‡	Add 25 μl (68 nMol) S-benzoyl-MAG$_3$ (1 mg in 1 ml MeCN/H$_2$O (9:1)).
4‡	Add 100 μl (442 nMol) freshly prepared SnCl$_2$.2H$_2$O solution (1 mg.ml^{-1}).
5§	Heat mixture in tube heater (A) at 100°C. Evaporate solvent under a stream of N$_2$ untill dry. Continue heating for another 15 min.
6	Put mixture on ice for 3 min.
7	Add 500 μl water for injection, vortex.
8¶,**	Bring pH between 5.7-6.3 with 490 μl 1 N H$_2$SO$_4$.
9¶,††	Add 200 μl 2,3,5,6-TFP, 100 mg in 1 ml MeCN/H$_2$O (9:1) and 50 mg EDC as a solid. Vortex, check pH and when necessary readjust pH with 1 N H$_2$SO$_4$ to pH = 5.7-6.3. Incubate at room temperature for 30 min.
10‡‡	Adjust the reaction mixture with H$_2$O to a volume of ± 8 ml.
11	Suck the reaction mixture through two conditioned Sep-pak C$_{18}$ cartridges in series via B,C,C' routing.
12	Suck 20 ml water for injection through the columns via B,C,C' routing for washing.
13	Suck 30 ml 20% (v/v) EtOH/0.01 M sodium phosphate, pH 7.0, through the columns via B,C,C' routing for washing.
14	Suck 10 ml water through the columns via B,C,C' routing for removal of EtOH/phosphate.
15	Suck 0.5 ml ethyl aether through the columns via B,C,C' routing for removal of most of the remaining water.
16¶,§§	Turn valve and elute active ester into the tube with 2.5 ml MeCN via B,D,E routing.
17	Evaporate solvent in the tube heater (A) at 30°C under a stream of N$_2$ via E,F routing.
18$^{\P\P,+\ast\ast}$	Solve active ester in 0.5 ml 0.9% NaCl and add antibody. Adjust pH with 0.05 M Na$_2$CO$_3$ to pH 9.5; incubate at room temperature for 30 min.
19†††	Purify antibody-conjugate by gel filtration on a PD-10 column equilibrated with 0.9% NaCl, elute with 0.9% NaCl.
20	Sterilize the antibody conjugate through a low protein binding 0.22 μm filter.

*Typical example starting from 27.9 nMol [^{186}Re]ReO$_4^-$ solution (1.03 mCi; spec. act. 36.9 μCi/nMol Re).

†Sulphite is added to neutralize the effect of "ageing" of the [^{186}Re]ReO$_4^-$ solution.

‡When using higher nMol amounts of Re, for optimal incorporation of Re into the complex, the Re:MAG$_3$ molar ratio should be taken at 1:2.3, the Re:Sn^{2+} molar ratio at 1:8.

§The tube heater avoids the use of a water- or oilbath in the sterile flow hood.

¶For analysis of the different chemical reaction steps, HPLC analysis can be performed at the end of these steps.

**With 800 nMol Re and consequently 6400 nMol Sn^{2+}, at this point a certain amount of tin colloid formation occurs; however, this does not affect the esterification process, while the colloids are removed/lost during the Sep-pak procedure.

††The amounts used here are in high excess to speed up the esterification process and are present in such amounts that these do not need to be adjusted when using higher nMol amounts of Re.

‡‡This step dilutes the original CH$_3$CN/H$_2$O (1:5) mixture, necessary to avoid elution of a part of the ester into the waste flask.

§§In general at this time 80 ± 5% of the activity is remaining in the form of pure ester.

¶¶Chemical half life of the esterbond in 0.9% NaCl is 7 hr.

$^{+\ast\ast}$The conjugation yield is 50 ± 5% when using 2 mg MAb IgG / F(ab')$_2$ in a reaction volume of 2.5 ml; the conjugation yields are higher when using higher amounts of protein.

†††The first sample consists of the 2.5 ml reaction volume; the labeled protein is collected in the next 3.5 ml fraction; with high ^{186}Re-activity this collection vessel already contains 175 μl of 100 mg.ml^{-1} ascorbic acid solution (final concentration 5 mg.ml^{-1}) for immediate protection against radiolytic decomposition. The next 2 ml fraction is discarded, whereafter the following 8 ml fraction contains the hydrolyzed ^{186}Re-MAG$_3$ (and some ^{186}ReO$_4^-$ formed by radiolytic decomposition during the conjugation process). This ^{186}Re-MAG$_3$ can be reused immediately by adding 200 μl TFP-solution and 50 mg EDC in solid form; after 30 min of incubation repeat steps 11-20, any ^{186}ReO$_4^-$ present is removed during the Sep-pak procedure.
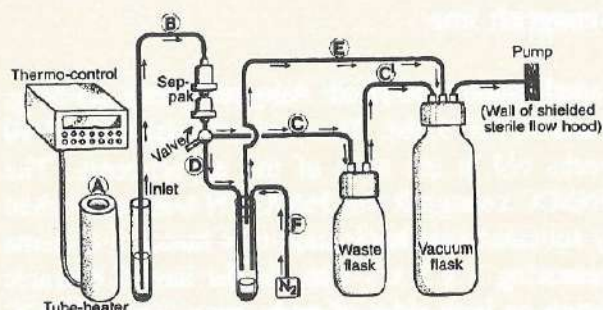
Fig. 2. Schematic presentation of the experimental set up for aseptical labeling of MAbs with ^{99m}Tc or ^{186}Re. For description of the synthe-sis routings see Table 1.

In vitro stability measurements

For measurement of the in vitro stability in relation to the radiolytic decomposition of ^{186}Re- and ^{99m}Tc-labeled MAG$_3$-TFP and MAG$_3$-MAb, aliquots were taken from a stock solution. For a meaningful comparison, all samples possessed the same geometry: 0.5 ml solutions in glass vessels with internal diameter 10 mm. As a result, for each individual isotope the percentage of the energy escaping from the solution or deposited in the glass is the same. As additives with the potential to retard the radiolytic decomposition gentisic acid (2,5-dihydroxybenzoic acid) and ascorbic acid (3-oxo-L-gulofuranolactone) were investigated. From these two additives 25 mg.ml^{-1} stock solutions were made; to 100 μl samples (for the blank, this was 100 μl water) an aliquot of radioactive solution was added, whereafter saline was used as the diluent to 0.5 ml (final concentration antioxidant 5 mg.ml^{-1}).

It is of note that solutions of 5 mg.ml^{-1} ascorbic acid and gentisic acid are acidic solutions (pH 2.3). To assess the stability in 5 mg.ml^{-1} ascorbic acid or gentisic acid solutions at higher pH, the

solutions were brought to that pH with 1 M Na$_2$CO$_3$ before addition of the labeled protein or ester. TLC analysis was performed after 0.5, 1, 2, 3, and 4 hour and subsequently every day untill the 21th day, HPLC analysis was performed once a day.

Monoclonal antibodies

Production and selection of MAb E48 has been described previously. MAb E48 detects a 22 kDa surface antigen, which in normal tissue is present only in stratified squamous and transitional epithelium. So far tested MAb E48 reacted with 90% of the primary head and neck tumors (N=110) and with the majority of cells within these tumors. A comparable reactivity pattern was observed in twenty-six tumor infiltrated lymph nodes from neck dissection specimens [16]. MAb JSB-1 [17], used as isotype matched control antibody in biodistribution studies, as well as 323A3 [13], K928 [14] and cSF-25 [15], used to evaluate the general applicability of the ^{186}Re-labeling procedure, have been described in detail elsewhere. Purification of the antibodies and preparation of F(ab')$_2$ fragments by pepsin digestion of IgG has been described previously [4]. Purity of whole IgG and F(ab')$_2$ preparations was evaluated by SDS polyacrylamide gel electrophoresis under non-reducing conditions and appeared to be more than 95%. The affinity constants were 1.5 x 10^{10} M^{-1} for E48 IgG and 1.2 x 10^{10} M^{-1} for E48 F(ab')$_2$ fragment as determined by Scatchard analysis.

Radioiodination

Radioiodination of F(ab')$_2$ fragments was performed essentially as described by Haisma et

al.[18]; 500 μg of F(ab')$_2$ fragment was mixed with 1 mCi ^{131}I or [125]I. After removal of unbound ^{131}I/[125]I (5-10%), the radiochemical purity was 96% for MAb E48 F(ab')$_2$ and 97% for JSB-1 F(ab')$_2$, respectively.

Immunoreactivity

In vitro binding characteristics of [131]I-, [99m]Tc- and [186]Re- labeled MAb E48 F(ab')$_2$ fragment or IgG were determined in an immunoreactivity assay essentially as described by Lindmo et al. [19]. In short, UM-SCC-22B cells were fixed in 0.1% paraformaldehyde and six serial dilutions, ranging from 5 x 10^{6} cells per tube to 3.1 x 10^{5} cells per tube, were made with 1% bovine serum albumin (BSA) in PBS. 10,000 cpm in case of ^{131}I and [186]Re, or 80,000 cpm in case of ^{99m}Tc, labeled MAb IgG or F(ab')$_2$ fragment were added to the tubes and the samples were incubated overnight at room temperature. Excess unlabeled MAb IgG or F(ab')$_2$ fragment was added to the last sample to determine non-specific binding. Cells were spun down and radioactivity in the pellet and supernatant was determined in a gamma counter and the percentage bound and free radioactivity was calculated (LKB-Wallac 1218 Compu-Gamma). Data were graphically analysed in a modified Lineweaver-Burk plot and the immunoreactive fraction was determined by linear extrapolation to conditions representing infinite antigen excess. The UM-SCC-22B squamous cell carcinoma cell line was derived from a lymph node metastasis of a hypopharyngeal tumor and was kindly provided by Dr. T. Carey, University of Michigan, Ann Arbor, MI [20].

Xenograft line

Female nude mice (Hsd: Athymic nu/nu, 25-32 g, Harlan/CPB, Zeist, The Netherlands) were 8-10 weeks old at the time of the experiments. The HNSCC xenograft line HNX-HN was established by subcutaneous implantation of tumor fragments measuring 3 x 3 x 1 mm, in the lateral thoracic region on both sides of nude mice. The HNSCC xenograft line was established from a T4N2 squamous cell carcinoma of the base of the tonque from a 54-year-old female patient. The expression of the E48 antigen in this xenograft line was demonstrated previously by immuno-histochemistry using the biotin-avidin peroxidase technique [4].

Radioimmunoscintigraphy

Mice were killed by cervical dislocation and scanned with an Ohio γ-camera (Sigma 410 S); 100,000 cpm were obtained and data were stored in a computer (PDP 1134 computer system) for further analysis and production of images.

Biodistribution

In vivo tissue distribution of radiolabeled MAb E48 IgG/F(ab')$_2$ was studied in nude mice bearing the HNSCC xenograft line HNX-HN (150-300 mm^3) or in tumor free nude mice, essentially as described earlier [4]. In short, mice were bled, killed and dissected 24 or 48 hr after i.v. injection of the radioimmunoconjugate. Organs were removed, placed in 5 ml plastic tubes and weighed. Samples were taken from blood, urine, tumor, liver, spleen, kidney, heart, stomach, ileum, colon, bladder, sternum, muscle, lung,

skin and tongue. After weighing, radioactivity in organs and tumors was counted in a gamma counter. The antibody uptake in the tumor and other tissues was calculated as the percentage of the injected dose per gram of tissue (% ID.g^{-1}). Three sets of biodistribution experiments were designed to investigate possible artefacts introduced by the described labeling procedures. In a first experiment to determine the influence of the conjugation of the Re-MAG$_3$ to the MAb on the biodistribution characteristics in tumor bearing nude mice, the biodistribution of ^{186}Re-E48 F(ab')$_2$ was compared with the biodistribution of equimolar amounts of ^{99m}Tc-E48 F(ab')$_2$. The biodistribution of ^{131}I-E48 F(ab')$_2$ and the ^{125}I-labeled control MAb JSB-1 F(ab')$_2$ was described earlier and was taken in this study as a mutual control for the in vivo behaviour of the ^{186}Re- and ^{99m}Tc- labeled E48 F(ab')$_2$. In a second experiment, the influence of the number of Re-MAG$_3$ molecules bound per MAb molecule on the biodistribution characteristics of E48 IgG, labeled with different numbers of Re-MAG$_3$ molecules, was determined. For a comparison, the biodistribution of equimolar amounts of analogously prepared ^{99m}Tc-E48 IgG was determined. To avoid a differential influence of tumors on the biodistribution characteristics of these radioimmunoconjugates in normal tissues, this experiment was performed using tumor free nude mice. Finally, in a third experiment, the tumor targeting properties of ^{186}Re-E48 IgG with a high Re-MAG$_3$:MAb molar ratio was determined.

In all experiments, the ^{99m}Tc-labeling was performed with the same amount of chemical ingredients as with the corresponding ^{186}Re-labeling; both according to the protocols described above. For each experiment, the exact chemical conditions and Re:MAb molar ratios are given in the legend of the corresponding figure.

Results

Chemistry

In the solid phase synthesis as outlined in Table 1 and Figure 1 and 2, [^{186}Re]ReO$_4^-$ was reduced by SnCl$_2$ at pH=11.7 in the presence of Na$_2$SO$_3$ and S-benzoyl-MAG$_3$ to give more than 90% of the ^{186}Re-MAG$_3$. The ^{186}Re-MAG$_3$ yield appeared highly dependent on the heating procedure applied. When the reaction mixture was heated for 10 min. at 100°C, conditions suitable for high yield ^{99m}Tc-MAG$_3$ synthesis, the yield of ^{186}Re-MAG$_3$ was found to be less than 1%. This yield did not increase upon prolonged heating. When the solvent of the reaction mixture was evaporated at 100°C under a stream of N$_2$ untill dry and heating was continued, ^{186}Re-MAG$_3$ formation occurred. In this solid phase synthesis a yield of 90 % or more ^{186}Re-MAG$_3$ was obtained within 15 min. Once formed, ^{186}Re-MAG$_3$ is a stable compound in aqueous solution. Under the reaction conditions described in the protocol (Table 1) the esterification is nearly quantitative. As a result, 80 ± 5% pure ester was obtained after the Sep-pak purification procedure, the experimental set up of which is outlined in Figure 2. In a reaction volume of 2.5 ml, the conjugation yield was 50 ± 5% when using 2 mg MAb IgG or F(ab')$_2$, but was found to be higher when using increasing amounts of protein in the same reaction volume (e.g. 75% with 8-10 mg IgG).

Depending on the amount of protein used, the overall yield was 40-60%. The major proportion of isotope loss is caused by the hydrolysis of

^{186}Re-MAG$_3$-TFP at pH=9.5 during the antibody conjugation step. However, ^{186}Re-MAG$_3$ formed in this way can be recovered from the PD-10 column and be reused immediately by adding 200 μl TFP solution and 50 mg EDC in solid form. After 30 min incubation, steps 11-20 of the protocol can then be repeated for another batch of ^{186}Re labeled antibody.

The concentrations given in the protocol are the standard concentrations used in the ^{99m}Tc labeling of MAbs, and can be applied for Re up to 30 nMol. When using higher nMol amounts of Re, optimal Re-MAG$_3$ formation was obtained when taking the molar ratios S-benzoyl-MAG$_3$:Re as 2.3:1 and Sn^{2+}:Re as 8.0:1. For optimal esterification, no adjustments to the standard protocol, provided by Table 1, are necessary due to the high excess of EDC and TFP. As an example, for a ^{186}Re-MAG$_3$-TFP preparation with 800 nMol [^{186}Re]ReO$_4^-$, 1840 nMol S-benzoyl-MAG$_3$ and 6400 nMol Sn^{2+}, the yield was routinely 80%. Addition of 8-10 mg MAb E48, 323A3, K928 or cSF-25 to this ^{186}Re-MAG$_3$-TFP preparation gave 7-8 Re-MAG$_3$ molecules per MAb molecule without *in vitro* denaturation or precipitation of the protein. As expected [9], the addition of cysteine or desferal as "challenging" agents did not affect the label.

In vitro analysis

Considering the fact that ^{186}Re is a strong ß-emitter, the ^{186}Re-MAG$_3$-MAb conjugate appeared to be fairly stable at low radioactivity concentration; e.g. for a ^{186}Re-MAG$_3$-E48 IgG preparation, 0.12 mCi.ml^{-1} (0.6 mg MAb.ml^{-1}, Re:IgG molar ratio 0.5:1), after 2, 24 and 120 hr at room temperature, the percentage protein bound ^{186}Re

Table 2. Stability of ^{186}Re-MAG$_3$-E48 IgG in 0.9% NaCl with or without ascorbic acid or gentisic acid.

	% protein bound ^{186}Re						
	4h	24h	65h	96h	120h	144h	21days
0.9% NaCl	90.2	65.3	29.0	17.0	10.7	7.5	-
gentisic acid (pH 2.3)	95.6	94.1	93.5	92.6	92.4	92.4	90.5
ascorbic acid (pH 2.3)	95.2	90.7	83.8	80.0	78.0	75.0	65.2
ascorbic acid (pH 3.5)	95.7	94.7	93.8	92.7	92.5	92.0	85.6

The ^{186}Re-labeled protein was added to ascorbic acid and gentisic acid 45 min after end of synthesis. At that time 96% of the ^{186}Re activity was protein bound. pH of the solution in the presence of MAb E48 has been indicated. Percentage protein bound Re was assessed by TLC analysis. Final radioactivity concentration: 2.5 mCi.ml^{-1} (1.16 mg MAb.ml^{-1}, Re:MAb = 3.5:1, specific activity ^{186}Re 92.3 μCi.nMol^{-1} Re). Final antioxidant concentration: 5 mg.ml^{-1}.

was 95.3, 91.0 and 82.8%, respectively (TLC analysis). The effect of radiolytic decomposition was more prominent at higher radioactivity concentrations as demonstrated in Table 2 for a ^{186}Re-MAG$_3$-E48 IgG preparation, 2.5 mCi.ml^{-1} (1.16 mg MAb.ml^{-1}, Re:MAb molar ratio 3.5:1). At 24 and 120 hr, the percentage protein bound ^{186}Re was 65.3 and 10.7%, respectively. The effects of the presence of the antioxidants gentisic acid or ascorbic acid (final concentration 5 mg.ml^{-1}) under the same geometric conditions are also shown in Table 2. The antioxidative capacity of gentisic acid appeared to be strongly pH dependent. Although gentisic acid was found

to be protective at pH 2.3, it became destructive at physiological pH: within 24 hr, all ^{186}Re was detached from the protein. In contrast, ascorbic acid still possessed protective capacity at physiological pH (half life of the ^{186}Re-MAb bond 4.5 days). The optimal antioxidative capacity of ascorbic acid was found to be at pH 3.5. Detach-

ment of [186]Re from the protein was a consequence of reoxidation of the chelated Re. HPLC analysis of the [186]Re-MAG$_3$-TFP ester under forementioned conditions revealed [186]ReO$_4^-$ formation. For the [186]Re-MAG$_3$-TFP ester stored in saline after the Sep-pak procedure (i.e. free from SO$_3^{2-}$ and Sn^{2+}), 75% [186]ReO$_4^-$ formation had taken place within 92 hr. In the presence of gentisic acid or ascorbic acid, this percentage was 11.0 and 11.9%, respectively, while again gentisic acid at physiological pH appeared to be destructive. It is of note that for the ^{99m}Tc-MAG$_3$-TFP ester in a radioactivity concentration of 40 mCi.ml^{-1} exactly the same phenomenon was observed. In saline, 19% [99m]TcO$_4^-$ formation had taken place after 45 hr, in the presence of gentisic acid or ascorbic acid this percentage was 5% in both cases. Also for ^{99m}Tc, gentisic acid was found to be destructive at physiological pH.

Dose calculations show that for relatively short time periods (1 day) addition of ascorbic acid to a final concentration of 5 mg.ml^{-1} is sufficient for protection against radiolytic decomposition. For example, a solution consisting of 9.7 mCi.ml^{-1} (2 mg MAb.ml^{-1}, Re:MAb molar ratio of 7.3:1), which had lost 6% label within 20 min (from 98 to 92%), only lost 0.9% label during the next 4 hr after addition of ascorbic acid, while after 24 hr 89% label was still protein bound. After 3 days this percentage was 75%. A corresponding sample without ascorbic acid showed almost complete loss of protein label at that time. On the basis of these results, collection of the [186]Re-labeled MAb preparation in ascorbic acid was made part of the technical protocol.

The immunoreactive fractions of [186]Re-, [99m]Tc- or ^{131}I-labeled E48 IgG and F(ab')$_2$ fragments at infinite antigen excess were > 95% in all experi-
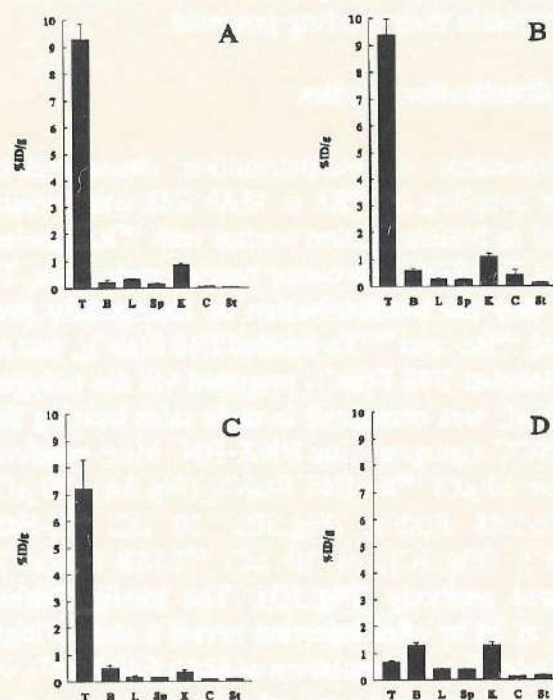
Fig. 3. Biodistribution of radiolabeled E48 F(ab')$_2$ in HNSCC bearing nude mice. (A) 10 µCi [186]Re-, (B) 70 µCi [99m]Tc-, (C) 10 µCi ^{131}I-E48 F(ab')$_2$, (D) 10 µCi ^{125}I-JSB-1 F(ab')$_2$ control antibody. At 24 hr following i.v. injection mice (n=4) were bled, killed, dissected, and the percentage injected dose per gram of tissue (%ID.g^{-1}) was calculated. T, tumor; B, blood; L, liver; Sp, spleen; K, kidney; C, colon; St, sternum. Uptake in organs not shown did not exceed 1%. Starting chemical conditions: 27.9 nMol [[186]Re]ReO$_4^-$ (spec. act. 36.9 µCi.nMol^{-1} Re); 68 nMol S-benzoyl-MAG$_3$; 442 nMol Sn^{2+}; 2 mg E48 F(ab')$_2$; final labeling result 203 µCi.mg^{-1} MAb (molar ratio Re:MAb = 0.55:1). For ^{99m}Tc the same S-benzoyl-MAG$_3$, Sn^{2+} and E48 F(ab')$_2$ amounts were used.

ments. This also holds true for [186]Re-immunoconjugates with the highest Re:MAb molar ratios prepared in these experiments, corresponding with seven to eight Re-MAG$_3$ molecules per MAb molecule, as assessed for MAb E48, 323A3, K928 and cSF-25. These data

indicate that upon coupling of ^{186}Re-MAG$_3$, MAbs fully retain their binding potential.

Biodistribution studies

Maintenance of biodistribution characteristics after coupling of ^{186}Re to MAb E48 was investigated in biodistribution studies with ^{186}Re-labeled MAb E48 F(ab')$_2$ in tumor bearing nude mice. To this end the biodistribution of analogously prepared ^{186}Re- and ^{99m}Tc-labeled E48 F(ab')$_2$, and of ^{131}I-labeled E48 F(ab')$_2$ prepared via the iodogen method, was compared in nude mice bearing the HNSCC xenograft line HNX-HN. Mice received either 10 μCi ^{186}Re-E48 F(ab')$_2$ (Fig.3A), 70 μCi ^{99m}Tc-E48 F(ab')$_2$ (Fig.3B), 10 μCi ^{131}I-E48 F(ab')$_2$ (Fig.3C), or 10 μCi ^{125}I-JSB-1 F(ab')$_2$ control antibody (Fig.3D). The biodistribution data at 24 hr after injection reveal a similar high and selective accumulation of MAb E48 F(ab')$_2$ in the tumor but not in any other organ, irrespective whether labeled with ^{186}Re-, ^{99m}Tc-, or ^{131}I. The %ID.g^{-1} in the tumor was 9.27 $\pm$ 0.58, 9.37 $\pm$ 0.60 and 7.22 $\pm$ 1.07 for ^{186}Re-, ^{99m}Tc- and ^{131}I-labeled E48 F(ab')$_2$ respectively. Uptake in other organs did not exceed 1%. Control ^{125}I-labeled F(ab')$_2$ did not show any specific accumulation in the tumor (Fig. 3d).

^{186}Re-E48 F(ab')$_2$ injected mice were scanned with a γ-camera 24 hr after i.v. injection. Figure 5 shows a representative immunoscintigraphic image with isotope localizing in the xenografts only.

The biodistribution characteristics of ^{186}Re-E48 IgG in nude mice were studied in relation to the number of Re-MAG$_3$ molecules attached to the antibody. Radioimmunoconjugates with either a low Re-MAG$_3$:MAb molar ratio of 0.95:1 or a
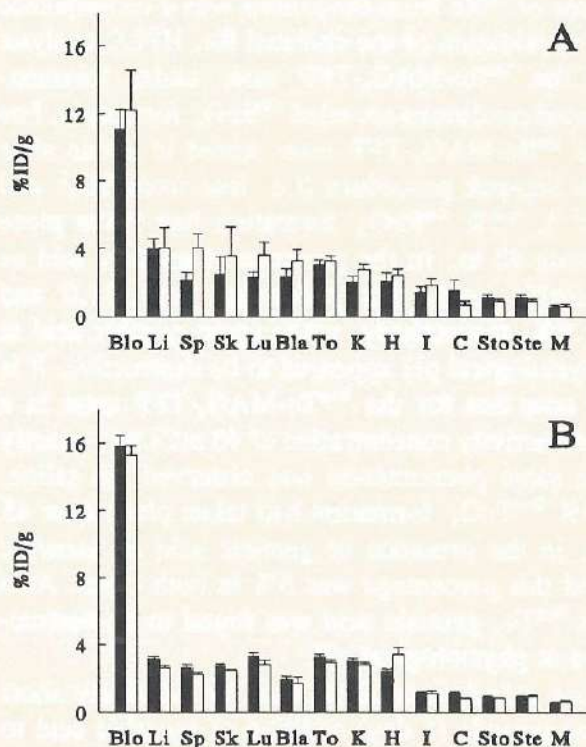
Fig.4. Biodistribution of ^{186}Re-E48 IgG labeled with different numbers of Re-MAG$_3$ molecules per MAb molecule and their corresponding ^{99m}Tc-conjugates in tumor-free nude mice. (A) 230 μCi ^{186}Re-E48 at a Re:MAb molar ratio of 7.17:1 (black bars), compared to 27 μCi ^{186}Re-E48 at a molar ratio of 0.95:1 (open bars), (B) 452 μCi ^{99m}Tc-E48 (black bars) compared to 53 μCi ^{99m}Tc-E48 (open bars) starting from the same amounts of S-benzoyl-MAG$_3$, Sn^{2+} and E48 IgG. At 24 hours following i.v. injection mice (n=6) were bled, killed, dissected, and the % injected dose per gram of tissue (%ID.g^{-1}) was calculated. Blo, blood; Li, liver; Sp, spleen; Sk, skin; Lu, lung; Bla ,bladder; To, tongue; K, kidney; H, heart; I, ileum; C, colon; Sto, stomach; Ste, sternum; M, muscle. Starting chemical conditions: 347 nMol [^{186}Re]ReO$_4^-$ (spec. act. 54.3 μCi.nMol^{-1} Re); 806 nMol S-benzoyl-MAG$_3$; 2.54 μMol Sn^{2+}. At step 18, after dissolution in 0.9% NaCl, the activity was divided in two samples in a ratio of 8:1 and each sample was conjugated to 2 mg E48 IgG (steps 19, 20). Final labeling result Re-"high": 2.57 mCi.mg^{-1} MAb (Re:MAb = 7.17:1); Re-"low": 336 μCi.mg^{-1} MAb (Re:MAb = 0.95:1).
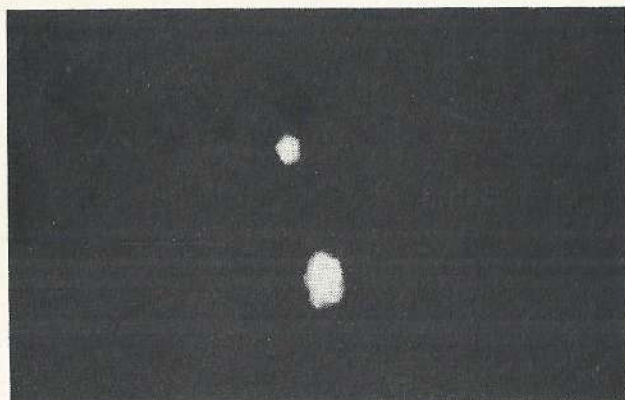
Fig. 5. Whole body scintigraphic image of a nude mouse bearing two subcutaneous HNX-HN xenografts in the flank. Images were taken 24 hr after i.v. injection of 20 μCi ^{186}Re-E48-F(ab')$_2$. Weight of the xenografts: upper 269 mg, lower 581 mg. Position of the mouse: head right, tail left.

Fig. 6. Biodistribution of 200 μCi ^{186}Re-E48 IgG labeled at a Re:MAb molar ratio of 7.35:1 in nude mice bearing HNSCC xenografts. At 48 hours following i.v. injection mice (n=4) were bled, killed, dissected, and the percentage injected dose per gram of tissue (%ID.g^{-1}) was calculated. Tu, tumor; Blo, blood; Li, liver; Sp, spleen; Sk, skin; Lu, lung; To, tongue; Bla, bladder; K, kidney; Sp, spleen; H, heart; Sto, stomach; Ste, sternum; I, ileum; C, colon; M, muscle. Starting chemical conditions: 782 nMol [^{186}Re]ReO$_4^-$ (spec. act. 77.3 μCi.nMol^{-1} Re); 1792 nMol S-benzoyl-MAG$_3$; 5.8 μMol Sn^{2+}; 8.9 mg E48 IgG. Final labeling result: 3.75 mCi.mg^{-1}IgG (Re:MAb = 7.35:1).

high molar ratio of 7.17:1 were injected i.v. at a dose of 27 and 230 μCi respectively, into tumor free nude mice. Mice receiving the ^{186}Re-conjugates were sacrificed 24 hr after injection. Tumor-free nude mice were used to avoid variability in biodistribution introduced by the tumor. The amount of ^{186}Re-activity delivered by the conjugates with low- and high Re-MAG$_3$:MAb molar ratio to the various organs, expressed as the average percentage of radioactivity of the injected dose per gram of tissue (%ID.g^{-1}), is shown in Figure 4A. No obvious differences were found between distribution of the conjugates with low and high Re-MAG$_3$:MAb molar ratios and no selective accumulation of ^{186}Re in any particular organ was observed. The biodistribution of ^{186}Re-conjugates appeared to be similar to the biodistribution of ^{99m}Tc-conjugates prepared starting with the same S-benzoyl-MAG$_3$, Sn^{2+} and MAb E48 IgG amounts and tested in a separate set of experiments (Fig.4B). The tumor targeting pro-

perties of ^{186}Re-E48 IgG with a high Re-MAG$_3$:MAb molar ratio were determined by injecting tumor bearing nude mice with 200 μCi ^{186}Re-E48 IgG. At 48 hr after injection, mice were sacrificed and biodistribution of the radioimmunoconjugate was determined (Fig.6). At this timepoint, 10.4 %ID.g^{-1} was localized in tumor, while only 2.8% ID.g^{-1} localized in the blood. In all other tissues, the %ID.g^{-1} did not exceed 1.2%. In all ^{186}Re-MAb biodistribution experiments described, TCA precipitation of serum samples revealed that 24 hr after injection more than 95% of the ^{186}Re was still protein bound. This percentage did not change during subsequent storage for 10 days at 4^{0}C.

Discussion

Recent data from an ongoing phase I/II trial with intravenously administered ^{99m}Tc-labeled MAb E48 F(ab')$_2$ and IgG in patients with squamous cell carcinoma of the head and neck indicate that both are highly capable of detecting metastatic and recurrent disease [5]. Moreover, MAb E48 was shown to be capable of eradicating head and neck squamous cell carcinoma xenografts grown in nude mice when labeled with ^{131}I [21]. As outlined in the introduction, the efficacy of radioimmunotherapy of head and neck cancer may improve when ^{186}Re-MAb conjugates become available.

In this paper a reproducible labeling procedure, leading to stable and sterile radioimmunoconjugates of MAb E48 with ^{186}Re using S-benzoyl-MAG$_3$, the precursor of ^{99m}Tc-MAG$_3$ used for renal function measurement, is provided in detail. High Re:MAb molar ratios were obtained without impairment of the immunoreactivity or biodistribution properties of the conjugate. For MAb 323A3, K928 and cSF-25 labeled to the same high Re:Mab molar ratio, a similar in vitro stability and retention of immunoreactivity was observed, indicating the general applicability of this labeling procedure (data not shown).

The labeling procedure described in this paper stems from a method developed by Fritzberg et al. [9,10] in which an active ester of TFP and N$_2$S$_2$-pentanoate carrying the radioisotope is prepared, which is subsequently conjugated to amino groups of the antibody. When using the MAG$_3$ chelator, the reported [9,10] reaction conditions to obtain ^{99m}Tc-MAG$_3$ and its corresponding ester appeared to give low and irreproducible yields. Optimal and reproducible yields were obtained when Sn^{2+} was used as reducing agent instead of S$_2$O$_4^{2-}$ while

the preparation of ^{99m}Tc-MAG$_3$-TFP was performed at pH 5.7-6.3 in the absence of phosphate buffer, and at room temperature instead of at 75°C; the presence of phosphate ions was found to retard the rate of esterification.

^{99m}Tc-MAG$_3$-conjugates of MAb E48, 323A3, K928 and cSF-25 F(ab')$_2$ and IgG prepared in this way have been administered (750 MBq, 1 mg) to 40 head and neck cancer patients up till now. The labeling procedure appeared to be highly reproducible and resulted in radioimmunoconjugates of constant quality. Of the conjugates prepared in for these studies, TLC analysis of serum samples taken up to 24 hr after injection revealed that >95% of the ^{99m}Tc was protein bound. HPLC analysis of these serum samples revealed that the protein bound radioactivity was confined to the MAb. Reanalysis after storage at 4°C for 24 hr gave the same results, affirming that this conjugation method does not give transchelation [9]. As determined by the modified Lineweaver-Burk plot, the immunoreactive fraction before injection was consistently > 0.70, while the radioimmunoconjugates retained full binding capacity up to 24 hr after injection.

Although the chemistry of corresponding 4d and 5d metals is often similar, the reaction conditions to form the corresponding compounds are in most of the cases different [21,22]. The MAG$_3$ complexes of Tc and Re form a good example of this difference. While ^{99m}Tc-MAG$_3$ is formed within 10 min of heating at 100°C in water, ^{186}Re only forms its ^{186}Re-MAG$_3$ complex after removal of all water molecules. With the Re concentrations used in this study (25-800 nMol), it appeared that this could easily be accomplished by heating for 15 min after evaporation of the water.

For reproducible labeling results, the presence of

SO_3^{2-} before the addition of S-benzoyl-MAG$_3$ and Sn^{2+} is required. Aqueous [^{186}Re]ReO$_4^-$ solutions suffer from the "ageing" process. A scala of highly reactive radicals and e.g. H$_2$O$_2$ are formed, possibly upto micromole amounts, due to the intense radiation (e.g. a 1 ml solution of 200 mCi [^{186}Re]ReO$_4^-$ - assuming that all ß-particles are absorbed in the solution - has obtained a dose of 3400 krads after 1 day). The amount of reactive species present in the [^{186}Re]ReO$_4^-$ solution to be used for labeling will vary with and depend on the amount/concentration of activity and the time delay between production and use for synthesis. Consequently, oxidation of sulphur atoms of the added MAG$_3$ and consumption of Sn^{2+} ions necessary for the reduction of Re will be variable and possibly complete. The large excess of SO_3^{2-} does not affect the Re-MAG$_3$ formation and is washed away during the Sep-pak procedure.

Once formed the ^{186}Re-MAG$_3$ complex is a stable compound in aqueous solution, that is to say at low specific activities and at low radioactivity concentration. The term "in vitro stability" is often a vague description of a very complex situation. For ^{99m}Tc it can be calculated that about 2% of the total energy is deposited in the solution. At low radioactivity this forms no problem with respect to radiolytic decomposition, but, especially because ^{99m}Tc is nearly carrier free, at high radioactivity this amount cannot be neglected. However, often reducing additives like Sn^{2+} or ß-mercaptoethanol are still present in the solution because a post-purification step was not carried out or the MAb contains internal reducing groups (SH-groups generated by the Schwartz or pre-tinning method [23,24]). For ^{186}Re the amount of energy deposited in the solution is several orders of magnitude higher than for ^{99m}Tc. As a result

the in vitro stability or speed of radiolytic decomposition of a ^{186}Re-protein bond is a function of the specific activity (with the same dose, at low specific activity the ^{186}Re compounds seem to be relatively more stable because more ^{185}Re atoms are reoxidized), the dose (the radioactivity concentration), time delay ("ageing" of the so-lution), the pH [25], the presence of other oxidizable groups (the MAb concentration or added HSA) [26,27], and finally the presence of other constituents of the solution to produce secondary reactive species (e.g. when phosphate ions were present we observed a faster radiolytic decomposition). So although there are undoubtedly diffe-rences in rates and redox chemistry of Tc and Re [21,22,28], these subtle differences are not the main reason why lower valent ^{186}Re compounds are apparently more easily reoxidized than their corresponding ^{99m}Tc compounds. The main reason lies in their differences in decay properties and their concomitant radiolytic decomposition. In this study, the use of antioxidants was shown to suppress the radiolytic decomposition. Addition of ascorbic acid or gentisic acid at low pH ensures the stability of ^{186}Re-MAG$_3$-MAb when stored in vitro untill injection. In contrast to ascorbic acid, gentisic acid at physiological pH caused rapid detachment of ^{186}Re from the protein. On the basis of these results we prefer to add ascorbic acid, which is a safe agent for parenteral administration, to ^{186}Re-MAG$_3$-MAb prepared for in vivo application. The mixture of dissociated and undissociated ascorbic acid molecules at pH 3.5 apparently is the most effective antioxidative additive.

After injection of the ^{186}Re-MAG$_3$-MAb into nude mice, no free ^{186}Re could be detected as became apparent after TCA precipitation of serum

samples directly after bleeding. Even after prolonged storage of these samples no free ^{186}Re could be detected, indicating the stability of the conjugate in serum.

From the three sets of biodistribution experiments described here, it can be concluded that when using the forementioned ^{186}Re labeling procedure, the intrinsic behaviour of the antibody molecule is not obscured by label, chemistry or concentration related artefacts: (1) the tumor targeting capacity of ^{186}Re-E48 F(ab')$_2$, prepared with S-benzoyl-MAG$_3$, Sn^{2+} and E48 F(ab')$_2$ amounts that are used routinely in the ^{99m}Tc protocol for patient studies, was comparable to that of analogously labeled ^{99m}Tc-E48 F(ab')$_2$ and to that of ^{131}I-E48 F(ab')$_2$, (2) biodistribution characteristics and immunoreactivity did not alter for ^{186}Re-E48 IgG conjugates when the Re-MAG$_3$:MAb molar ratio was increased to 7.3:1, and (3) these latter conjugates also appeared highly capable to selectively target to HNSCC xenografts in a way similar to ^{131}I-E48 IgG as shown in previous studies [3-5].

One aspect that might need further investigation is the observation that ^{186}Re-conjugates appear to show a slightly faster blood clearance than their corresponding ^{99m}Tc-conjugates (Fig. 3 and 4). This phenomenon might originate from inter-experimental variability (e.g. the use of a different batch of mice, different xenograft passages). However, it might be that this slightly faster blood clearance of the ^{186}Re-conjugates is a reflection of subtle differences in susceptibility to catabolic processes in the in vivo situation. Therefore, experiments in which ^{186}Re- and ^{99m}Tc-labeled E48 are compared directly upon coinjection in nude mice are currently being initiated.

Several methods for coupling of ^{99m}Tc to monoclonal antibodies have been described [29-33]. Besides methods for indirect coupling also methods for direct coupling are used successfully in clinical immunoscintigraphy studies. Whether direct labeling methods will be suitable for preparation of ^{186}Re-MAb conjugates to be used for clinical RIT studies is questionable in view of the reported in vivo instability of directly labeled ^{186}Re- as well as ^{188}Re-labeled MAbs [26,34]. Besides this, it can be anticipated that for clinical application of directly ^{186}Re-labeled MAbs the Re:MAb ratio should be higher than the 1.34:1 that was e.g. recently reported by Griffiths et al. [26]. With the clinical option in mind to use ^{99m}Tc-MAb imaging to identify ^{186}Re therapy candidates and possibly to use it also for dose calculations we regard direct labeling not the method of choice at this moment.

Methods for indirect labeling of ^{186}Re have also been reported by others. Najafi et al. described a method for ^{186}Re labeling using a N$_2$S$_4$ chelate precoupled to the protein [27,35]. In contrast to the method used here in which the radiolabeled chelate is conjugated to amino groups of MAbs, in this procedure the chelate is coupled to the MAb via a disulfide bond. Although these bonds are potentially less stable in the presence of cysteine or SH-groups of proteins, Najafi et al. showed that MAbs labeled in this way were capable to eradicate tumors in nude mice [27]. Whether this labeling procedure will have a value for general application of ^{186}Re is not clear. Also in this case it can be anticipated that for clinical application the N$_2$S$_4$:MAb molar ratio should be higher than the 1:1 molar ratio used. Higher molar ratios probably make the pre-coupled protein susceptible to aggregate formation.

Goldrosen *et al.* [12] described coupling of ^{186}Re to N_2S_2 or N_3S chelate esters via transchelation at pH$=3$ in the presence of Sn^{2+} and isopropanol at 95^{0}C. As already mentioned in the introduction, for the MAG$_3$ chelate this pre-ester method was found to be inconvenient due to rapid hydrolysis of the ester bond under these circumstances.

^{186}Re-MAb conjugates prepared by this pre-ester method using the N_3S butyrate chelate have been evaluated in animal radioimmunotherapy studies in tumor bearing nude mice [36], as well as in a clinical radioimmunotherapy trial which has been described by Breitz *et al.* [37]. In an editorial accompanying this latter paper, Goldenberg and Griffiths pose some doubts about the clinical utility of the ^{186}Re chemistry developed by this group [38]. For administration of 40-300 mCi ^{186}Re, 36 to 47 mg MAb was used. Assuming the use of ^{186}Re with a specific activity of 2.5 Ci.mg^{-1}, Goldenberg and Griffiths calculated that two to three Re-MAG$_2$-GABA chelates had been coupled to each antibody molecule. They argued that when using commercially available ^{186}Re, which has a lower specific activity (900 mCi.mg^{-1}, NEN Dupont), more antibody will be required than in the study of Breitz *et al.*, thereby limiting the more general application of this labeling technique.

From a chemical point of view the pre-ester method, implying a one-pot reduction, transchelation and conjugation, is with respect to the integrity of the ester bond and the antibody less flexible than the prelabeled chelate approach. The latter method allows a variety of chemical adjustments in chelation conditions before esterification, while the Sep-pak purification step removes all potentially disturbing chemical ingredients before conjugation. In view of the

high Re-MAG$_3$:MAb molar ratios of 7-8:1 that could be realized in this way without apparent impairment of the intrinsic behaviour of the MAb, we regard the specific activity of Re not necessarily a restrictive factor any longer. For administration of 300 mCi ^{186}Re-E48 IgG, ^{186}Re with a specific activity of 900 mCi.mg^{-1} Re can be coupled to 36 mg MAb, the same amount as administered in the study of Breitz *et al.* in which ^{186}Re of high specific activity was used. Obviously, the amount of antibody needed will be less when ^{186}Re of high specific activity becomes available more generally.

Applying labeling strategies described in this paper, initial therapy experiments with ^{186}Re-labeled MAb E48 IgG in nude mice bearing established HNSCC have been started recently. Preliminary results indicate that ^{186}Re-conjugates of MAb E48 are better suited to eradicate HNSCC xenografts than ^{131}I-conjugates. Using a single bolus injection of 400-600 μCi ^{186}Re-labeled MAb E48 IgG all tumors regressed while 36% of the tumors showed complete remission without regrowth during follow up ($>$ 4 months). We feel that the synthesis as outlined in the technical protocol is an important step in our aim to end up with an effective adjuvant radioimmunotherapy strategy for a group of HNSCC patients, who are at risk of developing distant metastases. Reaching the phase of routine clinical application, coupling of high doses of ^{186}Re to MAbs as schematically presented by Figure 2 can be easily automated in a way that recently has been realized at our institute for the synthesis of ^{18}FDG.

References

1. Quak JJ, Balm AJM, van Dongen GAMS, Brakkee JGP, Scheper RJ, Snow GB, Meijer CJLM. A 22-kDa surface antigen detected by monoclonal antibody E48 is exclusively expressed in stratified and transitional epithelia. *Am J Pathol* 136:191-197, 1990.

2. Schrijvers AHGJ, Gerretsen M, Fritz JM, van Walsum M, Quak JJ, Snow GB, van Dongen GAMS. Evidence for a role of the monoclonal antibody E48 defined antigen in cell-cell adhesion in squamous epithelia and head and neck squamous cell carcinoma. *Exp Cell Res* 196:264-269, 1991.

3. Quak JJ, Balm AJM, Brakkee JGP, Scheper RJ, Haisma HJ, Braakhuis BJM, Meijer CJLM, Snow GB. Localization and imaging of radiolabeled monoclonal antibody against squamous cell carcinoma of the head and neck in tumour bearing nude mice. *Int J Cancer* 44:534-538, 1989.

4. Gerretsen M, Quak JJ, Suh JS, van Walsum M, Meijer CJLM, Snow GB, van Dongen GAMS. Superior localization and imaging of radiolabelled monoclonal antibody E48 F(ab')2 fragment in xenografts of human squamous cell carcinoma of the vulva and of the head and neck as compared to monoclonal antibody E48 IgG. *Br J Cancer* 63:37-44, 1991.

5. Gerretsen M, Schrijvers AHGJ, van Walsum M, Braakhuis BJM, Quak JJ, Meijer CJLM, Snow GB, van Dongen GAMS. Radioimmunotherapy of human head and neck squamous cell carcinoma xenografts with 131I-labelled monoclonal antibody E48 IgG. *Br J Cancer* 66:496-502, 1992.

6. van Dongen GAMS, Leverstein H, Roos JC, Quak JJ, van den Brekel MWM, van Lingen A, Martens HJM, Castelijns JA, Visser GWM, Meijer CJLM, Teule GJJ, Snow GB. Radioimmunoscintigraphy of head and neck cancer using 99mTc-labeled monoclonal antibody E48 F(ab')2. *Cancer Res* 52:2569-2574, 1992.

7. Wessels BW, Rogus RD. Radionuclide selection and model absorbed dose calculations for radiolabeled tumour associated antibodies. *Med Phys* 11:638-645, 1984.

8. Coursey BM, Cessna J, Garcia-Torano E. The

standardization and decay scheme of rhenium-186. *Int J Radiat Appl Instrum Part A* **42**:865-869, 1991.

9. Fritzberg AR. Advances in 99mTc-labeling of antibodies. *Nucl Med* **26**:7-12, 1987.

10. Fritzberg AR, Abrams PG, Beaumier PL, Kasina S, Morgan Jr AC, Rao TN, Reno JM, Sanderson JA, Srinivasan A, Wilbur DS, Vanderheyden J-L. Specific and stable labeling of antibodies with technetium-99m with a diamide dithiolate chelating agent. *Proc Natl Acad Sci* **85**:4025-4029, 1988.

11. Kasina S, Rao TN, Srinivasan A, Sanderson JA, Fitzner JN, Reno JM, Beaumier PL, Fritzberg AR. Development and biologic evaluation of a kit for preformed chelate technetium-99m radiolabeling of an antibody Fab fragment using a diamide dimercaptide chelating agent. *J Nucl Med* **32**:1445-1451, 1991.

12. Goldrosen MH, Biddle WC, Pancook J, Bakshi S, Vanderheyden J-L, Fritzberg AR, Morgan Jr AC, Foon KA. Biodistribution, pharmacokinetic, and imaging studies with 186Re-labeled NR-LU-10 whole antibody in LS174T colonic tumor-bearing mice. *Cancer Res* **50**:7973-7978, 1990.

13. Edwards DP, Grzyb KT, Dressler LG. Monoclonal antibody identification and characterization of a Mr 34,000 membrane glycoprotein associated with human breast cancer. *Cancer Res* **46**:1306-1317, 1986.

14. Quak JJ, Schrijvers AHGJ, Brakkee JGP, Davis HD, Scheper RJ, Balm AJM, Meijer CJLM, Snow GB, van Dongen GAMS. Expression and charcterization of two differentiation antigens in stratified squamous epithelia and carcinomas. *Int J Cancer* **50**:507-513, 1992.

15. Takahashi H, Wilson B, Ozturk M, Motte P, Straus W, Isselbacher KJ, Wands JR. In vivo characterization of human colon adenocarcinoma by monoclonal antibody binding to a highly expressed cell surface antigen. *Cancer Res* **48**:6573-6579, 1988.

16. Quak JJ, Gerretsen M, Schrijvers AHGJ, Meijer CJLM, van Dongen GAMS, Snow GB. Detection of squamous cell carcinoma xenografts in nude mice with radiolabelled monoclonal antibodies. *Arch Otolaryngol /Head Neck Surg* 117:1287-1291, 1991.

17. Scheper RJ, Bulte JWM, Brakkee JGP, Quak JJ, van der Schoot E, Balm AJM, Meijer CJLM, Kuiper CM, Lankelma J, Pinedo HM. Monoclonal antibody JSB-1 detects a highly conserved epitope on the P-glycoprotein associated with multi-drug resistance. *Int J Cancer* **42**:389-394, 1988.

18. Haisma HJ, Hilgers J, Zurawski VR. Iodination of monoclonal antibodies for diagnosis and therapy using a convenient one-vial method. *J Nucl Med* **27**:1890-1895, 1986.

19. Lindmo T, Boven E, Cuttitta F, Fedorko J, Bunn Jr PA. Determination of the immunoreactive fraction of radiolabelled monoclonal antibodies by linear extrapolation to binding at infinite antigen excess. *J Imm Meth* **72**:77-78, 1984.

20. Grenman RG, Carey TE, McClatchey KD. In vitro radiation resistance among cell lines established from patients with squamous cell carcinoma of the head and neck. *Cancer* **67**:2741-2747, 1991.

21. Davison A, Orvig C, Trop HS, Sohn M, DePamphilis BV, Jones AG. Preparation of oxobis(dithiolato) complexes of technetOium (IV) and rhenium (V). *Inorg Chem* **19**:1988-1993, 1980.

22. Cotton FA, Wilkinson G. Technetium and rhenium: group VII B. In: *Advanced Inorganic Chemistry*, edited by Cotton FA, Wilkinson G. New York: Wiley, 1988, p. 847-867.

23. Schwarz A, Steinsträsser A. A novel approach to Tc-99m-labelled monoclonal antibodies. *J Nucl Med* **28**:721-727, 1987.

24. Rhodes BA, Zamora PO, Newell KD, Valdez EF. Technetium-99m labelling of murine monoclonal antibody fragments. *J Nucl Med* **27**:685-693, 1986.

25. Portenländer G, Heusinger H. Chemical reactions induced by ultrasound and ´-rays in aqueous solutions of L-ascorbic acid. *Carbohyd Res* **232**:291-301, 1992.

26. Griffiths GL, Goldenberg DM, Knapp Jr FF, Callahan AP, Chang CH, Hansen HJ. Direct radiolabeling of monoclonal antibodies with generator-produced rhenium-188 for radioimmunotherapy: labeling and animal biodistribution studies. *Cancer Res* **51**:4594-4602, 1991.

27. Najafi A, Alauddin MM, Sosa A, Ma GQ, Chen DCP, Epstein AL, Siegel ME. The evaluation of 186Re-labeled antibodies using N2S4 chelate in vitro and in vivo using tumor-bearing nude mice. *Nucl Med Biol* 19:205-212, 1992.

28. Quadri SM, Wessels BW. Radiolabeled biomolecules with 186Re: potential for radioimmunotherapy. *Int J Radiat Appl Instrum Part B* 13:447-451, 1986.

29. Eckelman WC, Paik CH, Steigman J. Three approaches to radiolabeling antibodies with 99mTc. *Int J Radiat Appl Instrum Part B* 16:171-176, 1989.

30. Verbruggen AM. Radiopharmaceuticals: state of the art. *Eur J Nucl Med* 17:346-364, 1990.

31. Hnatowich DJ. Antibody radiolabeling, problems and promises. *Int J Radiat Appl Instrum Part B* 17:49-55, 1990.

32. Srivastava SC, Mease RC. Progress in research on ligands, nuclides and techniques for labeling monoclonal antibodies. *Int J Radiat Appl Instrum Part B* 18:589-603, 1991.

33. Rhodes BA. Direct labeling of proteins with 99mTc. *Int J Radiat Appl Instrum Part B* 18:667-676, 1991.

34. Su F-M, Axworthy DB, Beaumier PL, Fritzberg AR. Pharmacokinetic comparison of Re-186 direct vs. chelate labeled NR-LU-10 MAb in tumored nude mice. *J Nucl Med* 33:910, 1992.

35. Najafi A, Alauddin MM, Siegel ME, Epstein AL. Synthesis and preliminary evaluation of a new chelate N2S4 for use in labeling proteins with metallic radionuclides. *Nucl Med Biol* 18:179-185, 1991.

36. Beaumier PL, Venkatesan P, Vanderheyden J-L, Burgua WD, Kunz LL, Fritzberg AR, Abrams PG, Morgan Jr AC. 186Re radioimmunotherapy of small cell lung carcinoma in nude mice. *Cancer Res* 51:676-681, 1991.

37. Breitz HB, Weiden PL, Vanderheyden J-L, Appelbaum JW, Bjorn MJ, Fer MF, Wolf SB, Ratliff BA, Seiler CA, Foisie DC, Fisher DR, Schroff RW, Fritzberg AR, Abrams PG. Clinical experience with rhenium-186-labeled monoclonal antibodies for radioimmuno-therapy: results of phase I trials. *J Nucl Med* 33:1099-1109, 1992.

38. Goldenberg DM, Griffiths GL. Radioimmunotherapy of cancer: arming the missiles. *J Nucl Med* 33:1110-1112

[186]Re-labeled monoclonal antibody E48 IgG mediated therapy of human head and neck squamous cell carcinoma xenografts

Martijn Gerretsen[1], Gerard W.M. Visser[2], Marijke van Walsum[1],
Chris J.L.M. Meijer[3], Gordon B. Snow[1]
and Guus A.M.S. van Dongen[1]

Departments of Otolaryngology / Head and Neck Surgery[1], Free University Hospital,
Radio Nuclide Center[2], Free University, and Department of Pathology[3],
Free University Hospital, Amsterdam, The Netherlands

Summary

In our laboratory, a solid-phase synthesis of ^{186}Re-MAG$_3$ for reproducible and aseptical production of stable ^{186}Re-monoclonal-antibody-conjugates was recently developed*. Monoclonal antibody (MAb) E48 IgG, when labeled with ^{99m}Tc according to the same labeling procedure, was recently shown to be highly capable of detecting recurrent and metastatic disease in patients with squamous cell carcinoma of the head and neck. In this study, MAb E48 was labeled with ^{186}Re and tested for its capacity to eradicate established human HNSCC xenografts in the nude mouse model. Experimental groups received a single bolus injection of 200 (number of mice (n)=6, number of tumors (t)=11), 400 (n=6, t=11), 500 (n=6, t=12) or 600 (n=5, t=9) μCi ^{186}Re-labeled MAb E48 IgG; control animals were given diluent (n=4, t=8). In the 200 μCi group, 5 of 11 tumors showed regression while the remaining tumors showed a decreased growth rate. In the other treatment groups, all tumors regressed. In all treated groups, complete remissions were observed (no regrowth within 3 months post injection). The number of complete remissions in the 200, 400, 500 and 600 μCi group were 2 of 11 (18.2%), 3 of 11 (27.3%), 6 of 12 (50%) and 3 of 9 tumors (33.3%), respectively. In comparison with the median tumor volume doubling time (TVDT) of the controls, the TVDT in the remaining tumors in the groups receiving 200, 400, 500 and 600 μCi was increased 5.5-, 7.8-, 8.7- and 11.3-fold, respectively. Dosimetry was based on the biodistribution of 200 μCi ^{186}Re-labeled MAb E48 IgG. In the group receiving 600 μCi, the absorbed cumulative radiation dose was 3432 cGy for tumor and 1356 cGy for blood. In other tissues, the accumulated dose was less than 17% of the dose delivered to tumor. Whole body dose was 11-fold lower than the dose delivered to tumor. Toxicity was limited to weight loss which did not exceed 12% and which returned to control levels within 2 weeks. No treatment related deaths occured. These data suggest RIT with ^{186}Re-labeled MAb E48 IgG to be a feasible approach for the treatment of head and neck cancer.

Introduction

Although improvement of surgery and radiotherapy has resulted in an increase in the locoregional control of HNSCC, no enhancement of the overall 5-year survival rate of patients has been achieved [1,2]. The major cause of death in this group of patients has gradually shifted from uncontrolled locoregional disease to distant metastases and second primary tumors, for which there is no adequate therapy at this moment. In search for more specific and effective therapeutical methods, we are focussing on the use of MAbs labeled with radioisotopes for RIT. An important rationale for this approach with respect to HNSCC, is the intrinsic sensitivity of this tumor type for radiation [3]. Experimental RIT has been described for various tumor types [4-10]. Sofar, introduction of RIT into the clinic has not answered to the high expectations yet [11]. From the first clinical trials it has become clear that the percentage of

injected dose taken up in large tumors is still an order of magnitude too low, and therapeutic ratios are still very low. At present RIT is most succesful in microscopic residual disease. Major issues that are currently under investigation are the generation of MAbs with higher specificity and the development of improved conjugates using radioisotopes with appropriate radiophysical characteristics. Re-cently, we have developed a panel of MAbs with high specificity to HNSCC [12-14]. One of these antibodies, designated E48, recognizes a 18-22 kDa cell surface molecule that is exclusively expressed on stratified squamous epithelia and transitional epithelium. Strong reactivity of MAb E48 towards primary as well as metastatic HNSCC was observed. Recent data indicate that the E48 antigen is involved in the structural organization of squamous tissue at the level of intercellular adhesion [15]. Ongoing phase I/II clinical studies with intravenously administered ^{99m}Tc-labeled MAb E48 IgG and F(ab')$_2$ fragment indicate that MAb E48 is highly capable of detecting metastatic and recurrent disease in patients with HNSCC [16]. In these studies, accumulation of the radioimmunoconjugate in tumors of 0.5-4.0 cm diameter was shown to be 0.030 %ID.g^{-1} (range 0.014-0.082, number of patients=7), implicating the possibility to achieve radiation doses in small tumor nodules and cell clusters that are sufficient for the treatment of minimal residual disease. In nude mice bearing HNSCC xenografts, we demonstrated a dose dependent growth delay, regression and complete remissions with injection of single doses ^{131}I-labeled MAb E48 IgG [17]. However, ^{131}I is not the isotope of choice for clinical applications because of the low percentage therapeutic ß-emission (32%), the high percentage γ-radiation (66%) and because of the rapid dehalogenation of ^{131}I-labeled conjugates. Therefor, we pursued the development of a MAb E48 radioimmunoconjugate labeled with [186]Re. With a half-life of 3.7 days, 9% γ-emission with ideal energy for imaging (137 KeV), and 91% ß-emission of 1.07 KeV, [186]Re theoretically seems to be better suited for RIT than [131]I. MAbs labeled with this isotope have already been described in experimental tumor localization and therapy studies [18-20] as well as in phase I clinical trials [21]. Despite the recent progress in [186]Re chemistry, further improvements are needed before [186]Re-MAb conjugates can be applied more generally for clinical purposes. A major limitation is the low specific activity of commercially available [186]Re [27]. In our laboratory, a solid phase synthesis of [186]Re-MAG$_3$ was developed, adapted from the method of Fritzberg et al. [21]. These studies resulted in a efficient and reproducable technical protocol for aseptic labeling of stable [186]Re-MAb conjugates with an isotope:Mab molar ratio as high as 7.3, enabling preparation of [186]Re-MAb conjugates for clinical purposes. Studies in HNSCC bearing nude mice with tracer doses revealed biodistribution characteristics of [186]Re-MAb E48 comparable to the biodistribution characteristics of [131]I- and ^{99m}Tc-labeled MAb E48. In the present study investigating the therapeutic efficacy of single doses [186]Re-labeled MAb E48 IgG, we observed a dose dependent growth delay and a high percentage of regressions and complete remissions of established tumors in HNSCC bearing nude mice.

Material and methods

Monoclonal antibodies

MAb E48, a murine antibody of the IgG1 sub-
class, was raised against a metastasis of a mod-
erately differentiated SCC of the larynx [12]. The
MAb E48 defined antigen is expressed by 90%
of the primary head and neck tumors tested
sofar (n=110) and by a majority of the cells
within these tumors. In 26 tumor infiltrated
lymph nodes from neck dissection specimens, a
comparable reactivity pattern was observed.
Affinity purified MAb E48 was obtained as an
aseptical and virus-inactivated solution from
Centocor Europe Inc., Leiden, The Nether-
lands.

Xenografts

Female nude mice (Hsd: Athymic nu/nu, 25-32
g, Harlan/CPB, Zeist, the Netherlands) were 8-
10 weeks old at the time of the experiments.
The HNSCC xenograft line HNX-HN was
established by subcutaneous implantation of
tumor fragments measuring 3x3x1 mm, in the
lateral thoracic region on both sides of nude
mice. Therafter, the xenograft line was main-
tained by serial transplantation [24]. The tumor
from which the HNX-HN line originates was a
T4N2M0 squamous cell carcinoma of the base
of the tongue from a 54-year-old female patient.
As determined by indirect immunoperoxidase
staining, the expression pattern of the MAb E48
defined antigen in the HNX-HN line was com-
parable to the pattern of the majority of human
HNSCC tumors [25].

^{186}Re labeling

^{186}Re-perrhenate (^{186}ReO$_4^-$) was obtained from
Mallinckrodt Medical, Petten, The Netherlands
at a specific activity of 78 μCi.nMol^{-1}, concen-
tration 47.1 mCi.ml^{-1}. 62.5 mCi ^{186}ReO$_4^-$ was
reduced by 1320 μl SnCl$_2$ (1 mg.ml^{-1}) in the
presence of 150 μl of 1 M Na$_2$CO$_3$, 150 μl
NaSO$_3$ (100 mg.ml^{-1}), and 700 μl S-benzoyl-
mercaptoacetyltriglycerine (MAG$_3$, 1 mg in 1
ml MeCN:H$_2$O=9:1). The final pH of this
mixture was 11.7. MAG$_3$ or betiatide, the
chelating agent used for renal function measure-
ment, was a gift from Mallinckrodt. The mix-
ture was heated under a stream of N$_2$ until dry,
and from that time on the heating was continued
for another 15 minutes. Esterification and coup-
ling of ^{186}Re-MAG$_3$ was performed essentially
as described by Fritzberg et al. [23]. In short, the
pH was brought between 5.7-6.3 by addition of
440 μl of 1 N H$_2$SO$_4$ and the ^{186}Re-MAG$_3$ com-
plex was esterified with 200 μl 2,3,5,6-tetraflu-
orophenol (TFP, Jansen Chimica, Beerse, Bel-
gium, 100 mg in 1 ml MeCN/H$_2$O=9:1) in the
presence of 50 mg 1-ethyl-3-(3-dimethylamin-
opropyl)-carbodiimide (EDC, Jansen Chimica).
The resulting active ester was purified by two
conditioned C$_{18}$ cartridges (Waters, Millipore,
MA, USA). The mixture was loaded on these
colums and washed with 20 ml H$_2$O, 30 ml
20% (vol/vol) ethylalcohol/0.01 M sodium
phosphate, pH=7.0, 10 ml H$_2$0, and 0.5 ml
ethyl aether. The active ester was eluted with
2.5 ml MeCN and the solvent was subsequently
evaporated at 30^{0}C under a stream of N$_2$. The
purified ester was solved in 0.5 ml 0.9%NaCl,
and 2 ml MAb E48 IgG (4.5 mg.ml^{-1}) was
added. The pH was adjusted with 0.05 M

Na_2CO_3 to pH=9.5. After 30 min. at room temperature, the ^{186}Re-MAG$_3$-E48 IgG conjugate was purified by gelfiltration on a Sephadex-G25 column (Pharmacia-LKB, Woerden, The Netherlands) equilibrated with 0.9% NaCl. For protection against radiolytic self-decomposition, vitamin C was added to the purified radioimmunoconjugate, to a final concentration of 5 mg.ml^{-1}, pH=3.5. The labeling procedure is schematically presented in Fig.1.

Quality control and stability of ^{186}Re-labeled MAb E48 IgG

HPLC analysis of the ^{186}Re-labeled MAG$_3$ and the corresponding MAG$_3$-TFP ester was performed on a LKB 2150 HPLC pump coupled to a LKB 2152 LC controller with a gradient elution on a 250 x 4.6 mm lichrosorb 10 RP 18 column (Chrompack, Middelburg, The Netherlands). Solution A consisted of a 5:95 mixture of EtOH and a 0.01 M sodium phosphate buffer + 0.015 M sodium azide pH = 6 solution; solution B was a 9:1 mixture of MeOH and H_2O. Gradient (flow rate 1 ml.min^{-1}): 10 min 100% A, 10 min 100% A → 100% B, 10 min 100% B. Radioactivity was detected continuously by an Ortec 406A single channel analyzer connected to a Drew 3040 Data collector (Betron Scientific, Rotterdam, The Netherlands) and fractions of 1 ml were collected on a LKB 2212 Helirac. Comparison of the injection standard with the total effluent from the HPLC column showed in all cases a quantitative recovery of the activity (>98%) from the HPLC column. Analysis of labeled MAb E48 IgG was performed by thin layer chromatography (TLC) on silicagel impregnated glass fiber sheets (Gel-
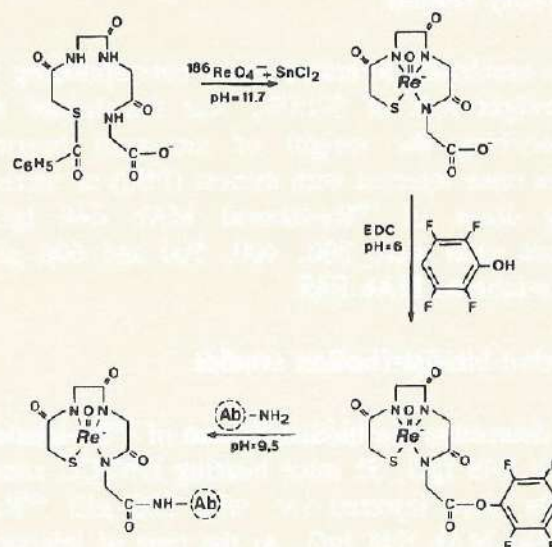
Figure 1: Schematic presentation of the solid phase synthesis of Re-MAG$_3$, esterification of the Re-MAG$_3$ complex and its conjugation to MAb E48 IgG.

man Sciences Inc., Ann Arbor, MI, USA), thickness 0.3 mm, eluent 0.1 M citric acid, pH 7.0.

After labeling, the immunoreactive fraction of the radioimmunoconjugate was determined essentially as described by Lindmo et al.[26]. Using paraformaldehyde fixed cells of the cell line UMSCC-22B, a gift from Dr T.E. Carey (Ann Arbor, MI, USA), a serial dilution was incubated with 10,000 cpm of ^{186}Re-labeled MAb E48. Radioactivity in pellet and supernatant were determined and data were graphically analyzed in a modified Lineweaver-Burke plot. Immunoreactivity was calculated by extrapolation to conditions representing infinite antigen excess.

Toxicity studies

The maximum tolerated dose, corresponding to a weight loss of 5-15%, was determined by monitoring the weight of xenograft bearing nude mice injected with diluent (PBS) or increasing doses of [186]Re-labeled MAb E48 IgG. Doses used were 200, 400, 500 and 600 μCi [186]Re-labeled MAb E48.

In vivo biodistribution studies

To determine the biodistribution of [186]Re-labeled MAb E48 IgG, 33 mice bearing HNSCC xenografts were injected i.v. with 200 μCi [186]Re-labeled MAb E48 IgG. At the time of injection the estimated xenograft volume was 405 ± 271 mm^3 (n=51) as determined by measuring the tumor in 3 dimensions with calipers ((LxWxH)/2). Mice were bled, killed and dissected 3 and 8 hours and 1, 2, 4, 7, and 10 days after i.v. injection. Organs were immediately removed, placed in 5 ml plastic tubes and weighed. Samples were taken from blood, urine, tumor, liver, spleen, kidney, heart, stomach, ileum, colon, bladder, sternum, muscle, lung, skin and tongue. After weighing, radioactivity in all organs and tumors was counted in a gamma counter. The antibody uptake in the tumor and other tissues was calculated as the percentage of the injected dose per gram of tissue (% ID.g^{-1}).

Therapy studies

Mice bearing 1 or 2 xenografts with a volume between 50 and 250 mm^3 were given a single intravenous injection of 200 (n=6, t=11), 400 (n=6, t=11), 500 (n=6, t=12) or 600 (n=5, t=9) μCi [186]Re-labeled MAb E48 IgG. Control groups were given diluent (n=4, t=8). Groups were randomized for initial tumor volume, for diluent 157 ± 52 (mean $\pm$ s.e.m.), for 200 μCi 191 ± 114, for 400 μCi 112 ± 68, for 500 μCi 125 ± 69 and for 600 μCi 140 ± 60. At day 1, 2, and 3, and thereafter weekly, cages were cleaned to remove excreted radioactivity. During the first week mice were weighed daily and tumor size was determined daily as described earlier. After the first week weight and tumor size were determined twice a week. Mice were sacrificed when total tumor burden exceeded 1000 mm^3.

Dosimetry calculations

Dosimetry calculations were performed using the data of the biodistribution of 200 μCi [186]Re-labeled MAb E48 IgG. Complete and uniform ß-particle absorption was assumed in both tumor and whole body, ignoring the contribution of γ-energy absorption. The absorbed cumulative radiation dose for tumor and various organs was calculated using the trapezoid integration method for the area under the curve [27]. The final segment of the area under the curve was calculated based on the biological halflife: dose of last segment = dose previous segment (day 7 - day 10) x 0.693(t½ in previous segment)$^{-1}$. cGy were further calculated by multiplying the μCi.h.g^{-1} by the g.cGy.(μCi.h)$^{-1}$ factor published by the Medical Internal Radiation Dose commitee for [186]Re of 0.73 [28]. For the estimation of whole body dose, blood, skin, muscle and bone were taken as 8.0, 18.4, 44.5, and 4.7% of the body weight, respectively, as
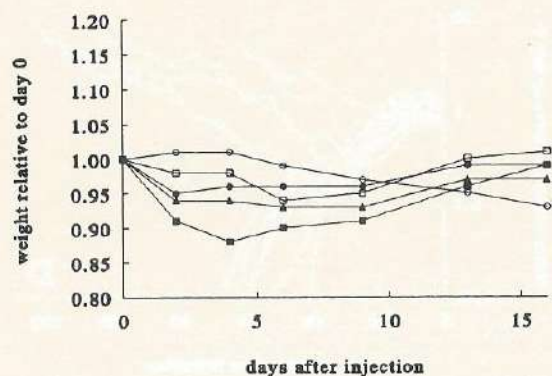
Figure 2: Toxicity of [186]Re-labeled MAb E48 in nude mice bearing HNX-HN xenografts monitored as the bodyweight relative to day 0, diluent (o), 200 μCi (●), 400 μCi (▲), 500 μCi (□) and 600 μCi (■). Values are the mean of 5-6 mice per dose, standard deviations were less than 3%.

Figure 3: Biodistribution of 200 μCi [186]Re-labeled MAb E48 in nude mice bearing HNX-HN xenografts. Mice were bled, killed and dissected 3 and 8 hrs and 1, 2, 3, 7, and 10 days after injection and the % injected dose.gram[-1] (%ID.g[-1]) was calculated and plotted vs time. Tumor (■), blood (●) and liver (▲) are shown.

determined by Beaumier et al. [19]. The mean weight of liver, spleen, kidney, heart, stomach and lung was calculated from the 33 mice used inthe biodistribution study. These tissues accounted for 84% of the total body weight, for which the estimated dose was corrected.

Evaluation of therapeutic efficacy

Tumor bearing mice were treated with RIT when tumors reached a volume of at least 50 mm³ (range 50-250 mm³). Tumors smaller than 50 mm³ at the time of injection were not included in the determination of the tumor volume doubling time because of inaccuracy in measuring these tumors. Tumor growth was expressed as the tumor volume at each timepoint relative to the tumor volume at day 0. Efficacy of RIT was expressed by the increase in the mean tumor volume doubling time (TVDT) of the treated animals as compared to the TVDT of the control group. Prolonged sur-

vival (survival defined as the time period between day 0 and the timepoint of sacrifice, being when total tumor burden exceeded 1000 mm³) was determined by comparing experimental groups with treatment groups using the Mann-Whitney U-test.

Results

Labeling and *in vitro* analysis

The efficiency of [186]Re incorporation in MAG$_3$ was 87%, after which 86% was recovered as active ester. Conjugation of 73% of the active ester to the MAb resulted in an overall yield of radioactivity of 54.6%. Specific activity of the conjugate was 3.8 mCi.mg^{-1}, which corresponds with a Re:MAb ratio of 7.35:1. *In vitro* stability studies showed that in the presence of vitamin C, 96% of the radioactivity was bound to IgG at the moment of injection, whereas 87% of the radioactivity was still bound to protein
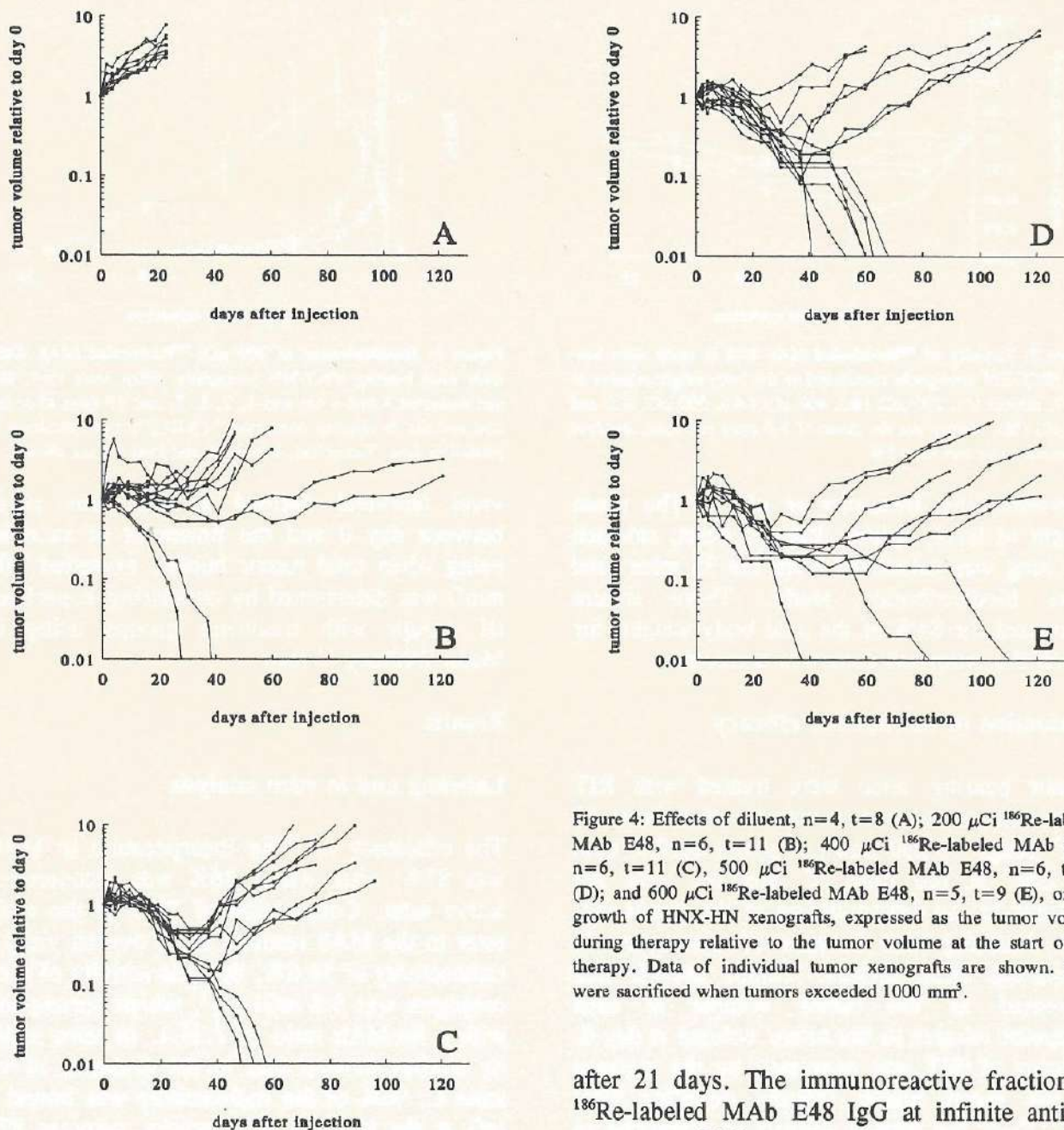
Figure 4: Effects of diluent, n=4, t=8 (A); 200 μCi [186]Re-labeled MAb E48, n=6, t=11 (B); 400 μCi [186]Re-labeled MAb E48, n=6, t=11 (C), 500 μCi [186]Re-labeled MAb E48, n=6, t=12 (D); and 600 μCi [186]Re-labeled MAb E48, n=5, t=9 (E), on the growth of HNX-HN xenografts, expressed as the tumor volume during therapy relative to the tumor volume at the start of the therapy. Data of individual tumor xenografts are shown. Mice were sacrificed when tumors exceeded 1000 mm³.

after 21 days. The immunoreactive fraction of [186]Re-labeled MAb E48 IgG at infinite antigen excess was 95%.

Toxicity studies

The MTD, defined as the dose resulting in a maximum reversible weight loss of 15%, was determined at 600 μCi (Fig.2). At this dose, no treatment related deaths were observed.

Biodistribution and *in vivo* stability

The biodistribution of 200 μCi ^{186}Re-labeled MAb E48 IgG is shown in Figure 3. Radioactivity measured in the blood is 14.9 %ID.g^{-1} at 3 hours post injection and thereafter rapidly decreases. Radioactivity in tumors increases during the first 2 days to 10.4% ID.g^{-1} and thereafter gradually decreases to 3% ID.g^{-1} at day 10. No specific or nonspecific accumulation is observed in any other tissue. For *in vivo* stability determination, TCA precipitation of serum samples taken at day 1, 2, 3 and 4 was performed immediately and after 10 days and revealed more than 95% of the activity to be protein bound at both timepoints.

Therapeutic efficacy

Tumor growth expressed as the tumor volume at each timepoint relative to the tumor volume at day 0 for control and treatment groups is shown in Figure 4A-4E. Tumors in the groups receiving diluent (Fig.4A) showed exponential growth. Median tumor volume doubling time in the group receiving diluent was 6.3 days. Tumors in the group receiving 200 μCi ^{186}Re-labeled MAb E48 IgG (Fig.4B) showed delay of growth (3 of 11) or regression (6 of 11) with a median tumor volume doubling time of 39.8 days, while 2 out of 11 tumors showed com-

plete remission without regrowth during follow-up (> 4 months). All tumors in the group receiving 400 μCi ^{186}Re-labeled MAb E48 IgG (Fig.4C) regressed, with a median tumor volume doubling time of 58.5 days (t=7, 1 tumor did not reach a double volume during follow up), while 3 out of 11 tumors showed complete remission. In the group receiving 500 μCi ^{186}Re-labeled MAb E48 IgG, all tumors showed regression with a median tumor volume doubling time of 64.9 days (t=6), while 6 out of 12 tumor showed complete remission (Fig.4D). Finally, in the group receiving 600 μCi ^{186}Re-labeled MAb E48, again all tumors showed regression, with a median tumor volume doubling time of 84.6 days (t=5, 1 tumors did not reach a double volume during follow up), while 3 out of 9 tumors showed complete remission (Fig.4E). The increase in mean TVDT for the 200, 400, 500 and 600 μCi group was 5.5, 7.8, 8.7, and 11.3, respectively. Statistical analysis showed significant differences in survival between control and all treatment groups (p < 0.05). When treatment groups were compared with each other, only the 200 and 600 μCi group differed significantly. When the 200 μCi group was compared with the 400, 500, and 600 μCi group as a whole, these groups did differ significantly. After sacrificing animals with complete remissions, no evidence of tumor could be detected at the site of implantation.

Dosimetry

For the group receiving 600 μCi, the absorbed cumulative radiation dose for tumor and various organs, based on the area under the curve of the biodistribution data of 200 μCi ^{186}Re-labeled
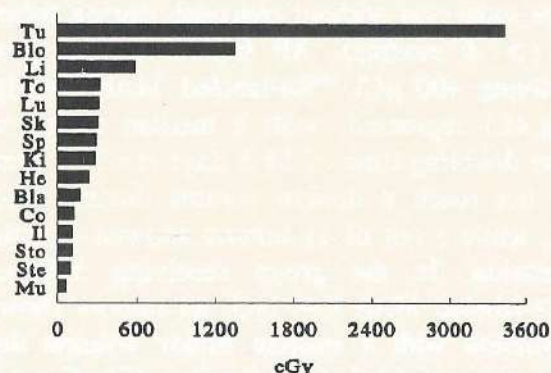
Figure 5: Total accumulated radiation dose in cGy, calculated using the trapezoid integration method for the area under the curve. Tu, tumor; Blo, blood; Li, liver; To, tongue; Lu, lung; Sk, skin; Sp, spleen; Ki, kidney; He, heart; Bla, bladder; Co, colon; Il, ileum; Sto, stomach; Ste, sternum; Mu, muscle.

MAb E48 IgG, is shown in Figure 5. The ratio doses of tumor : blood was 2.5, tumor : liver 5.8, tumor : tongue 10.6 and for all other tissues this ratio was always greater than 11.6. The ratio tumor dose : whole body dose was 11.

Discussion

With respect to physical parameters of importance for the development of radioimmunoconjugates for radioimmunotherapy, ^{186}Re is a very suitable isotope. In our laboratory, an efficient and reproducible solid-phase synthesis of ^{186}Re-MAG$_3$ for the aseptical production of stable ^{186}Re-MAb conjugates, adapted from the method described by Fritzberg et al. [23], was developed. In this way, rasioimmunoconjugates were obtained from MAbs E48, 323A3 [29], K928 [13], and chimeric SF-25 [30] with a Re:MAb ratio of 7:1 to 8:1 without loss of immunoreactivity. In this study we examined the efficacy of the thus

obtained ^{186}Re-labeled MAb E48 (ratio Re:MAb = 7.35:1) to eradicate human squamous cell carcinoma xenografts in the nude mouse model. With the dose range used in this study (200 - 600 µCi), growth delay, regression and complete remissions of established tumors was observed. Dose dependency was observed only when comparing the 200 µCi group versus the 400, 500 and 600 µCi group as a whole, although when comparing the latter groups there was a tendency of increasing tumor volume doubling time with increasing dose. Dosimetry calculations showed that with an accumulated dose in the range of 1144-3432 cGy, complete remissions of 18.2-50% could be achieved. Moreover, the low toxicity that was observed indicates that even higher doses might be tolerated without causing treatment related deaths. In pilot experiments preceeding these studies, injection of an intermediate dose of 400 µCi ^{186}Re-labeled isotype-matched control antibody (Myoscint^R, Centocor, Malvern) did not affect tumor growth.

TCA-precipitation of serum samples obtained from animals used for determination of the biodistri-bution of the radioimmunoconjugate indicated that the conjugate was highly stable in vivo. More than 95% of the radioactivity was found to be protein bound in serum samples obtained 1-4 days p.i.. This percentage did not change during subsequent storage for 10 days at 4^{0}C. In vitro, the ^{186}Re-MAb preparation used for injection and containing the antioxidant vitamin C also appeared highly stable.

The small differences in anti-tumor efficacy between the 4 treatment groups as observed in this study may be due to the heterogeneous distribution of the radioimmunoconjugate

throughout the tumor, resulting in overkill in certain tumor areas, and leaving other areas relatively unaffected. Heterogeneous distribution is more likely a result of restricted penetration of the conjugate into the tumor rather than of heterogeneous E48 antigen expression in the HNX-HN xenograft line [25]. Preliminary data indicate that the efficacy of RIT with 600 μCi [186]Re-labeled MAb E48 IgG is better when treating small tumors. Mice bearing HNX-HN xenografts with a mean volume of 70 mm[3] were all cured. These data indicate that for treatment of large tumors, serial doses of [186]Re-labeled MAb E48 may be recommended, thus overcoming heterogeneous dose delivery.

In therapy experiments described by Beaumier et al. [19], with [186]Re-labeled NR-LU-10 labeled according to the protocol described by Fritzberg et al. [23], 23% complete remissions were obtained in a multiple dose-protocol, with total doses of 400 and 600 μCi. When taking the groups receiving 400, 500 or 600 μCi in our study as a whole, 33% complete remissions were obtained with single bolus injections. Moreover, Beaumier et al. report an estimated LD$_{50/30}$ of 600 μCi, corresponding with a total body dose of 880 cGy. In our study, the total body dose at 600 μCi, calculated as described by Beaumier et al, was only 312 cGy, possibly explaining the low toxicity observed. Most likely, these differences can be explained by the differences in antibody characteristics like isotype, rather than by differences in the [186]Re labeling procedure used in these studies. In the study of Beaumier et al., an IgG2b MAb was used, showing a relatively slow clearance from the blood and thus contributing to a high total body dose.

Using a labeling procedure in which the chelating agent N,N,N,N,-tetrakis(2-mercaptoethyl)ethylenediamine (N_2S_4) was used to label MAbs with [186]Re, Najafi et al. [20] describe partial and complete remissions of tumors in RIT experiments after 1 or 2 injections of 500 μCi. No biodistribution data are available to determine accumulated doses in tumor and normal tissues. Moreover, as was also stressed by Goldenberg and Griffiths [22], it remains doubtfull whether this method of labeling will yield conjugates with specific activities that are high enough to allow patient studies.

Recently, we reported on the efficacy of RIT with ^{131}I-labeled MAb E48 IgG in the same nude mouse model [17]. In this study, a single bolus injection of 400 μCi ^{131}I-labeled MAb E48 IgG, resulted in growth delay and regression of tumors but no complete remissions. After a single bolus injection of 800 μCi ^{131}I-labeled MAb E48 IgG, corresponding with an accumulated dose of 12,170 cGy in the tumor, 2 of 7 tumors (29%) showed complete remission without regrowth during follow up (>3 months). In the studies performed with [186]Re-labeled MAb E48 IgG, complete remission were observed with all doses, with 33% complete remissions in a dose range of 2,288 - 3,432 cGy. Based on these data it is tempting to speculate that [186]Re-labeled MAb E48 IgG is more effective in irradicating HNSCC than ^{131}I-labeled MAb E48 IgG under conditions resulting in apparent equivalent radiation doses delivered to the tumor. However, the validity of directly compa-

ring the efficacy of the radioimmunoconjugates used in these two studies in relation to dosimetry is questionable, since apparent differences in tumor accumulation and retention of the conjugates were observed. These differences may be due to (1) the fact that for the assessment of the biodistribution of radiolabeled MAb E48 and subsequent dosimetry calculations, different doses of ^{131}I- and ^{186}Re-labeled MAb E48 were used, (2) minor differences in xenograft passages with respect to tumor volume doubling time and antigen expression, or (3) differences in the intrinsic behaviour of ^{131}I- and ^{186}Re-labeled MAb E48. This latter possibility however, does not seem likely, since administrations of tracer doses of ^{131}I- and ^{186}Re-labeled MAb E48 to nude mice bearing HNX-HN xenografts of the same passage showed similar biodistribution characteristics[*].

Experiments in which ^{131}I- and ^{186}Re-labeled MAb E48 IgG are compared directly with respect to biodistribution and therapeutic efficacy in the nude mouse model are currently being performed.

MAb E48 is the first MAb to be described for succesfull RIT of human squamous cell carcinoma of the head and neck in nude mice. Shikani et al. [31] reported on ^{90}Y-labeled antibody therapy for squamous cell carcinoma of the head and neck. In this study a polyclonal antibody preparation was used, which implicates limitations with respect to availibility and excludes the possibility of humanization or chimerization, thus increasing the possibility of HAMA-responses when using such a preparation in a multiple-dose regimen in clinical trials. Moreover, with the dose range used in their study, severe toxicity was observed with the higher doses, whereas no complete remissions were obtained. Finally, biodistribution and dosimetry data provided in their study are restricted to the ratio of deposited activity between tumor and normal organs, being 2 to 3 times higher in tumor. It remains questionable if such experimentally obtained ratios will result in ratios with therapeutic efficacy in a clinical setting.

Most clinical trials with radiolabeled MAb for diagnosis or therapy of solid neoplasms have reported MAb uptake in large tumors in the range of 0.001-0.01 %ID.g^{-1} [32,33]. Preliminary data on the localization of ^{99m}Tc-labeled MAb E48 IgG indicate accumulation of the conjugate in tumors of 0.5-4.0 cm diameter up to a mean of 0.030 % ID.g^{-1} at 44 hrs (range: 0.014-0.082, number of patients=7). This looks very promising indeed, when taking into account the higher accumulation of MAbs in small tumor loads. Chatal et al. [34] reported on the biodistribution of ^{111}In-labeled MAb OC125 intraperitoneally injected into patients with ovarian carcinoma, demonstrating low accumulation in large tumors (0.0014-0.0032 %ID.g^{-1}) but significantly higher accumulation in small tumor nodules (0.13 $\pm$ 0.08 %ID.g^{-1}) and malignant cell clusters (median 0.33 with a maximum of 4.16 %ID.g^{-1}). Assuming that this size correlation also applies for head and neck tumors and assuming that patients will tolerate a dose of 60 mCi.m^{-2} ^{131}I-labeled MAb E48 [6,10], we previously stated that achieving radiation doses in tumor tissue enabling elimination of minimal residual disease lies within reach. As shown in this paper, ^{186}Re-labeled MAb E48 might even be better suited for RIT, especially when taking into account that patients seem to tolerate much

higher doses of [186]Re-labeled MAbs than of ^{131}I-labeled MAbs. As demonstrated by Breitz, the first phase I clinical trials investigating the pharmacokinetics, toxi-city and MTD of a [186]Re-labeled MAb IgG and F(ab')$_2$ fragments showed that dose-limiting myelosup-pression was observed at 120 mCi.m^{-2} for IgG and at 150 mCi.m^{-2} for F(ab')$_2$ for heavily pretreated patients [21]. In patients with minimal treatment prior to entering this trial, no MTD for F(ab')$_2$ was reached at 200 mCi.m^{-2}. At our department, preparations for a phase I clinical trial with [186]Re-labeled chimeric MAb E48 IgG are currently in progress.

References

1. Choksi AJ, Dimery IW, Hong WK. Adjuvant chemotherapy of head and neck cancer: the past, the present and the future. *Seminars in Oncol* 15:45s-49s, 1988.

2. Cognetti EV, Pinnaro P, Carlini P, Ruggeri EM, Impiobato FA, Rosarion Del Vecchio M, Gianarelli D, Perrino A. Neoadjuvant chemotherapy in previously untreated patients with advanced head and neck squamous cell cancer. *Cancer* 62:251-261, 1988.

3. Wessels BW, Harisiadis L, Carabell SC. Dosimetry and radiobiological efficacy of clinical radioimmunotherapy. *J Nucl Med* 30:827, 1989.

4. Lee Y-C, Washburn LC, Sun TT, Byrd BL, Crook JE, Holloway EC, Steplewski Z. Radioimmunotherapy of human colorectal carcinoma xenografts using 90Y-labeled monoclonal antibody CO17-1A prepared by two bifunctional chelating techniques. *Cancer Res* 50:4546-4551, 1990.

5. Lee Y-S, Bullard DE, Zalutsky MR, Coleman RE, Wikstrand CJ, Friedman HS, Colapinto EV, Bigner DD. Therapeutic efficacy of antiglioma mesenchymal extracellular matrix ^{131}I-labeled murine monoclonal antibody in a human glioma xenograft model. *Cancer Res* 48:559-566, 1988.

6. Ward B, Mather S, Shepherd J, Crowther M, Hawkins L, Britton KE, Slevin ML. The treatment of intraperitoneal malignant disease with monoclonal antibody guided ^{131}I radiotherapy. *Br J Cancer* 58:658-662, 1988.

7. Smith A, Groscurth P, Waibel R, Westera G, Stahel RA. Imaging and therapy of small cell carcinoma xenografts using ^{131}I-labeled monoclonal antibody SWA11. *Cancer Res* 50:980s-984s, 1990.

8. Senekowitsch R, Reidel G, Mollenstadt S, Kriegel H, Pabst H-W. Curative radioimmunotherapy of human mammary carcinoma xenografts with iodine-131-labeled monoclonal antibodies. *J Nucl Med* 30:537, 3092.

9. Chiou RK, Vessella RL, Limas C, Shafer RB, Elson MK, Arfman EW, Lange PH. Monoclonal antibody-targeted radiotherapy of renal cell carcinoma using the nude mouse

model. *Cancer* 61:1766-1775, 1988.

10. Rosen ST, Zimmer AM, Goldman-Leikin R, Gordon LI, Kazikiewicz JM, Kaplan EH, Variakojis D, Marder RJ, Dykewicz MS, Piergies A, Silverstein EA, Roenigk HH, Spies SM. Radioimmuno-detection and radioimmunotherapy of cutaneous T cell lymphomas using an ^{131}I-labeled monoclonal antibody: an Illinois Cancer Council Study. *J Clin Oncol* 5:562-573, 1987.

11. Britton KE, Buraggi GL, Bares R, Bischof-Delaloye A, Buell U, Emrich D, Granowska M. A brief guide to the practice of radioimmunoscintigraphy and radioimmunotherapy in cancer. Report of the European Association of Nuclear Medicine Task Group on the clinical utility of radiolabeled antibodies. *Int J Biol Markers* 4:106-118, 1989.

12. Quak JJ, Balm AJM, van Dongen GAMS, Brakkee JGP, Scheper RJ, Snow GB, Meijer CJLM. A 22-kd surface antigen detected by monoclonal antibody E48 is exclusively expressed in stratified and transitional epithelia. *Am J Path* 136:191-197, 1990.

13. Quak JJ, Schrijvers AHGJ, Brakkee JGP, Davis HD, Scheper RJ, Balm AJM, Meijer CJLM, Snow GB, van Dongen GAMS. Expression and characterization of two differentiation antigens in stratified epithelia and carcinomas. *Int J Cancer* 50:507-513, 1992.

14. Quak JJ, van Dongen GAMS, Gerretsen M, Hayashida D, Balm AJM, Brakkee JGP, Snow GB, Meijer CJLM. Production of a monoclonal antibody (K931) to a squamous cell carcinoma associated antigen identified as the 17-1A antigen. *Hybridoma* 9:377-387, 1990.

15. Schrijvers AHGJ, Gerretsen M, Fritz JM, van Walsum M, Quak JJ, Snow GB, van Dongen GAMS. Evidence for a role of the monoclonal antibody E48 defined antigen in cell-cell adhesion in squamous epithelia and head and neck squamous cell carcinoma. *Exp Cell Res* 196:264-269, 1991.

16. van Dongen GAMS, Leverstein H, Roos JC, Quak JJ, van den Brekel MWM, van Lingen A, Martens HJM, Castelijns JA, Visser GWM, Meijer CJLM, Teule GJJ, and Snow GB. Radioimmuno-scintigraphy of head and neck cancer using ^{99m}Tc-labeled monoclonal antibody E48 F(ab')2. *Cancer Res* 52:2569-2574, 1992.

17. Gerretsen M, Schrijvers AHGJ, van Walsum M, Braakhuis BJM, Quak JJ, Meijer CJLM, Snow GB, van Dongen GAMS. Radioimmunotherapy of human head and neck squamous cell carcinoma xenografts with ^{131}I-labelled monoclonal antibody E48. *Br J Cancer* 66:496-502, 1992.

18. Goldrosen MH, Biddle WC, Pancook J, Bakshi S, Vanderheyden J-L, Fritzberg AR, Morgan Jr AC, Foon KA. Biodistribution, pharmacokinetics and imaging studies with [186]Re-labeled NR-LU-10 whole antibody in LS174T colonic tumor-bearing mice. *Cancer Res* 50:7973-7978, 1990.

19. Beaumier PL, Venkatesan P, Vanderheyden J-L, Burgua WD, Kunz LL, Fritzberg AR, Abrams PG, Morgan Jr AC. [186]Re radioimmunotherapy of small cell lung carcinoma xenografts in nude mice. *Cancer Res* 51:676-681, 1991.

20. Najafi A, Alauddin MM, Sosa A, Ma GQ, Chen DCP, Epstein AL, Siegel ME. The evaluation of [186]Re-labeled antibodies using N2S4 chelate in vitro and in vivo using tumor-bearing nude mice. *Nucl Med Biol* 19:205-212, 1992.

21. Breitz HB, Weiden PL, Vanderheyden J-L, Appelbaum JW, Bjorn MJ, Fer MF, Wolf SB, Ratlif BA, Seiler CA, Foisie DC, Fisher DR, Schroff RW, Fritzberg AR, Abrams PG. Clinical experience with rhenium-186-labeled monoclonal antibodies for radioimmunotherapy: results of phase I trials. *J Nucl Med* 33:1099-1109, 1992.

22. Goldenberg DM, Griffiths GL. Radioimmunotherapy: arming the missiles. *J Nucl Med* 33:1110-1112, 1992.

23. Fritzberg AR, Abrams PG, Beaumier PL, Kasina S, Morgan Jr AC, Rao TN, Reno JM, Sanderson JA, Srinivasan A, Wilbur DS, Vanderheyden J-L. Specific and stable labeling of antibodies with technetium-99m with a diamide dithiolate chelating agent. *Proc Natl Acad Sci USA* 85:4025-4029, 1988.

24. Braakhuis BJM, van Dongen GAMS, Bagnay M, van Walsum M, Snow GB. Preclinical chemotherapy of human head and neck cancer xenografts grown in athymic nude mice. *Head & Neck* 11:511-515, 1989.

25. Gerretsen M, Quak JJ, Suh JS, van Walsum M, Meijer CJLM, Snow GB, van Dongen GAMS. Superior localisation and imaging of radiolabelled monoclonal antibody E48 F(ab')2 fragment in xenografts of human squamous cell carcinoma of the head and neck and of the vulva as compared to monoclonal antibody E48 IgG. *Br J Cancer* 63:37-44, 1991.

26. Lindmo T, Boven E, Luttita F. Determination of the immunereactive fraction of radiolabelled monoclonal antibodies by linear extrapolation to binding at infinite antigen excess. *J Imm Methods* 72:77-89, 1984.

27. Badger CC, Krohn KA, Shulman H, Flournoy N, Bernstein ID. Experimental radioimmunotherapy of murine lymphoma with ^{131}I-labeled anti-T cell antibodies. *Cancer Res* 46:6223-6228, 1986.

28. Dillman LT. Radionuclide Decay Schemes and Nuclear Parameters for Use in Radiation-Dose Estimation. *MIRD Pamphlet No.4. New York: The Society of Nuclear Medicine.* 1969.

29. Edwards DP, Grzyb KT, Dressler LG, Mansel RE, Zava DT, Sledge GW, McGuire WL. Monoclonal antibody identification and characterization of a Mr 43,000 membrane glycoprotein associated with human breast cancer. *Cancer Res* 46:1306-1317, 1986.

30. Takahashi H, Wilson B, Ozturk M, Motte P, Strauss W, Isselbacher KJ, Wands JR. In vivo localization of human colon carcinoma by monoclonal antibody binding to a highly expressed cell surface antigen. *Cancer Res* 48:6573-6579, 1988.

31. Shikani AH, Richtsmeier WJ, Klein JL, Kopher KA. Radiolabeled antibody therapy for squamous cell carcinoma of the head and neck. *Arch Otolaryngol /Head Neck Surg* 118:521-525, 1992.

30. Goldenberg DM. Challenges to the therapy of cancer with monoclonal antibodies. *J Natl Cancer Inst* 83:78-79, 1991.

31. Epenetos AA, Kosmas C. Monoclonal antibodies for imaging and therapy. *Br J Cancer* 59:152-155, 1989.

32. Chatal J-F, Saccavini J-C, Thedrez P, Curtet C, Kremer M, Guerreau D, Nolibe D, Fumoleau P, Guillard Y. Biodistribution of Indium-111-labeled OC125 monoclonal antibody intraperitoneally injected into patients operated on for ovarian carcinomas. *Cancer Res* 49:3087-3094, 1989.

Direct comparison of the biodistribution of ^{131}I- and ^{186}Re-labeled monoclonal antibody E48 IgG in tumor-bearing nude mice; complete ablation of small head and neck squamous cell carcinoma xenografts with ^{186}Re-labeled monoclonal antibody E48 IgG

Martijn Gerretsen[1], Gerard W.M Visser[2], Ruud H. Brakenhoff[1],
Marijke van Walsum[1], Gordon B. Snow[1],
Guus A.M.S. van Dongen[1]

Department of Otolaryngology / Head and Neck Surgery[1], Free University Hosptital,
Radio Nuclide Center[2], Free University, Amsterdam, The Netherlands

Summary

Direct comparison of the biodistribution of simultaneously injected [131]I- and [186]Re-labeled MAb E48 IgG in nude mice bearing small (58 $\pm$ 31 mm^3) head and neck squamous cell carcinoma (HNSCC) xenografts revealed differences in terms of maximum percentage of the injected dose per gram (%ID.g^{-1}) in tumor and in terms of differences in distribution in non-tumor tissues. ^{131}I-labeled MAb E48 IgG reached a maximum %ID.g^{-1} of 78.3% at day 7, the maximum %ID.g^{-1} of [186]Re-labeled MAb E48 IgG was 53.1% at day 7. The relatively high maximum %ID.g^{-1} in tumor of both radioimmunoconjugates in the small xenografts used in comparison with previous experiments using larger xenografts strongly suggest a correlation between size of the tumor and the amount of localizing radioactivity. In non-target organs, a significant higher uptake of [186]Re-labeled MAb E48 IgG vs. ^{131}I-labeled MAb E48 IgG was observed after 2 hrs in the liver, 12.3 $\pm$ 1.3 vs. 6.8 $\pm$ 1.2. The initial high uptake of the [186]Re-conjugate rapidly decreased and reached ^{131}I-conjugate levels within 48 hrs. These data may be indicative for different metabolic patterns of these radioimmunoconjugates.

To investigate whether the therapeutic efficacy of RIT will be enhanced when treating small xenografts, mice bearing 75 $\pm$ 17 mm^3 HNSCC xenografts were treated with 600 μCi [186]Re-labeled MAb E48 IgG. All tumors completely regressed and did not regrow during follow-up (> 150 days). Control tumors showed exponential growth. One mouse in the treatment group died after recovering from an unacceptable weight loss of 35%. In all other mice weight loss did not exceed 10%. These data implicate that [186]Re-labeled MAb E48 may be especially suited to cure small tumors.

Introduction

In Chapters 4 and 6, the efficacy of respectively [131]I- and [186]Re-labeled monoclonal antibody (MAb) E48 IgG in eradicating established head and neck squamous cell carcinoma (HNSCC) xenografts was investigated. In order to perform dosimetric calculations in these studies, the biodistribution characteristics of [131]I- and [186]Re-labeled MAb E48 IgG were also determined. Data obtained from these studies implicated considerable differences in biodistribution characteristics of these radioimmunoconjugates. Using 800 μCi ^{131}I-labeled MAb E48 IgG in nude mice bearing xenografts of 323 $\pm$ 244 mm^3, a maximum %ID.g^{-1} in tumor of 19.4% was reached at day 3 while %ID.g^{-1} in tumor at day 28 was still 8.1%. Using 200 μCi [186]Re-labeled MAb E48 IgG in nude mice bearing xenografts of 407 $\pm$ 271 mm^3, the maximum %ID.g^{-1} in tumor only reached a value of 10.4% at day 3 and thereafter decreased to 3% at day 10. However, since these experiments were not carried out under the exact same conditions, definite conclusions could not be made. Factors like xenograft passage; tumor size; batch of animals; amount of injected radioimmunoconjugate, in terms of radioactivity as well as protein; these are all likely to be of influence on the biodistribution of radioimmunoconjugates. In order to make a direct comparison of the biodistribution characteristics of [131]I- and [186]Re-labeled MAb E48 IgG, the two radioimmunoconjugates were injected simultaneously into nude mice bearing HNSCC xenografts.

In a report describing one of the first studies on

the utility of [186]Re-labeled MAbs for RIT, Beaumier *et al.* mentioned preliminary data showing increased efficacy of RIT when treating small xenografts [1]. In 16 mice bearing tumors of 65.8 $\pm$ 50.4 mm^3, 3 remissions of > 140 days and a prolonged mean tumor growth delay of 53 days was observed. In 10 mice with tumors of 17 mm^3, 100% durable complete remissions were achieved. In Chapter 6, a single dose of 600 μCi [186]Re-labeled MAb E48 IgG was shown to give an 11.3-fold increase in the tumor volume doubling time, and 33.3% complete remissions. The initial volume of these tumors was 140 $\pm$ 60 mm^3. Based on the biodistribution of 200 μCi [186]Re-labeled MAb E48 IgG, the absorbed cumulative tumor dose in animals receiving 600 μCi was estimated to be 3,432 cGy. To assess a possible size-respons relationship in our xenograft model, mice bearing small xenografts (75 $\pm$ 17 mm^3) were injected with a single bolus injection of 600 μCi [186]Re-labeled MAb E48 IgG.

Material and methods

Animals and xenografts

Femal nude mice (Hsd: Athymic nu/nu, 20-25 g, Harlan/CPB, Zeist, The Netherlands) were 6 weeks old at the time of the experiments. The HNSCC xenograft line HNX-HN, described in Chapters 3, 4, 5 and 6, was used.

[131]I- and [186]Re-labeling

Labeling of MAb E48 IgG with [186]Re was performed as described in Chapter 5 and 6.
Labeling of MAb E48 IgG with ^{131}I was performed as described in Chapter 3, 4, 5 and 6.

Quality control of [131]I- and [186]Re-labeled MAb E48 IgG

In vivo and *in vitro* stability and immunoreactivity of the radioimmunoconjugates was performed as described in Chapter 5 and 6.

Biodistribution studies

Nude mice bearing HNX-HN xenografts were simultaneously injected with 100 μCi [186]Re-labeled MAb E48 IgG (15.5 μg) and 10 μCi ^{131}I-labeled MAb E48 IgG (3.2 μg). At the time of injection the estimated xenograft volume, as determined by measuring the tumor in 3 dimensions with calipers ((LxWxH)/2), was 58 $\pm$ 31 mm^3. Mice were bled, killed and dissected 2 and 8 hours and 1, 2, 3, 7, 10 and 13 days after i.v. injection. Organs were immediately removed, placed in 5 ml plastic tubes and weighed. Samples were taken from blood, tumor, liver, spleen, kidney, heart, stomach, ileum, colon, bladder, sternum, muscle, lung, skin, lung and skin. After weighing, radioactivity in organs and tumor was counted in a dual isotope gamma counter. Standards were included to correct for the contribution of both isotopes to each other's window setting. The antibody uptake for both isotopes was calculated as the percentage of the injected dose per gram of tissue (%ID.g^{-1}).

Radioimmunotherapy

Mice bearing 2 xenografts were given a single i.v. injection of 600 μCi [186]Re-labeled MAb E48 IgG (n=6, t=12) or diluent (n=6, t=12). Initial tumor volumes for the 600 μCi group and the control group was 75 $\pm$ 17 mm^3 and 54 $\pm$ 18

mm³, respectively. To monitor toxicity, mice were weighed daily the first week and thereafter twice a week untill they had recovered from weight loss. Tumors were measured once a week.

Dosimetry estimations

Dosimetry calculations were performed using the biodistribution data of 100 μCi ^{186}Re-labeled MAb E48 IgG. The absorbed dose for tumor and various organs were calculated using the trapezoid integration for the area under the curve as described in Chapter 6. The final segment of the area under the curve was calculated based on the biological half life: dose of last segment = dose of previous segment (day 10-13) x 0.693 x (t½ in previous segment)$^{-1}$. Uniform biodistribution of radioactivity was assumed. cGy were further calculated by multiplying the μCi.h.g^{-1} by the g.cGy.(μCi.h)$^{-1}$ factor for ^{186}Re of 0.73, as published by the Medical Internal Radiation Dose commitee. Furthermore, correction for non-absorbed radiation was performed by multiplying with an infinit volume boundary correction factor of 0.75. This absorbed fraction was calculated as follows: for a number of emissions (n=10), the decay location and emission direction were randomly selected. For each ß-particle, the average fraction of its energy absorbed in the tumor was calculated using a point kernel approach [2,3]. For the estimation of whole body dose, blood, skin, muscle and bone were taken as 8.0, 18.4, 44.5, and 4.7% of the body weight, respectivily. The mean weight of liver, spleen, kidney, heart, stomach, and lung were calculated from the 25 mice used in the biodistribution study. These tissues account for 84% of the total body weight, for which the estimated dose was corrected.
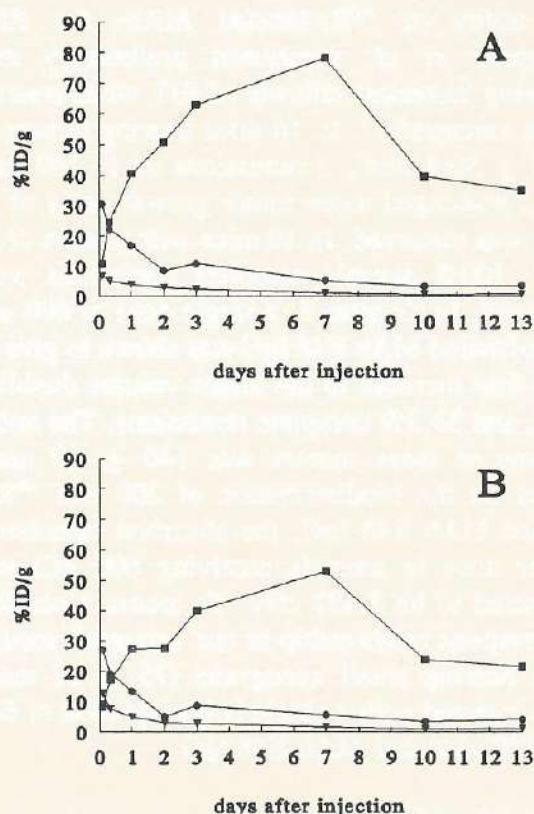
Figure 1: Biodistribution of 10 μCi ^{131}I- (A) and 100 μCi ^{186}Re-labeled MAb E48 (B) in nude mice bearing HNX-HN xenografts. Mice were bled, killed and dissected 2 and 8 hrs and 1, 2, 3, 7, 10, and 13 days after injection. The % injected dose.gram^{-1} (%ID.g^{-1}) was calculated and plotted vs time. Tumor (■), blood (●) and liver (▲) are shown.

Results

Labeling, quality control and immunoreactivity

The specific activity of ^{131}I-labeled MAb E48 IgG was 3.12 mCi.mg^{-1}. MAb E48 IgG was labeled with ^{186}Re to a Re : MAb molar ratio of 8.8 : 1. The specific activity of ^{186}Re-labeled MAb E48

Table I. Tumor to non-tumor ratios for [131]I- and [186]Re-labeled MAb E48 IgG.

| | 2 hrs | | 8 hrs | | day 1 | | day 2 | | day 3 | | day 7 | | day 10 | | day 13 | |
	[186]Re	[131]I	[186]Re	[131]I	[186]Re	[131]I	[186]Re	[131]I	[186]Re	[131]I	[186]Re	[131]I	[186]Re	[131]I	[186]Re	[131]I
Blood	0.31	0.34	0.95	1.11	1.99	2.43	6.03	7.21	4.68	5.82	9.48	14.99	8.19	12.80	6.15	11.10
Liver	0.65	1.53	2.33	4.87	5.50	10.52	9.82	18.71	14.59	26.73	35.10	68.31	27.47	60.01	23.14	49.54
Spleen	1.45	1.95	4.61	6.31	8.21	11.35	16.36	21.35	20.35	27.11	42.96	77.00	48.45	80.32	31.74	60.22
Lung	1.45	1.77	3.32	4.09	7.98	9.77	11.56	12.45	13.94	16.12	39.84	48.73	22.20	32.06	20.57	32.36
Muscle	17.85	20.48	22.94	26.38	42.33	50.22	69.85	81.29	72.31	89.48	213.87	305.57	102.29	143.41	114.98	150.26
Kidney	1.56	1.91	4.63	5.62	9.72	12.50	16.75	20.51	21.60	28.96	45.81	69.02	33.78	57.06	26.04	46.28
Heart	1.42	1.62	3.53	4.22	7.83	9.62	15.26	17.26	31.29	39.24	56.31	97.70	55.27	75.89	36.45	58.60
Colon	7.69	9.46	17.18	21.54	38.13	47.39	53.72	66.18	54.11	62.42	148.05	208.87	77.66	115.90	65.18	124.10
Ileum	4.36	4.01	14.43	12.43	32.67	33.14	51.14	48.62	68.48	77.02	125.27	161.01	129.90	156.77	81.30	152.99
Stomach	5.50	5.41	15.57	17.48	28.21	21.38	46.25	35.55	71.02	68.63	147.05	101.59	100.09	92.51	77.73	56.55
Bladder	4.99	5.49	9.82	11.79	9.76	11.82	14.37	14.71	20.47	22.35	28.67	43.51	23.22	42.04	20.70	34.73
Sternum	4.89	5.77	9.71	11.52	20.29	24.95	31.45	39.19	51.64	62.60	89.64	156.85	66.23	104.57	46.38	91.24
Tongue	1.93	2.15	4.00	4.64	8.61	10.40	14.27	15.65	22.13	26.39	33.12	46.05	33.41	54.54	22.23	40.86
Skin	3.08	3.35	4.96	5.85	7.38	8.67	13.40	14.71	19.45	21.48	34.05	42.73	32.36	40.27	23.64	37.55

E48 IgG was 6.44 mCi.mg⁻¹. Immunoreactivity of [131]I- and [186]Re-labeled MAb E48 IgG was > 70%.

Biodistribution of [131]I- and [186]Re-labeled MAb E48 IgG

The biodistribution of 10 μCi ^{131}I-labeled MAb E48 IgG and 100 μCi [186]Re-labeled MAb E48 IgG are shown in Figure 1A and 1B. For ^{131}I, the initial %ID.g⁻¹ in blood was 30.3% at 2 hrs, 15.4% at 24 hrs, and thereafter steadily decreased. Activity in tumor increased from 10.6% at 2 hrs to 78.3% at 7 days, and thereafter decreased. No abnormal nonspecific accumulation in any organ was observed. For [186]Re, the initial %ID.g⁻¹ in blood was 26.4% at 2 hrs, 17.0% at 24 hrs, and thereafter steadily decreased. Activity in tumor increased from 8.2% at 2 hrs to 53.1%

at day 7, and thereafter decreased. No abnormal nonspecific accumulation was observed except in liver, where after 2 hrs, 12.3 %ID.g⁻¹ was observed (vs. 6.8 %ID.g⁻¹ for ^{131}I). This nonspecific accumulation thereafter decreased but consequently remained approximately 2-fold higher than ^{131}I accumulation in the liver. The tumor to non-tumor ratios at each time point of both radioimmunoconjugates are shown in Table I. For [131]I- as well as [186]Re-labeled MAb E48 IgG, all ratios increased during the first 7 days and then started to decrease from day 10 on. The ratio [131]I : [186]Re shows a tendency to increase slightly, indicating somewhat better retention characteristics for ^{131}I-labeled MAb E48 IgG. Due to the high uptake in tumor of both radioimmunoconjugates, the ratios observed in this study were higher than observed in previous experiments.
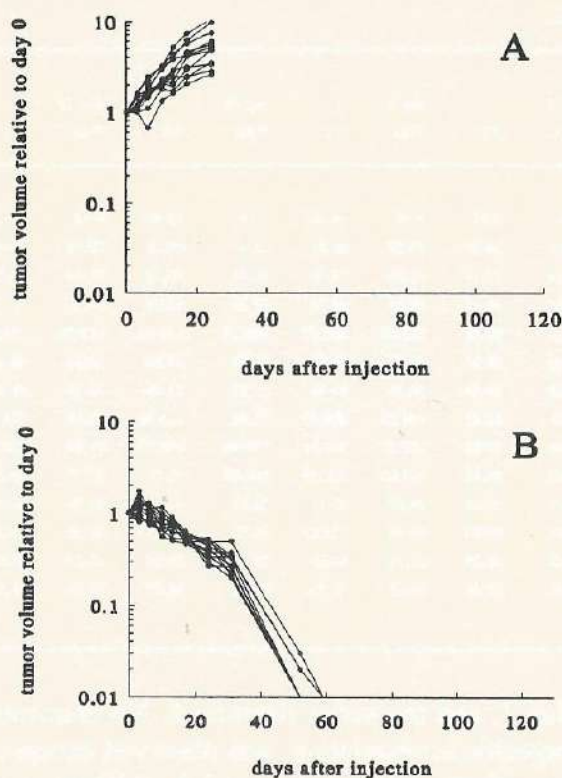
Figure 2. Effects of diluent (n=4, t=8) (A) and 600 μCi ^{186}Re-labeled MAb E48 IgG (n=6, t=12) (B), on the growth of HNX-HN xenografts, expressed as the tumor volume during therapy relative to the tumor volume at the start of therapy. Mice were sacrificed after passing a number of tumor volume doubling times or when tumor size exceeded 1000 mm^3.

Radioimmunotherapy

Tumor growth expressed as the tumor volume at each timepoint relative to the tumor volume at day 0 for control and treatment group is shown in Figure 2A and 2B. Tumors in the group receiving diluent (Fig.2A) showed exponential growth. All tumors in the group receiving 600 μCi ^{186}Re-labeled MAb E48 completely regressed. Tumors
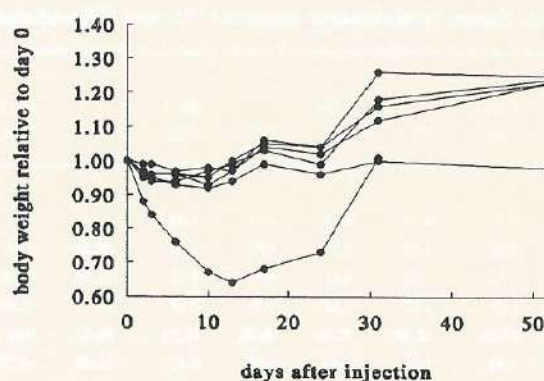
Figure 3. Toxicity of 600 μCi ^{186}Re-labeled MAb E48 IgG in nude mice bearing HNX-HN xenografts, monitored as the individual body weight relative to day 0.

did not show regrowth during follow up (>150 days). However, one mouse died at 31 days, after recovering from a weight loss of 35%. Toxicity, monitored by the individual body weight of the treatment group at each time point relative to day 0, is shown in Figure 3. At the time of death, recovery of weight loss had occurred up to 85%. No visible sign of tumor was observed after dissection. In all other mice, weight loss did not exceed 10%.

Dosimetry

For the group receiving 600 μCi ^{186}Re-labeled MAb E48 IgG, the absorbed cumulative radiation dose for tumor and various organs, based on the area under the curve of the biodistribution data of 100 μCi ^{186}Re-labeled MAb E48 IgG, is shown in Figure 4. The ratio of doses of tumor : blood was 4.3, tumor : non-tumor ratios ranged from 12.3 (tumor : liver) to 80.5 (tumor : muscle). The ratio tumor dose : whole body dose was 14.0.
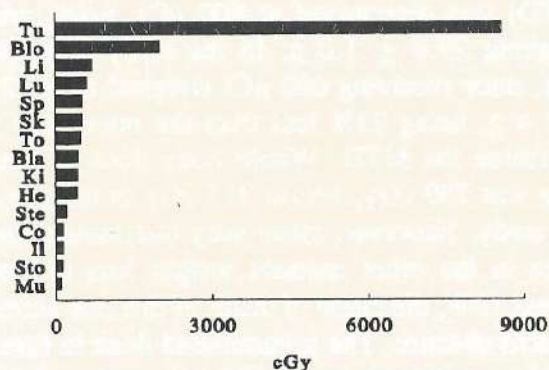
Figure 4. Total accumulated radiation dose in cGy, calculated using the trapezoid integration method for the area under the curve. Tu, tumor; Blo, blood; Li, liver; Lu, lung; Sp, spleen; Sk, skin; To, tongue; Bla, bladder; Ki, kidney; He, heart; Ste, sternum; Co, colon; Il, ileum; Sto, stomach; Mu, muscle.

Discussion

In this addendum experiments are described in which the biodistribution of ^{131}I-labeled and ^{186}Re-labeled MAb E48 IgG are compared directly by simultaneous injection into HNSCC xenograft bearing mice. Data obtained from therapy experiments described in Chapter 4 and Chapter 6 indicated possible differences in biodistribution characteristics, but factors like xenograft passage, batch of animals, amount of injected radioimmunoconjugate, in terms of radioactivity as well as protein, all likely to be of influence on the biodistribution of radioimmunoconjugates, were not the same in these experiments. In the study described here, differences in biodistribution characteristics were indeed observed. For ^{131}I-labeled MAb E48, a higher maximum %ID.g^{-1} was observed than for ^{186}Re-labeled MAb E48 IgG. This difference seemed to be generated during the first 3 days, after day 3, the biodistribution patterns ran practically in parallel. In non-target organs, the only significant difference observed was a initial higher accumulation of ^{186}Re-labeled MAb E48 IgG in the liver as compared to ^{131}I-labeled MAb E48 IgG. This non-specific accumulation rapidly decreased and reached levels comparable to ^{131}I-labeled MAb E48 IgG. Since in this experiment the two radioimmunoconjugates were simulataneously injected, the differences observed are a reflection of intrinsic characteristics of these compounds. Whether these intrinsic characteristics are a consequence of the chelate used for the labeling of ^{186}Re or determined by the isotope itself remains a question to be answered by future experiments. A possible explanation of the observed differences might be found in different metabolic patterns of the two radioimmunoconjugates. Differences in catabolism of ^{186}Re-conjugates depending on the method of chelation have been described by Fritzberg et al. [4] While minimal hepatic and renal retention were observed when using MAG$_2$-GABA chelating agents, very high gut excretion occurred in patients due to catabolism of the conjugates in the liver to ^{186}Re-N,S chelate lysine conjugates. Insertion of a cleavable succinyl ester based on a beta amido alcohol of the N,S ligand, mercaptoacetylglycylglycylglycylserine, resulted in an 80% reduction in intestinal radioactivity in animals. Differences in metabolic patterns between iodinated versus radiometal chelated radioimmunoconjugates have also been described. In a study comparing the tumor targeting, pharmacokinetics, and metabolic patterns of iodinated *versus* radiometal (^{177}Lu) chelated anticarcinoma single-chain Fv molecules (sFv), significant higher uptake of ^{177}Lu-sFv in liver, spleen and kidney was observed [5]. According to the authors, the most likely explanation for these differences appears to be that for both the

liver, spleen and kidney was observed [5]. According to the authors, the most likely explanation for these differences appears to be that for both the iodinated and the radiometal chelated sFv similar metabolism occurs but that dehalogenation of the iodinated forms takes place [6]. Subsequently, iodine is expelled from the body, whereas free ^{177}Lu and/or ^{177}Lu chelate complex appears to be maintained in the cells metabolizing the conjugates. Comparable phenomena have been described in other studies using metal-conjugated MAb IgG and their fragments [7,8]. Further experiments comparing ^{131}I- and ^{186}Re-labeled MAb E48 IgG with special emphasis on pharmacokinetics and intestinal excretion will have to be performed to answer the questions raised by the observations made in the study described here.

Increased uptake of radioactivity in small tumors as compared to larger tumors has been described in experimental [9,10] as well as clinical studies [11]. In addition, in experimental [1] as well as clinical studies [12], this increased uptake was shown to increase the respons to RIT of small tumor loads when compared to larger tumors. In a pilot experiment investigating such a possible relation between tumor size and therapeutic efficacy of RIT in our xenograft model, the injection of a single bolus of 600 μCi ^{186}Re-labeled MAb E48 IgG resulted in 100% complete remission of tumors of 75 $\pm$ 17 mm^3. In earlier experiments using ^{131}I- and ^{186}Re-labeled MAb E48 IgG, the highest percentage complete remissions sofar was 50%, using tumors of 125 $\pm$ 69 mm^3. One possibly treatment related death was observed. At the time of death, no visible evidence of tumor was present after dissection. In previous experiments with ^{186}Re, the maximum tolerable dose

(MTD) was determined at 600 μCi, using mice weighing 29.4 $\pm$ 1.0 g. In the study described here, mice receiving 600 μCi weighed only 22.7 $\pm$ 1.4 g, being 23% less than the mice used to determine the MTD. Whole body dose of these mice was 759 cGy, *versus* 312 cGy in the previous study. However, since only one mouse died while in the other animals weight loss did not exceed 10%, the cause of death of this one animal remains obscure. The accumulated dose in tumor in this experiment was 8,580 cGy *versus* 3,432 cGy in the experiments described in Chapter 6. Data from this pilot therapy experiment clearly indicates the enhanced efficacy of RIT in relatively small tumors. The tumor dose observed in these small tumors is in the order of magnitude known to be sufficient for sterilization of HNSCC by means of external beam irradiation.

References

1. Beaumier PL, Venkatesan P, Vanderheyden J-L, Burgua WD, Kunz LL, Fritzberg AR, Abrams PG, Morgan Jr AC. [186]Re radioimmunotherapy of small cell lung carcinoma xenografts in nude mice. *Cancer Res* 51:676-681, 1991.

2. Jungerman JA, Yu KHP, Zanelli CI. Radiation absorbed dose estimates at the cellular level for some electron-emitting radionuclides for radioimmunotherapy. *Int J App Rad Isot* 35:883-888, 1984.

3. Prestwich WV, Nunes J, Kwok CS. Beta-dose point kernels for radionuclides of potential use in radioimmunotherapy. *J Nucl Med* 30:1036-1046, 1989.

4. Fritzberg AR, Beaumier PL, Kasina S, Srinivasan A, Su FM, Vanderheyden J-L. Targeting and therapeutic studies of rhenium-186 NR-LU-10 with stable and cleavable linkages. *The sixth IRIST symposium on immunoscintigraphy and immunotherapy* Lausanne, 1991.

5. Schott ME, Milenic DE, Yokota T, Whitlow M, Wood JF, Fordyce WA, Cheng RC, Schlom J. Differential metabolic patterns of iodinated *versus* radiometal chelated anticarcinoma single-chain Fv molecules. *Cancer Res* 52:6413-6417, 1992.

6. Carrasquillo JA, Krohn KA, Beaumier P, McGuffin RW, Brown JP, Hellström KE, Hellström I, Larson SM. Diagnosis and therapy for solid tumors with radiolabeled antibodies and immune fragments. *Cancer Treat Rep* 68:317-328, 1984.

7. Buchsbaum D, Randall B, Hanna D, Chandler R, Loken M, Johnson E. Comparison of the distribution and binding of monoclonal antibodies labeled with 131-iodine or 111-indium. *J Nucl Med* 10:398-402, 1985

8. Sharkey RM, Motta-Hennessey C, Pawlyk D, Siegel JA, Goldenberg DM. Biodistribution and radiation dose estimates for yttrium- and iodine-labeled monoclonal antibody IgG and fragments in nude mice bearing human colonic tumor xenografts. *Cancer Res* 50:2330-2336, 1990.

9. Matzku S, Tilgen W, Kalthoff H, Schmiegel WH, Broecker E. Dynamics of antibody transport and internalization. *Int J Cancer* 2:11s-14s, 1988.

10. Hagan PL, Halpern SE, Dillman RO, Shawler DL, Johnson DE, Chen A, Krishan L, Frincke J, Bartholomew L, David GS, Carlo D. Tumor size: effect of monoclonal antibody uptake in tumor models. *J Nucl Med* 27:422-426, 1986.

11. Chatal J-F, Saccavinni J-C, Thedrez P, Curtet C, Kremer M, Guerreau D, Nolibe D, Fumoleau P, Guillard Y. Biodistribution of Indium-111-labeld OC125 monoclonal antibody intraperitoneally injected into patients operated on for ovarian carcinomas. *Cancer Res* 49:3087-3094, 1989.

Chapter 7

Summary and conclusions

The long term goal of these studies is to have available an effective adjuvant systemic therapy for patients with minimal residual disease. In the case of head and neck cancer this would apply to patients with stage III and IV disease. In these patients locoregional recurrences occur after conventional therapy in 50-60%, while 15-25% develop distant metastases.

In **Chapter 1**, the rationale for our studies is given. In spite of the increase in the locoregional control of head and neck squamous cell carcinoma, this has not resulted in an improved 5-year survival of patients. More patients are exposed to the risk of developing distant metastases and "second primary" tumors. Since at present no adequate therapy is available for patients with distant metastases, there is a need for an effective adjuvant systemic therapy. To achieve this long term goal, the development of MAbs with specificity for head and neck cancer for RIT was started several years ago. MAbs with this specificity were developed, and biodistribution studies with MAbs E48 IgG, K984 IgG and recently U36 IgG have demonstrated the capacity of these MAbs for specific delivery of radioisotopes to HNSCC xenografts. At the start of this dissertation, MAb E48 was shown to be the most promising MAb available. The work presented in this thesis was aimed at further investigating the suitability of the antigen recognized by MAb E48 as a target for RIT of head and neck cancer. Furthermore, studies initiated to characterize the antigen recognized by MAb E48 were continued. One of the main reasons to pursue the possibility of RIT for the treatment of patients with distant metastases is the intrinsic sensitivity of head and neck cancer for radiation. The development of new MAbs was necessary because available

MAbs did not possess the characteristics needed for RIT. From the overview of clinical RIT trials it has become clear that in large solid tumors only a low percentage of injected radioactivity accumulates, explaining the low therapeutic ratios. The observed higher accumulation in smaller tumor loads and the correlation between tumor size and respons to RIT indicate that RIT has the potential to be most useful in adjuvant therapy when minimal residual disease is present. This does not exclude the possibility, however, to use RIT for treatment of large tumors, e.g. in combination with external beam irradiation for treatment of lymph node metastases in the neck. In this approach, RIT can probably provide an additional 1,000-2,000 rads, needed for curative treatment. The major disadvantages of the most used isotopes in clinical trials sofar, ^{131}I and ^{90}Y, are discussed and the reasons for pursuing the development of radioimmunoconjugates with the isotope ^{186}Re are given. Finally, the validity of the nude mouse model for the preclinical evaluation of radioimmunoconjugates is discussed.

In **Chapter 2**, the subcellular localization of the MAb E48 defined antigen in normal oral mucosa is investigated by means of immunoelectronmicroscopy. In this tissue, the expression of the E48 antigen at the cellular level appears to be restricted to the cell surface and in particular to desmosomes. *In vitro* experiments with HNSCC cells growing in collagen gels show that in the presence of MAb E48, cells do not grow out to colonies but instead form clusters of dispersed cells. These data indicate a role for the E48 antigen in cell-cell adhesion in squamous epithelia and their neoplastic counterparts. In order to ultimately clone the gene encoding the E48 antigen, recently an immunoaffinity protocol has

been developed to purify the E48 antigen from extracts of HNSCC xenografts. The first amino-acid sequence analysis studies performed with purified E48 antigen show no sequence homology of the N-terminus with any mammalian sequences described sofar (Gerretsen *et al*, unpublished data).

In **Chapter 3**, the biodistribution and imaging characteristics of MAb E48 IgG and its F(ab')$_2$ fragment were investigated. Trying to reflect the expression pattern of the E48 antigen as observed in clinical specimens, a squamous cell carcinoma xenograft line with a low, heterogenous expression, and a squamous cell carcinoma xenograft line with a strong, homogenous cell surface expression were used. Whole IgG as well as F(ab')$_2$ accumulated specifically in the xenograft line with high expression, and clear images of tumors could be taken from F(ab')$_2$ injected mice after 24 hours, and from IgG injected mice after 3 days. In mice bearing xenografts with low E48 antigen expression, only F(ab')$_2$ showed specific localisation and allowed images of tumors to be obtained after 24 hours. The apparent superior localization and imaging characteristics of F(ab')$_2$ were reason to start a clinical phase I/II radio-immunoscintigraphy (RIS) trial, in which the safety and diagnostic accuracy of ^{99m}Tc-labeled MAb E48 F(ab')$_2$ for the detection of metastatic disease in patients with histologically proven HNSCC and with clinical evidence of lymph node involvement was started. No adverse reactions were observed. An unexpected finding in this study was the consistent uptake of activity in the adrenal glands. Untill now, no clear explanation for this phenomenon has been found. Immunohistochemical examination of frozen sections of adrenal tissue sofar has not shown any reactivity

with MAb E48. In addition to the uptake observed in the adrenal glands, uptake was observed in the nose and mouth region. The ^{99m}Tc-labelled 323A3 F(ab')$_2$ fragment, which is not reactive with normal oral mucosa, did not show any accumulation in this region. Therefore, it is thought that uptake of activity in the nose and mouth region as observed with MAb E48 F(ab')$_2$ is due to a specific antigen-antibody interaction in which the antibody has overcome the natural barriers formed by the capillary endothelium and the basement membrane of the mucosal epithelium. From subsequent patient studies using MAb E48 IgG instead of F(ab')$_2$, preliminary data indicate that the use of IgG results in a decreased accumulation of activity in the adrenal glands as well as the nose and mouth region. Strategies to further decrease the uptake in adrenals and normal mucosa are currently under investigation. When comparing the biodistribution data of IgG and F(ab')$_2$ in these trials, no clear advantage for either conjugate could be observed with respect to the observed tumor to non-tumor ratios. This finding, the uptake in the adrenals and the antigen-specific accumulation in normal mucosa were not predicted from the findings in our animal studies. This confirms, at least for MAb E48, the limitations of the model as described in Chapter 1, especially with respect to the absence of the antigen in mouse tissues. However, the specific accumulation in tumor was confirmed. Data on the localisation of ^{99m}Tc-labeled MAb E48 IgG indicate accumulation of the conjugate in tumours of 0.5-4.0 cm diameter up to a mean of 0.03 %ID.g^{-1} at 44 hours (range: 0.014-0.082, number of patients=7). This looks very promising indeed when taking into account the higher accumulation in small tumour loads.

From the comparison of the value of MAb E48 RIS with the value of computerized tomography (CT), magnetic resonance imaging (MRI) and palpation, always tested by the histopathological outcome of the neck dissection specimen, a similar or somewhat better sensitivity and specificity for RIS was observed in comparison with MRI, CT and palpation. Yet, when taking into account the relative substantial costs of RIS, the additional value of RIS over CT and MRI at the present does not seem high enough to consider this diagnostic modality for routine application in the clinic. More important with respect to the further perspectives for RIT, the accumulation of radioactivity in tumour tissue as proven in our clinical RIS trial suggest the E48 antigen to be a suitable target for RIT. Thus, the development of radioimmunoconjugates for RIT of HNSCC was further pursued. From this point of view, RIS can be regarded as a prelude to RIT.

In **Chapter 4**, the capacity of ^{131}I-labeled MAb E48 IgG for RIT in the nude mouse model was shown. Using single bolus injections, dose dependent tumor growth delay, tumor regression and complete remissions were obtained. A very good retention of the radioimmunoconjugate was observed, which resulted in a high cumulative absorbed radiation dose in the tumor. Comparison of RIT with a number of clinically used and experimental chemotherapeutic agents clearly showed a higher therapeutic efficacy of RIT. Also when compared with therapeutic data of other radioimmunoconjugates in different tumor models, the efficacy of ^{131}I-labeled MAb E48 IgG appeared to be high.

However, it has been recognized that ^{131}I is not the isotope of choice for clinical application, due to the *in vivo* dehalogenation and the high percentage toxic γ-radiation. With respect to the physical parameters of importance for the development of radioimmunoconjugates for RIT, ^{186}Re is a very suitable isotope. Therefore, the development of radioimmunoconjugates for application in the clinic was pursued with this isotope.

In **Chapter 5**, the development of a technical protocol for the labeling of MAbs with ^{186}Re, using the MAG$_3$ chelate, is described. Although a number of labeling techniques for ^{186}Re had already been described, there remained serious doubt about the stability and specific activities of conjugates thus obtained, the latter question in part being caused by the restricted commercial availability of ^{186}Re with high specific activity. With our technical protocol, which was shown to be generally applicable for a number of MAbs, these criteria were met. First, the generated conjugates were highly stable *in vitro* and *in vivo*. Second, with the ratios Re : MAb obtained in this way, the applicability of this protocol is not restricted by the low specific activity of commercially available ^{186}Re. Moreover, the labeling procedure appeared to be highly reproducible and suited for routine automated application. Immunoreactivity was preserved with all MAbs labeled, and pilot biodistribution experiments with ^{99m}Tc- and ^{186}Re-labeled MAb E48 showed comparable biodistribution and tumor targeting characteristics. The latter observation may be reason to assume that ^{186}Re-conjugates will show comparable tumor targeting in patients as observed with ^{99m}Tc-labeled MAb E48 in our trials. As far as our information goes, ^{186}Re with a specific activity of 1-1.5 Ci.mg^{-1} will become commercially available at large scale in 1993. It can be anticipated that availability of ^{186}Re in combination with the development of suitable labeling procedures will

result in a widespread use of ^{186}Re-labeled MAbs. In **Chapter 6**, the efficacy of ^{186}Re-labeled MAb E48 IgG mediated therapy for RIT was investigated. Upon single bolus injection of increasing doses of ^{186}Re-conjugate, dose dependent tumor growth delay, tumor regression and up to 50% complete remissions were observed. Based on the numbers of complete remissions and the absorbed cumulative dose in tumor in the therapy experiments with ^{131}I- and ^{186}Re-labeled MAb E48 IgG, it was tempting to speculate that the latter is more effective in eradicating HNSCC under conditions resulting in apparent equivalent radiation doses delivered to the tumor. However, direct comparison of these two radioimmunoconjugates is not valid, since interexperimental variation in important parameters cannot be excluded. For instance, apparent differences in tumor accumulation and retention of the conjugates were observed. To further address these questions, pilot biodistribution experiments of simulateneously injected ^{131}I- and ^{186}Re-labeled MAb E48 IgG were performed, described in the **Addendum**. Data obtained from these experiments indicate possible differences in metabolic patterns of these conjugates. As demonstrated in this Chapter, a slight increased uptake of ^{186}Re-labeled MAb E48 IgG in the liver was observed when compared with ^{186}I-labeled MAb E48 IgG. This phenomenon may be due to the MAG$_3$ chelator used for ^{186}Re labeling. As demonstrated by Fritzberg *et al.* for ^{186}Re-MAG$_3$-GABA conjugates very high gut excretion of activity may occur due to the catabolism of the conjugates in the liver to ^{186}Re-N,S-chelate-lysine derivatives. Also in a proportion of head and neck cancer patients receiving ^{99m}Tc-MAG$_3$-MAb we have observed intestinal accumulation of radioactivity. In this respect, the metabolic patterns of MAbs labeled with a high MAG$_3$: MAb ratio will have to be investigated in the clinic. Another important point to be considered is the possible immunogenicity of MAG$_3$, since some chelators for radiometals, like DOTA for chelation of ^{90}Y, are known to be immunogenic in humans.

Also described in the **Addendum** are pilot experiments investigating the efficacy of ^{186}Re-labeled MAb E48 IgG to treat small tumor xenografts. When mice bearing relatively small xenografts were injected with 600 μCi, all tumors were abolished. A very high accumulation of activity in tumor was observed. In Chapter 2, the *in vitro* expression of the E48 antigen was shown to be dependent on the three dimensional organization of the cell cultures. In this respect, it is not yet clear if and to what extent the E48 antigen will be expressed in small tumor nodules and cell clusters in patients. Unfortunately, at present no suitable metastasis model for head and neck cancer is available to determine the efficacy of RIT to treat disseminated disease. In this respect, the introduction of the SCID (severe combined immune deficient) mouse may open new avenues for the development of a relevant metastasis model, thus permitting the design of experiments addressing these questions.

In conclusion, the MAb E48 antigen seems a very suitable target for RIT with ^{186}Re-labeled MAb E48 IgG. To design a therapy trial, a well defined group of patients with a high risk of harbouring minimal residual disease is needed. It has been shown that defining such a patient group, with a high risk of developing distant metastases, is possible. Definition of this group of patients is based on the number of involved lymph nodes. Analysis of a group of 281 patients with head and

neck cancer revealed that when 4 or more nodes were involved, the risk of developing distant metastases was found to be almost 50%. At our department, preparations for a phase I clinical trial with [186]Re-labeled chimeric MAb E48 IgG in patients with metastatic disease after conventional therapy are currently in progress. When this trial demonstrates that [186]Re-RIT is well tolerated, the efficacy of [186]Re-RIT will be further evaluated in an adjuvant setting for the treatment of patients with locoregional disease, who are at high risk for developing distant metastases.

Het uiteindelijke doel van deze studies is om te kunnen beschikken over een effectieve adjuvant therapie voor patiemten met "minimal residual disease". Daarbij bestaat in het bijzonder behoefte bij patiënten met stadium III en IV hoofd-hals kanker. Bij deze patiëntengroepen komen na conventionele behandeling in 50-60% locoregionale recidieven voor, terwijl zich in 15-25% van de gevallen metastasen op afstand ontwikkelen.

In **Hoofdstuk 1** wordt de rationale voor onze studies gegeven. Ondanks een verbetering in de locoregionale controle van plaveiselcel carcinomen van het hoofd-hals gebied heeft dit niet geleid tot verbetering van de 5-jaars overleving van patienten met deze ziekte. Meer patiënten raken blootgesteld aan het gevaar van de ontwikkeling van metastasen op afstand en "tweede primaire" tumoren. Daar op dit moment geen afdoende therapie beschikbaar is voor patiënten met metastasen op afstand, bestaat behoefte aan een effectieve systemische adjuvant therapie. Om dit lange termijn doel te bereiken werd enkele jaren geleden een start gemaakt met de ontwikkeling van monoclonale antilichamen (MAb) met specificiteit voor hoofd-hals tumoren. MAbs met deze specificiteit werden ontwikkeld, en biodistributie studies met MAbs E48, K984 en recentelijk U36 hebben de capaciteit van deze MAbs om specifiek radioisotopen naar hoofd-hals tumor transplantaten in naakte muizen te leiden aangetoond. Bij de start van het onderzoek voor deze dissertatie toonde MAb E48 zich het meest veelbelovende antilichaam. Het in dit proefschrift geëvalueerde werk is er op gericht de geschiktheid van het E48 antigeen als doelwit voor radioimmunotherapie (RIT) van hoofd-hals carcinomen te onderzoeken. Tevens werden eerder geïni-

tieerde studies met als doel het antigeen dat herkend wordt door MAb E48 te karakteriseren voortgezet.

Eén van de belangrijkste redenen om de mogelijkheid van RIT voor de behandeling van patienten met metastasen op afstand te onderzoeken is de intrinsieke gevoeligheid van hoofd-hals tumoren voor bestraling. De ontwikkeling van nieuwe MAbs was noodzakelijk omdat de beschikbare MAbs niet beschikten over de eigenschappen vereist voor RIT. Uit het overzicht van de clinische trials is het duidelijk geworden dat grote solide tumoren slechts een laag percentage van de geïnjiceerde radioaktiviteit opnemen, hetgeen de lage therapeutische index verklaart. De waargenomen hogere ophoping in kleinere tumoren en de correlatie tussen tumor grootte en respons op RIT geven aan dat RIT in potentie veel waarde heeft als adjuvant therapie bij "minimal residual disease". Dit sluit de mogelijkheid echter niet uit dat RIT tevens gebruikt kan worden bij de behandeling van grote tumoren, bijvoorbeeld in combinatie met conventionele bestraling voor de behandeling van lymfeklier metastasen in de nek. Bij deze benadering kan RIT waarschijnlijk een extra 1000-2000 rads opleveren, hetgeen nodig is voor curatieve behandeling. De belangrijkste nadelen van de tot dusver in de kliniek meest gebruikte isotopen, ^{131}I en ^{90}Y, worden besproken, en redenen voor de ontwikkeling van radio-immunoconjugaten met het isotope ^{186}Re worden gegeven. Ten slotte wordt de waarde van het naakte muizemodel voor de preklinische evaluatie van radioimmunoconjugaten besproken.

In **Hoofdstuk 2** wordt de subcellulaire lokalisatie van het door MAb E48 herkende antigeen in normale orale mucosa, onderzocht door middel van immunoelectronenmikroskopie, beschreven.

In dit weefsel lijkt de expressie van het E48 antigeen op cellulair niveau beperkt tot het celoppervlak, in het bijzonder tot desmosomen. *In vitro* experimenten met uit hoofd-hals tumoren geïsoleerde cellen die in collageen gels groeien tonen aan dat in aanwezigheid van MAb E48 cellen niet uitgroeien tot kolonies maar klusters van verspreide cellen vormen. Deze gegevens impliceren dat het E48 antigeen een rol speelt bij cel-cel adhesie in plaveiselcel epithelia en neoplasiën die uit deze weefsels kunnen ontstaan. Ten einde het gen dat codeert voor het E48 antigeen te kloneren is recentelijk een immunoaffiniteits protocol ontwikkelt om het E48 antigeen te zuiveren uit hoofd-hals tumor transplantaten. De eerste aminozuur-sequentie-analyse studies met gezuiverd E48 antigeen laten geen sequentie homologie van het N-terminale gedeelte zien met tot nu toe beschreven sequenties van zoogdieren (Gerretsen *et al.*, ongepubliceerd).

In **Hoofdstuk 3** worden de biodistributie en "imaging" eigenschappen van MAb E48 IgG en F(ab')$_2$ beschreven. Om te proberen een afspiegeling te geven van het expressie patroon van het E48 antigeen zoals dat wordt gezien in klinische monsters werden een plaveisel cel tumortransplantaat met een lage, heterogene expressie en een plaveiselcel tumortransplantaat met een hoge, homogene celoppervlak expressie gebruikt. Zowel het complete IgG als F(ab')$_2$ fragment van MAb E48 hoopten met name op in de tumortransplantaten met hoge expressie. Duidelijke "images" van tumoren konden gemaakt worden van met MAb E48 F(ab')$_2$ ingespoten muizen na 24 uur, en van met MAb E48 IgG ingespoten muizen na 3 dagen. In muizen met tumortransplantaten met lage E48 antigeen expressie toonde alleen MAb E48 F(ab')$_2$ specifieke lokalisatie en konden

hiermee "images" van tumoren na 24 uur verkregen worden. De geconstateerde superieure lokalisatie en "imaging" eigenschappen van F(ab')$_2$ hebben aanleiding gegeven tot de start van een klinische fase I/II radioimmunoscintigrafie (RIS) trial. In deze studie werd de veiligheid en diagnostische gevoeligheid van ^{99m}Tc-gelabeled MAb E48 F(ab')$_2$ voor de detectie van halskliermetastasen onderzocht bij patienten met een histologisch aangetoond plaveiselcel carcinoom uitgaande van het slijmvlies in het hoofd-halsgebied met klinisch evidente halskliermetastasen. Tijdens deze studie werden geen schadelijke bijwerkingen waargenomen. Een onverwachte observatie was de consistente opname van aktiviteit in de bijnieren. Tot nu toe kan geen verklaring voor dit fenomeen gegeven worden. Immunohistochemisch onderzoek van vriescoupes van bijnieren heeft tot dusver geen reaktiviteit met MAb E48 laten zien. Naast opname in de bijnier werd tevens opname in het gebied van de neus en mond gezien. ^{99m}Tc-gelabeled MAb 323A3, dat geen reaktiviteit heeft met normale orale mucosa, liet geen opname zien in dit gebied. Dientengevolge wordt aangenomen dat opname van aktiviteit in het gebied van de neus en mond zoals waargenomen met MAb E48 het gevolg is van een specifieke antigeen-antilichaam interactie, waarbij het antilichaam natuurlijke barrières die gevormd worden door het capillair endotheel en de basale membraan van het mucosa epitheel gepasseerd is. Uit verdere patienten studies, waarbij MAb E48 IgG gebruikt werd in plaats van MAb E48 F(ab')$_2$, impliceren dat het gebruik van IgG resulteert in een verlaagde opname van aktiviteit in zowel de bijnieren als het gebied van de neus en mond. Strategiën om de opname in bijnieren en normale mucosa nog verder te verlagen worden momenteel onderzocht.

Wanneer de biodistributie data van MAb E48 IgG en $F(ab')_2$ in deze studies worden vergeleken kan geen duidelijke voorkeur voor een der conjugaten geconstateerd worden met betrekking tot de waargenomen ratios tussen tumor en normale weefsels. Deze bevinding, de opname in de bijnieren en de antigeen-specifieke opname in normale mucosa waren niet voorspeld uit de bevindingen van onze dierexperimenten. Dit bevestigt, althans voor MAb E48, de beperkingen van het model zoals beschreven in Hoofdstuk 1, met name met betrekking tot het ontbreken van het E48 antigeen in muizeweefsels. De specifieke ophoping in tumor werd echter bevestigd. Data met betrekking tot de lokalisatie van ^{99m}Tc-gelabeled MAb E48 IgG laten zien dat in tumoren van 0,5-4,0 cm gemiddeld 0.03% (0,014-0,082) van de ingespoten dosis per gram accumuleert na 44 uur. Dit is inderdaad zeer veelbelovend wanneer rekening gehouden wordt met de hogere ophoping in kleinere tumoren en tumor haardjes.

Wanneer de waarde van RIS met MAb E48 wordt vergeleken met die van "computerized tomography" (CT), die van "magnetic resonance imaging" (MRI), en die van palpatie, steeds getoetst aan de histologische bevindingen in nek dissectiepreparaten, blijkt een vergelijkbare of een licht verhoogde sensitiviteit en specificiteit van RIS ten opzichte van de andere diagnostische methoden. Wanneer echter rekening wordt gehouden met de relatief hoge kosten van RIS lijkt de additionele waarde van RIS in vergelijking met CT en MRI niet hoog genoeg om RIS als routine toepassing in de kliniek te overwegen. Belangrijker met betrekking tot de perspectieven voor RIT is het feit dat de ophoping van radioaktiviteit in tumor weefsel, zoals aangetoond in onze klinische trial, impliceren dat het E48 antigeen een geschikt doelwit is

voor RIT. Dientengevolge werd de ontwikkeling van radioimmunoconjugaten voor RIT van hoofd-hals tumoren voortgezet. Vanuit dit standpunt kan RIS als een inleiding voor RIT beschouwd worden.

In **Hoofdstuk 4** wordt de capaciteit van ^{131}I-gelabeled MAb E48 IgG voor RIT, aangetoond in het naakte muizemodel, beschreven. Met eenmalige bolus injecties werden dosis afhankelijke tumor groei vertraging, tumor regressie en complete remissies verkregen. Een zeer goede retentie van het radio-immunoconjugaat werd waargenomen, welke resulteerde in een hoge cumulatieve geabsorbeerde stralingsdosis in de tumor. Vergelijking van RIT met een aantal klinisch toegepaste en experimentele chemotherapeutica lieten een duidelijk hogere therapeutische doeltreffendheid zien van RIT. Ook in vergelijking met therapeutische data van andere radioimmunoconjugaten in verschillende tumor modellen bleek de doeltreffendheid van ^{131}I-gelabeled MAb E48 hoog.

Momenteel wordt echter aangenomen dat ^{131}I niet het eerste keus isotoop is, met name door de snelle *in vivo* dehalogenatie en het hoge percentage schadelijke γ-straling. Met betrekking tot de physische eigenschappen die van belang zijn voor de ontwikkeling van radioimmunoconjugaten voor RIT is ^{186}Re een zeer geschikt isotoop. Daarom werd de ontwikkeling van radioimmunoconjugaten voor toepassing in de kliniek vervolgd met dit isotoop.

In **Hoofdstuk 5** wordt de ontwikkeling beschreven van een technisch protocol voor de labeling van MAbs met ^{186}Re, gebruik makend van de MAG_3 chelator. Hoewel een aantal labelings technieken voor ^{186}Re reeds beschreven waren werd sterk getwijfeld aan de stabiliteit en specifieke aktiviteit van langs deze weg verkregen conju-

gaten. Het laatste punt wordt ten dele veroorzaakt door de beperkte commerciële beschikbaarheid van ¹⁸⁶Re met hoge specifieke aktiviteit. Met de ontwikkeling van ons technisch protocol, waarvan aangetoond werd dat dit algemeen toepasbaar was voor een aantal MAbs, werd aan deze criteria voldaan. Ten eerste bleken de gegenereerde conjugaten zeer stabiel *in vitro* en *in vivo*. Ten tweede bleek dat met de resulterende Re : MAb ratio de toepasbaarheid van dit protocol niet gelimiteerd wordt door de lage specifieke aktiviteit van commerciëel beschikbare ¹⁸⁶Re. Tevens bleek de labelingsprocedure zeer reproduceerbaar en geschikt voor geautomatiseerde routine toepassing. De immunoreactiviteit werd behouden bij alle MAbs die gelabeled werden, en pilot biodistributie experimenten met ⁹⁹mTc- en ¹⁸⁶Re-gelabeled MAb E48 lieten vergelijkbare biodistributie en tumor lokalisatie eigenschappen zien. De laatste observatie kan reden zijn om aan te nemen dat ¹⁸⁶Re-conjugaten een vergelijkbare tumor lokalisatie in patienten zal laten zien als ⁹⁹mTc-gelabeled MAb E48 in onze patiënten trial. Zover onze informatie gaat zal ¹⁸⁶Re met een specifieke activiteit van 1-1,5 Ci per mg op grote schaal commerciëel beschikbaar komen in 1993. Aangenomen kan worden dat de beschikbaarheid van ¹⁸⁶Re gecombineerd met de ontwikkeling van relevante labelingsprocedures zullen uit monden in een wijdverspreid gebruik van MAbs gelabeled met ¹⁸⁶Re.

In **Hoofdstuk 6** wordt de doeltreffendheid van ¹⁸⁶Re-gelabeled MAb E48 IgG gemediëerde therapie voor RIT beschreven. Na eenmalige bolus injectie van toenemende doses ¹⁸⁶Re-conjugaat werd dosis afhankelijke tumor groeivertraging, tumor regressie en tot 50% complete remissies bereikt. Gebaseerd op de aantallen complete

remissies en de cumulatieve geabsorbeerde dosis in tumor in de therapie experimenten met ¹³¹I- en ¹⁸⁶Re-gelabeled MAb E48 IgG was het aantrekkelijk om te speculeren dat laatstgenoemde effectiever is in het opruimen van tumor transplantaten onder omstandigheden waarbij schijnbaar overeenkomende stralingsdoses worden afgegeven aan de tumor. Direkte vergelijking van deze radioimmunoconjugaten is niet valide, daar interexperimentele variaties in belangrijke parameters niet uitgesloten mag worden. Zo werden bijvoorbeeld schijnbare verschillen in tumor ophoping en retentie geobserveerd. Om deze vragen verder te onderzoeken werden pilot biodistributie experimenten met gelijktijdig ingespoten ¹³¹I- en ¹⁸⁶Re-gelabeled MAb E48 IgG uitgevoerd. Deze experimenten worden beschreven in het **Addendum**. Data uit deze experimenten impliceren mogelijke verschillen in metabolisme van deze conjugaten. Zoals beschreven in het Addendum werd een licht verhoogde opname van ¹⁸⁶Re-gelabeled MAb E48 IgG in de lever gezien in vergelijking met ¹³¹I-gelabeled MAb E48 IgG. Dit fenomeen is mogelijk het gevolg van de MAG₃ chelator die gebruikt word voor de labeling. Zoals werd aangetoond door Fritzberg *et al.* voor ¹⁸⁶Re-MAG₃-GABA conjugaten kan hoge darm excretie van aktiviteit plaats vinden door afbraak van conjugaten in de lever tot ¹⁸⁶Re-N,S-chelate-lysine derivaten. Ook in een aantal patienten met hoofd-hals kanker die ⁹⁹mTc-MAG₃-MAb toegediend kregen werd ophoping van radioaktiviteit in de darmen gezien. Het is daarom zaak de patronen van metabolisme van MAbs gelabeled met hoge MAG₃ : MAb ratios in de kliniek te onderzoeken. Een ander belangrijk punt waar rekening mee gehouden dient te worden is de mogelijke immunogeniciteit van MAG₃. Voor sommige chelatoren, zoals bijvoorbeeld

DOTA voor de chelatie van ^{90}Y, is namelijk beschreven dat deze immunogeen in de mens te zijn.

Ook beschreven in het **Addendum** zijn pilot experimenten waarin de doeltreffendheid van ^{186}Re-gelabeled MAb E48 IgG voor de behandeling van kleine tumoren wordt onderzocht. Wanneer muizen met relatief kleine tumor transplantaten werden ingespoten met 600 μCi verdwenen alle tumoren. Een zeer hoge ophoping van aktiviteit in tumorweefsel werd gezien. In Hoofdstuk 2 werd aangetoond dat de expressie van het E48 antigeen afhankelijk is van de driedimensionale organisatie van de celkweken. In dit verband is het nog niet duidelijk of en in welke mate het E48 antigeen tot expressie gebracht wordt in kleine tumor klompjes en tumorcel haardjes in patiënten. Helaas is op dit moment geen geschikt metastase model voor hoofd-hals tumoren beschikbaar om de doeltreffendheid van RIT voor de behandeling van metastasen te onderzoeken. De introductie van de SCID (severe combined immune deficient) muis kan nieuwe mogelijkheden bieden voor de ontwikkeling van een relevant metastase model, waardoor experimenten opgezet kunnen worden waarmee deze vraagstellingen getoetst kunnen worden.

Geconcludeerd kan worden dat het E48 antigeen een zeer geschikt doelwit is voor RIT met ^{186}Re-gelabeled MAb E48 IgG. Vanzelfsprekend dient deze therapie getest te worden in een zorgvuldig opgezette studie bij een groep patiënten met een sterk verhoogd risico op "minimal residual disease" na conventionale behandeling. Daarvoor lijkt in het bijzonder in aanmerking te komen de groep patiënten bij wie in het nek dissectiepreparaat bij pathologisch anatomisch onderzoek 4 of meer halskliermetastasen worden aangetoond. Het is namelijk gebleken dat zich binnen 2 jaar in bijna de helft van deze populatie metastasen op afstand voordoen. Op onze afdeling zijn momenteel voorbereidingen gaande voor een fase I klinische trial met ^{186}Re-gelabeled chimeer MAb E48 IgG, bij patiënten die reeds metastasen hebben ontwikkeld na conventionale therapie. Indien deze studie aantoont dat ^{186}Re-RIT goed getolereerd wordt zal de doeltreffendheid van ^{186}Re-RIT als adjuvant therapie direct aansluitend op conventionele behandeling getest worden bij de eerder genoemde patiëntengroep met een zeer hoog risico op metastasen op afstand.

Dankwoord

Publications

1. Van Wijnen AJ, Wright KL, Massung RF, **Gerretsen M**, Stein JL, Stein GS. Two target sites for protein binding in the promotor region of a cell cycle regulated human H1 histon gene. Nucleic Acids Res **16**:571-592, 1988.

2. Quak JJ, van Dongen GAMS, **Gerretsen M**, Hayashida D, Balm AJM, Brakkee JPG, Snow GB, Meijer CJLM. Production of monoclonal antibody (K931) to a squamous cell carcinoma antigen identified as the 17-1A antigen. Hybridoma **9**:377-387, 1990.

3. Quak JJ, **Gerretsen M**, Schrijvers AHGJ, Meijer CJLM, van Dongen GAMS, Snow GB. Detection of squamous cell carcinoma xenografts in nude mice by radiolabeled monoclonal antibody E48. Arch Otolaryngol / Head Neck Surg **117**:1287-1291, 1991.

4. **Gerretsen M**, Quak JJ, Schrijvers AHGJ, van Walsum M, Meijer CJLM, Snow GB, van Dongen GAMS. Radioimmunoscintigraphy of squamous cell carcinoma. In: Monoclonal antibodies: Applications in clinical oncology. Epenetos AA editor, Chapman & Hall Medical. pp 87-102, 1991.

5. **Gerretsen M**, Quak JJ, Suh JS, van Walsum M, Meijer CJLM, Snow GB, van Dongen GAMS. Superior localization and imaging of radiolabelled monoclonal antibody E48 F(ab')₂ fragment in xenografts of human squamous cell carcinoma of the head and neck and of the vulva as compared to monoclonal antibody E48 IgG. Br J Cancer **63**:37-44, 1991.

6. Van Dongen GAMS, Quak JJ, Schrijvers AHGJ, **Gerretsen M**, van Walsum M, van Essen HE, Braakhuis BJM, Leverstein H, Snow GB. Tumor targeting with monoclonal antibodies in head and neck cancer. In: Immunobiology in Otology, Rhinology and Laryngology. McCabe BF and Veldman JE, editors. pp 281-287, 1991.

7. Schrijvers AHGJ, **Gerretsen M**, Quak JJ, Fritz J, van Walsum M, Snow GB, van Dongen GAMS. Evidence for a role of the monoclonal antibody E48 defined antigen in cell-cell adhesion in squamous epithelia. Exp Cell Res **196**:264-269, 1991.

8. Schrijvers AHGJ, **Gerretsen M**, van Walsum M, Braakhuis BJM, Quak JJ, Snow GB, van Dongen GAMS. Potential for targeting head and neck squamous cell carcinoma with monoclonal antibody K984. Cancer Immunol Immunother, **34**:252-258, 1992.

9. **Gerretsen M**, Schrijvers AHGJ, van Walsum M, Braakhuis BJM, Snow GB, van Dongen GAMS. Radioimmunotherapy of head and neck squamous cell carcinoma with 131I-labeled monoclonal antibody E48. Br J Cancer, **66**:496-502, 1992.

10. Van Dongen GAMS, **Gerretsen M**, Schrijvers AHGJ, Leverstein H, Brakenhoff RH, Quak JJ, Snow GB. Monoclonal antibody-based therapy of head and neck cancer. In: Head and Neck Cancer, Volume III. Johnson JT, Didolkar MS, editors, Excerpta Medica, Amsterdam, London, New York, Tokyo. pp 135-143, 1993.

11. **Gerretsen M**, Visser GWM, van Walsum M, Meijer CJLM, Snow GB, van Dongen GAMS. ¹⁸⁶Re-labeled monoclonal antibody E48 IgG mediated therapy of human head and neck squamous cell carcinoma xenografts. Cancer Research, in press.

12. **Gerretsen M**, Visser GWM, Brakenhoff RH, Snow GB, van Dongen GAMS. Complete ablation of small human head and neck squamous cell carcinoma xenografts with ¹⁸⁶Re-labeled monoclonal antibody E48 IgG. Appl Biochem Biotechnol, in press.

13. **Gerretsen M**, Quak JJ, Brakenhoff, Snow GB, van Dongen GAMS. The feasibility of radioimmunotherapy in head and neck cancer. Oral Oncology, Eur J Cancer Part B. In press.

14. Visser GWM, **Gerretsen M**, Herscheid JDM, Snow GB, van Dongen GAMS. Labeling of monoclonal antibodies with ¹⁸⁶Re using the MAG₃ chelate for radioimmunotherapy of cancer: a technical protocol. Submitted.

Curriculum Vitae

*De schrijver van dit proefschrift werd op 28 november 1960 geboren te Haarlem. In 1980 behaalde hij
het diploma Atheneum B aan het Hertog-Jan College te Valkenswaard. In dat zelfde jaar werd een
begin gemaakt met de studie Biologie aan de Rijks Universiteit te Utrecht. In 1984 behaalde hij zijn
kandidaatsexamen Biologie. Daarna volgde een bijvak Moleculaire Neurobiologie op het Rudolf
Magnus Instituut voor Farmacologie te Utrecht (Prof.Dr. V.M. Wiegant), een hoofvak Experimentele
Pathologie op de afdeling H5 van het Nederlands Kanker Instituut te Amsterdam (Dr. J. Hilgers) en
een hoofdvak Moleculaire Biologie op de afdeling Moleculair Biology and Biochemistry (Prof. G.S.
Stein en Prof. J.L. Stein) aan de University of Florida, in Gainesville, USA. Het doctoraal examen B5
werd afgelegd in juni 1988. Vanaf september 1988 tot maart 1993 was hij werkzaam als AIO bij de
afdelingen Keel-, Neus- en Oorheelkunde en Pathologie van het Academisch Ziekenhuis der Vrije
Universiteit te Amsterdam.*